REPORT DOCUMENTATION PAGE

Form Approved
OMB No. 0704-0188

1. REPORT DATE *(DD-MM-YYYY)*	2. REPORT TYPE	3. DATES COVERED *(From - To)*
15-12-2005	Bi-annual Performance/Technical Report	06/01/2005 - 11/30/2005

4. TITLE AND SUBTITLE

Bi-annual (6/2005--11/2005) Performance/Technical Report
for ONR YIP Award under Grant N00014-03-1-0466
Energy Efficient Wireless Sensor Networks Using Fuzzy Logic

5a. CONTRACT NUMBER

5b. GRANT NUMBER
N00014 – 03 –1 –0466

5c. PROGRAM ELEMENT NUMBER

6. AUTHOR(S)
Liang, Qilian

5d. PROJECT NUMBER

5e. TASK NUMBER

5f. WORK UNIT NUMBER

7. PERFORMING ORGANIZATION NAME(S) AND ADDRESS(ES)
University of Texas at Arlington
Office of Sponsored Projects
PO Box 19145
Arlington, TX 76019

8. PERFORMING ORGANIZATION REPORT NUMBER

9. SPONSORING/MONITORING AGENCY NAME(S) AND ADDRESS(ES)
Office of Naval Research
800 North Quincy Street
Arlington, VA 22217-5660

10. SPONSOR/MONITOR'S ACRONYM(S)
ONR

11. SPONSOR/MONITOR'S REPORT NUMBER(S)

12. DISTRIBUTION/AVAILABILITY STATEMENT
Approved for Public Release; Distribution is Unlimited.

13. SUPPLEMENTARY NOTES

14. ABSTRACT

During the period of 6/1/2005 -- 11/30/2005, we have performed different studies on wireless sensor networks. 1) We studied multi-target detection in radar sensor networks. 2) We made interference analysis and performance evaluation on UWB Sensor Networks in hostile environment. 3) An energy consumption and latency estimation scheme based on statistical modeling and maximal-likelihood detection was investigated for wireless sensor networks. 4) Self-organization in underwater acoustic sensor networks was studied. 5) We designed a cross-layer optimization scheme for mobile ad hoc networks using fuzzy logic systems. 6) A distributed query processing algorithm for data-centric sensor networks was proposed. 7) We investigated an asynchronous energy-efficient MAC protocol for UWB Sensor Networks. Ten papers were produced during the past six months, and are attached to this report.

15. SUBJECT TERMS
Wireless Sensor Network, Energy Efficiency, Fuzzy Logic, Radar, UWB.

16. SECURITY CLASSIFICATION OF:			17. LIMITATION OF ABSTRACT	18. NUMBER OF PAGES	19a. NAME OF RESPONSIBLE PERSON
a. REPORT	b. ABSTRACT	c. THIS PAGE			Qilian Liang
U	U	U	UU	124	19b. TELEPHONE NUMBER *(Include area code)* 817-272-1339

Bi-annual (6/1/2005–11/30/2005) Performance/Technical Report for ONR YIP Award under Grant N00014-03-1-0466 Energy Efficient Wireless Sensor Networks Using Fuzzy Logic

Qilian Liang
Department of Electrical Engineering
University of Texas at Arlington
Arlington, TX 76019-0016 USA
Phone: 817-272-1339, Fax: 817-272-2253
E-mail: liang@uta.edu

Abstract

During the period of 6/1/2005 – 11/30/2005, we have performed different studies on wireless sensor networks.

1. We studied multi-target detection in radar sensor networks.
2. We made interference analysis and performance evaluation on UWB Sensor Networks in hostile environment.
3. An energy consumption and latency estimation scheme based on statistical modeling and maximal-likelihood detection was investigated for wireless sensor networks.
4. Self-organization in underwater acoustic sensor networks was studied.
5. We designed a cross-layer optimization scheme for mobile ad hoc networks using fuzzy logic systems.
6. A distributed query processing algorithm for data-centric sensor networks was proposed.
7. We investigated an asynchronous energy-efficient MAC protocol for UWB Sensor Networks.

Ten papers were produced during the past six months, and are attached to this report.

1 Multi-Target Detection in Radar Sensor Networks

Radar as a powerful sensor system has been employed for the detection and location of reflecting objects such as aircraft, ships, vehicles, people and natural environment. By radiating energy into space and detecting the echo signal reflected from an object or target, the radar system can determine the presence of a target. Furthermore, by comparing the received echo signal with the transmitted signal, the location of a target can be determined along with other target information.

Conventional radar system operates as independent entity. While in a resource-constrained wireless sensor network, such detached operation may lead to deteriorated performance and waste of limited resources. Cooperative techniques such as joint coding and joint detection appear to be very promising in optimizing system performance under constrained resources. In [1], we studied data fusion in a multi-target radar sensor network.

A lot prior research in data fusion are based on the assumption of lossless communication, i.e., the information sent from local sensors is perfectly recovered at the fusion center. Other researchers

addressed the problem of distributed detection with constrained system resources, most of which provided the solutions to optimize sensor selection. In another hand, decision fusion with non-ideal communication channels is studied at both fusion center level and at the sensor level. Channel-aware decision fusion rules have later been developed using a canonical distributed detection system where binary decisions from multiple parallel sensors are transmitted through fading channels to a fusion center. Lin extended the channel aware decision fusion rules to multi-hop WSNs. The above results, however, are mostly obtained based on one target or one event detection which is not applicable to multi-target situations. Furthermore, in a radar sensor system, when clutter, the unwanted echoes from the natural environment is much larger than receiver noise, detection can be quite different from that when the noise is dominant.

In [1], we presented the theoretical formulation of decision fusion problem for multi-target case. The objective of this work is to extend the channel-aware decision fusion rules developed to multi-target radar sensor system. We made the assumption that the multiple targets are stationary targets in clutter. We used Rayleigh target fluctuation model and Gaussian clutter as our first stage study. Particularly, we assume the radar when receiving, is a constant false alarm receiver (CFAR). CFAR automatically raises the threshold level to keep clutter echoes and external noise from overloading, which performs as a good rejection of clutter.

2 UWB Sensor Networks in Hostile Environment

Since 2002 there has been great increasing popularity of commercial applications based on Ultra WideBand. This has ignited interest in the use of this technology for sensor networks. Actually, UWB systems have potentially low complexity and low cost; have a very good time domain resolution, which facilitates location and tracking applications. So, UWB wireless sensor networks are promising.

One of the most important applications of WSN is in battle field, which means there exist hostile interferences. Frequency Hopping (FH) technology offers an improvement in performance when the communication systems is attacked by hostile interference and reduce the ability of a hostile observer to receive and demodulate the communication signal. This kind of inherent property finds it a potential position in the UWB sensor networks. Based on the UWB definition released by the FCC (FCC, 2002) that a signal is UWB if its bandwidth exceeds 500 MHz, the overall 7.5 GHz bandwidth, that is, frequencies in the range 3.1 GHz to 10.6 GHz as based on the FCC ruling, can be split into smaller frequency bands of at least 500 MHz each. This character inspired us to design a hybrid FH/TH-PPM UWB system in [2].

In [2], we studied the performance of a FH/TH UWB sensor network with hostile partial-band (PB) tone interference and multi-user interferences. Interferences due to the hostile environment and the Multi-User Access are critical factors affecting performance of the Wireless Sensor Networks. There is clearly a need of a system that can survive from the severe interference. In this paper, an analysis is also made for precisely calculating the bit error rates in the presense of multitone/pulse (tone in frequency domain and pulse in time domain) interference and Multi-User Interference.

3 Energy Consumption and Latency Estimation Based on Statistical Modeling and ML Detection

In [3], we modeled the end-to-end distance for given hops in Wireless Sensor Networks. We derived that the single-hop distance follows the distribution $2r/R^2$, where R is the transmission range. The end-to-end distance shows beta distribution for two hops, and approaches Gaussian distribution

when the number of hops is beyond three. As an application example, we proposed Statistical Distance Estimation, which shows less distance error than Hop-TERRAIN and APS (Ad hoc Positioning System). Our results are also applicable to other applications for Wireless Sensor Networks.

Based on this theoretical observation, we applied it to energy consumption and latency estimation based on the number of hops prediction[4][5]. The potential applications of WSN, such as environment monitor, often emphasize the importance of location information. Accordingly geographic routing was proposed to handle such requirement. Most likely, a packet is not routed to a specific node, but a given location. An interesting question arises as "how many hops does it take to reach a given location?" The prediction of the number of hops is important not only in itself but also in helping estimating the latency and energy cost, which are both important to the viability of WSN.

The question could become very simple if the sensor nodes are manually placed. However, if sensor nodes are deployed in a random fashion, which is the case for most potential application, the answer is beyond the reach of simple geometry. The stochastic nature of the random deployment calls for a statistical study. A natural and obvious estimation would be dividing the distance by the average inter-node distance (i.e., the average single-hop distance). However, such estimation may be unable to provide the required accuracy. We propose making a Maximum Likelihood (ML) decision,

$$H = \arg\max_{max} f(H|r), H = 1, 2, 3, \cdots . \tag{1}$$

Considering

$$f(H|r) = \frac{f(H,r)}{f(r)}, \tag{2}$$

the decision rule can be translated into

$$H = \arg\max_{max} f(H,r), \tag{3}$$

where $f(H,r)$ is also called objective function.

Generally, for $H = n$, we have

$$p(H_n, r_n|r_1, r_2, \cdots, r_n - 1) = \begin{cases} e^{-\lambda\pi[(R+\sum_{i=1}^{n-1} r_i)^2 - (\sum_{i=1}^{n} r_i)^2]} - e^{-\lambda\pi[(R+\sum_{i=1}^{n-1} r_i)^2 - (\sum_{i=1}^{n-1} r_i^2]} & \\ & R < r \leq nR \\ 0 & otherwise \end{cases} \tag{4}$$

and

$$p(H_n, r_n) = \int_R^{(n-1)R} \int_R^{(n-2)R} \cdots \int_0^R p(H_n, r_n|r_1, r_2, \cdots, r_n - 1) \\ f(H_{n-1}, r_{n-1}|r_1, r_2, \cdots, r_n - 2) \cdots f(H_1, r_1) dr_1 \cdots dr_{n-2} dr_{n-1} \tag{5}$$

Theoretically, we can take derivative of (5) with respect to r to obtain the objective function, use (3) to decide the most likely H given r and give the probability of error for such a decision. However, (5) is awkward to evaluate and the computational cost could limit the applicability of such a decision scheme. Therefore, we propose Attenuated Gaussian Approximation for the joint pdf based on the histogram collected from the simulations. The skewness and kurtosis tests show a good fit between our approximation and the simulation data. Also, we found the following properties.

1. $\sigma_n \approx \sigma_{n-1}$, which means the neighboring joint pdf's have similar spread.
2. $m_n - m_{n-1} \approx m_{n+1} - m_n$, which means the joint pdf's are evenly spaced.
3. $3 < \frac{m_n - m_{n-1}}{\sigma_n} < 5$, which means the overlap between the neighboring joint pdf's is small but not negligible. (As a rule of thumbs, $Q(3)$ is considered relatively small and $Q(5)$ is regarded negligible.)
4. $\frac{m_n - m_{n-2}}{\sigma_n} \gg 5$, which means the overlap between the non-neighboring joint pdf's is negligible.
5. $\alpha < 1$. For large density λ, $\alpha \to 1$. Along with Property 1, this tell us that the neighboring joint pdf's have nearly identical shape.

These properties visibly simplify the decision rule and error analysis.

$$\text{we decide } H = \hat{n} \text{ if } d_{\hat{n}-1} < r \leq d_{\hat{n}}, \tag{6}$$

where d_n is the decision boundary given by

$$d_n = \frac{\sigma_n^2 m_{n+1} + \sigma_{n+1}^2 m_n}{\sigma_n^2 + \sigma_{n+1}^2} \tag{7}$$

And the probability of error is

$$p(\epsilon) \approx \alpha^2 Q(\frac{m_3 - m_2}{2\sigma_2}) + \sum_{n=3}^{\infty} \alpha^n [Q(\frac{m_n - m_{n-1}}{2\sigma_n}) + Q(\frac{m_{n+1} - m_n}{2\sigma_n})] \tag{8}$$

Based on this result, for latency estimation, a good estimator of the total latency of a l-bit message is

$$l[T_{tx} + (\hat{n} - 1)(T_{tx} + T_{rx}) + T_{rx}] = l\hat{n}(T_{tx} + T_{rx}) \tag{9}$$

And for energy cost, we have

$$\bar{E}_{total}(l, r) = 2\hat{n}lE_{elec} + 2\epsilon_{fs}\Delta \sum_{1}^{\hat{n}} m_n, \tag{10}$$

where E_{elec} is the unit energy consumed by the electronics to process one bit of message, ϵ_{fs} is the amplifier factor for free-space path loss.

4 Self-Organization for Underwater Acoustic Sensor Networks

In [6], we are concerned with the optimal cluster size in underwater acoustic sensor networks. An UnderWater Acoustic Sensor Network (UW-ASN) can be thought of as an *ad hoc* network consisting of sensors linked by an acoustic medium to perform distributed sensing tasks. To achieve this objective, sensors must self-organize into an autonomous network which can adapt to the characteristics of the underwater environment. UW-ASNs share many communication technologies with traditional ad hoc networks and terrestrial wireless sensor networks, but there are some vital differences such as limited energy and bandwidth constraint, thus the protocols developed for traditional wireless ad hoc networks are not necessarily well suited to the unique features of WSNs. When a wireless sensor may have to operate for a relatively long duration on a tiny battery, energy efficiency becomes a major concern. Another issue in shallow water communications is that due to the limit

of bandwidth in shallow water communications, multi-hop communication could introduce heavy interference between cluster members, therefore, each sensor in a cluster communicate directly to its cluster head and intra-cluster communication should be coordinated by the cluster head in order to maximize the bandwidth usage. We showed that the optimal cluster size is also relevant to the working frequency of the acoustic transmission. Furthermore, we showed that assigning working frequency to cluster members according to their distances to the cluster head could minimize the energy consumption. Clustering has been widely used in pattern recognition, and we use it to obtain the energy-efficient organization for UW-ASN. Consider a heterogeneous UW-ASN, in which the low-capacity sensors serves as cluster members and are randomly distributed, and the high-capacity sensors serve as cluster heads and are manually positioned. If we obtain the optimal cluster size, then the required number of high-capacity sensors and their ideal positions can also be determined. If we assume the high-capacity sensors have virtually unlimited energy reserve compared to the low-capacity ones, only the energy consumption of the low-capacity sensors need to be counted. Under such circumstances, we derived the optimum cluster size, and we observed that the frequency allocation could be designed to minimize the energy consumption. Although the optimum frequency allocation is still elusive, we proposed an objective function, which can be used to seek such a frequency allocation algorithm.

5 Cross-Layer Design in Mobile Ad Hoc Networks

The demand for Quality of Service (QoS) in mobile ad hoc networks is growing in a rapid speed. To enhance the QoS, in [7][8], we considerred the combination of physical layer and data-link layer together, a cross-layer approach. We proposed to use Fuzzy Logic System (FLS) for packet transmission delay analysis and prediction. We applied both a singleton type-1 FLS and an interval type-2 FLS for the analysis and prediction. Theoretical analysis and simulation data demonstrate that a type-2 fuzzy membership functions (MFs), i.e., the Gaussian MFs with uncertain variance is most appropriate to model Bit Error Rate (BER). Recent research and simulation data discovered that the lognormal distribution could match for the MAC layer service time. So we could also use the Gaussian MFs to mode the logarithm of MAC layer service time. We used Guassian membership functions (MFs) to represent the antecedents and the consequent and two FLSs: a singleton type-1 FLS and an interval type-2 FLS are designed to predict the packet transmission delay based on the BER and MAC layer service time. After that, we could adjust the transmission power according to the predicted packet transmission delay. Therefore average delay, energy consumption and throughput performances will change. We implemented the simulation model using the OPNET modeler. For type-1 FLS, We chose Gaussian membership function as antecedents; for interval type-2 FLS, we used Gaussian primary MF's with fixed mean and uncertain STD for the antecedents. The steepest decent algorithm was used to train all the parameters based on the 300 data sets. After training, the rules were fixed, and we tested the FLS based on the remaining 300 data sets. We summarized the root-mean-square-errors (RMSE) between the estimated packet transmission delay and the actual delay. Simulation result showed that the interval type-2 FLS performs better than the type-1 FLS. And we used the outcomes of FLS predictors to control the transmission powers. We assume we could know the actual transmission delay as ideal algorithm before we adjusted the transmission power. So we could use he simulation result to compare the performances of three algorithms (type-2 FLS, type-1 FLS, and ideal case). For average delay prediction, a type-2 FLS is better than the type-1 FLS, and the idea case is the best among the three. For energy efficiency, the type-2 FLS is better than the type-1 FLS, and the idea case is the lower bound. For throughput, the type-2 FLS is better than the type-1 FLS, and the idea case was set as the upper bound.

6 Energy Efficient Query Processing in Data-Centric Wireless Sensor Networks

The widespread deployment of sensor nodes is transforming the physical world into a computing platform. Sensor nodes not only respond to physical signals to produce data, they also embed computing and communication capabilities. They are thus able to store, process locally and transfer the data they produce. From a data storage point of view, wireless sensor network (WSN) can be regarded as a kind of database, distributed sensor database system (DSDS). DSDS, compared to traditional database systems, stores data within the network and allow queries to be injected anywhere through query processing operators in the network. Even though data query processing methods have been studied extensively in traditional database systems. Few of them can be directly applied into sensor database systems due to the characteristics of sensor networks: decentralized nature of sensor networks, limited computational power, imperfect information recorded, and energy scarcity of individual sensor nodes.

The goal of monitoring through sensor nodes is to infer information about objects from measurements made from remote locations. Since inference processes are always less than perfect, there is an element of uncertainty regarding the answers. When viewed from this perspective, the problem of uncertainty, which stands for the quality of query answers, is central to monitoring applications. Thus, to build useful information systems, it is necessary to learn how to represent and reason with imperfect information. Considerring quality requirement and power constraint, we made analysis and classification on sources of imperfect information and energy waste for an environmental temperature monitoring application in [9]. In the context of our analyzing and understanding of query answer uncertainty, we utilized image chain method to express the nature and the source of uncertainty on temperature information derived from remote sensing. There are three main sources of imperfect information: measurement quality of nodes, which introduces uncertainty and imprecise information into query answers, point spread function of nodes, which introduces ambiguity into query answers, and link quality, which introduces incompleteness into query answers. Fixing other conditions, such as node density, communication range, sensing range and network coverage, we change those imperfect information sources separately to check the influences of those imperfect information sources on the correctness of query answers. Simulation results showed that with measurement errors, misrepresent errors, or missing information increased, the errors included in query answers are obviously increased and therefore the confidence of query answers is reduced. In energy waste source, we considerred that within a network, not all available nodes provide useful information that improves the accuracy of final results. Furthermore, some information might be redundant because nodes close to each other would have similar data. From this prospect, collecting raw readings from all nodes to front-end nodes involves large amounts of raw readings, which will lead to shorter lifetime, especially for energy-limited WSNs.

In additions, we proposed a quality-guaranteed and energy-efficient algorithm (QGEE) for sensor database systems in [9]. We employed an in-network query processing method to task sensor networks through declarative queries. In query answer confidence control, we modeled the problem-determining optimal locations for a query, as a k-partial set cover problem and adaptively determine the value of the radius of disks according to users' quality requirements instead of fixing it when considering the influence of PSF of nodes on uncertainty of query answers. We formed our query vector space model (QVSM) to express the correlation between a query and all candidate nodes. We chose location, measurement quality and remaining battery capacity of nodes as the elements of QVSM. The decision-which nodes are active to respond queries-is based on their query correlation. That is, nodes with highest query correlation among their one-hop neighbors are chosen

to participate in related query processing. In QGEE, active nodes are chosen locally leveraging cooperation among nodes. Besides those, we also controlled the sample size to ensure the sampling distribution of estimators meet users' pre-specified target precision, and utilized a multipath, power-aware and mobility aware routing scheme to control information collection. Bases on these strategies, our QGEE can adaptively form an optimal query plan in terms of energy efficiency and query quality. That is, only a subset of nodes within a network will be chosen to acquire readings or samples corresponding to the fields or attributes referenced in queries. The goal of our approach is to reduce interference coming from measurements with extreme errors and to minimize energy consumption by providing service that is considerably necessary and sufficient for the need of applications. Moreover, we employed probabilistic method to formulate the distribution of imperfect information sources in terms of probability distribution function (PDF). Since a statistic measurement on samples can rarely, if ever, be expected to be exactly equal to a parameter, it is important that a statement describing the precision accompanies estimation. We utilized confidence intervals to state both how close the value of a statistic being likely to be value of a parameter and the chance of being close. Hence, using our QGEE scheme, probabilistic query answers can be acquired on uncertain data. The probabilities to an answer allow users to place appropriate confidence in it. The simulation results demonstrated that, compared with the query processing algorithm which has no query optimization, our algorithm can reduce resource usage about 50% on processing same number of queries, the frame loss rate about 20%. The simulation results for MAXIMUM, MINIMUM and AVERAGE aggregation operation showed that our QGEE can successfully obtain suitable confidence intervals to guarantee the true value of query answers locating within this interval with a probability, which is equal to or larger than the pre-specified probability by users according to various query answer confidence requirement.

7 Energy Efficient Asynchronous MAC protocol for UWB Systems

Ultra wideband (UWB) technology offers unique advantages for wireless communications: precise location-timing capabilities, low power, low complexity, and low cost. However, no existing wireless network successfully takes advantage of the properties of this technology because of the lack of an efficient medium access control (MAC) technology. Multi-antenna systems have been studied intensively in recent years due to their potential to dramatically increase the channel capacity in fading channels. It has been shown that multi-input-multi-output (MIMO) systems can support higher data rates under the same transmit power budget and bit-error-rate performance requirements as a single-input single-output (SISO) system. However, direct application of multi-antenna techniques to sensor node impractical due to the limited physical size of a sensor node, which typically can only support a single antenna. In recent years, virtual MIMO conception have been proposed, which allows individual single-antenna nodes to cooperate on information transmission and/or reception. A cooperative MIMO system can be constructed such that energy-efficient MIMO schemes can be deployed.

In [10], we proposed an energy-efficient MAC protocol: asynchronous MAC protocol for UWB communications (A-MAC-UWB). From energy efficiency aspect, since, for UWB communication, circuit energy consumption is comparable to or even dominates the transmission energy since UWB is low power consumption i.e., a bit rate of 100Kpbs over 5 meters with no more than 1mW power consumption, we utilize virtual MIMO technology to reduce the idle time for waiting for sending/receiving next symbol. Virtual MIMO strategy can also increase the data rate, and substitute space diversity for time diversity to improve system performance. Besides this, we also exploit

multiple working models: sleep and active models. The idle time for waiting to transmit/receive next data packet is reduced through enforcing nodes into sleep mode to archive energy reservation. But the latency of data packets is traded off.

In addition, since UWB can support multiple access, our A-MAC-UWB protocol does not use mutual exclusion (as is commonly done by random access or TDMA protocols) but, in contrast, allows interference to occur and adapt to it. That is, competing sources are allowed to send concurrently, causing rate reduction instead of collisions. Slot ALOHA scheme is used in A-MAC-UWB. One of the advantages for our algorithm is removing the overhead of control packets for carrier sensing to avoid collision, such as RTS/CTS for CSMA/CA scheme, but also ensuring successful transmission. For multiuser interference, we set a model to adaptively adjust the data rate to ensure certain SNR at receiver side, since a Shanon capacity of a multipath fading additive white Gaussian noise (AWGN) wideband channel is a linear function of SNR. We formulate the relationship between probability of bit error and signal to noise and multiuser interference ratio (SNIR).

For optimum design for power on/off phase duration, we considerred the traffic whose arrival interval follows heavy tailed distribution, instead of Poisson distribution. Based on that, we acquired the probability density function (pdf) for power off phase duration for our algorithm. We also set up a objective function to carry out not only extend the power off duration as long as possible, but also ensure as less as possible chance for buffer overflowing for nodes within a cluster. For power on duration design, we also set up an object function to choose the highest date rate, which can ensure the BER acquired at receiver side to satisfy with the requirement. Compared with our previous work, we tried to find a better method to trade off between data packet latency and energy reservation.

References

[1] H. Shu, Q. Liang, " Data Fusion in a Multi-Target Radar Sensor Network," to be submitted to *IEEE Transactions on Aerospace and Electronic Systems.*

[2] L. Wang, Q. Liang, " UWB Sensor Networks in Hostile Environment: Interference Analysis and Performance Study," submitted to *EURASIP Journal on Wireless Communications and Networking.*

[3] L. Zhao, Q. Liang "Modeling End-to-end Distance for Given Number of Hops in Wireless Sensor Networks ," submitted to *IEEE Wireless Communications and Networking Conference*, April 2006, Las Vegas, NV.

[4] L. Zhao, Q. Liang "Resource Allocation and Latency Estimation in Wireless Sensor Networks Using Maximum Likelihood Decision ," submitted to *IEEE Transactions on Computers.*

[5] L. Zhao, Q. Liang "Resource Allocation and Latency Estimation in Wireless Sensor Networks Using Maximum Likelihood Decision ," submitted to *IEEE Intl Conference on Information Processing in Sensor Networks*, Nashville, TN, April 2006.

[6] L. Zhao, Q. Liang "Optimal Cluster Size for Underwater Acoustic Sensor Networks," to be submitted to *IEEE Globecom*, Nov 2006, San Francisco, CA.

[7] X. Xia, Q. Liang "Cross-Layer Optimization for Mobile Ad Hoc Networks Using Fuzzy Logic Systems," submitted to *IEEE Wireless Communications and Networking Conference*, April 2006, Las Vegas, NV.

[8] X. Xia, Q. Liang "Cross-Layer Optimization for Mobile Ad Hoc Networks Using Fuzzy Logic Systems," to be submitted to *IEEE Trans on Fuzzy Systems.*

[9] Q. Ren, Q. Liang "A Distributed Query Processing Algorithm for Wireless Sensor Networks," submitted to *IEEE Wireless Communications and Networking Conference*, April 2006, Las Vegas, NV.

[10] Q. Ren, Q. Liang "An Asynchronous Energy-Efficient MAC Protocol for Ultra-wideband Communications over Wireless Sensor Networks," to be submitted to *IEEE Globecom*, Nov 2006, San Francisco, CA.

Data Fusion in a Multi-Target Radar Sensor Network

Haining Shu and Qilian Liang

Department of Electrical Engineering

University of Texas at Arlington

Arlington, TX 76019-0016 USA

E-mail: shu@wcn.uta.edu, liang@uta.edu

Abstract

In this paper, we consider the decision fusion of Rayleigh fluctuating targets in multi-radar sensor networks. Decision fusion and data fusion in Wireless Sensor Networks (WSNs) has been widely studied in order to save energy. Radar system as a special sensor network, when implemented for battlefield surveillance, faces bandwidth constraint in real-time applications instead of energy restriction. A reliable detection of multiple targets in clutter is perhaps the most important objective in such an echo-location system. In this work, we study the decision fusion rules of multiple fluctuating targets in multi-radar (MT-MR) sensor networks. The MT-MR decision fusion problem is modeled as a multi-input multi-output (MIMO) system. We assume that each radar makes binary decision for each target from the observation, i.e. if the target is present or not. We derive our *MIMO fusion* rules based on the target fluctuation model and compare against the optimal likelihood ratio method (LR), maximum ratio combiner (MRC) and equal gain combiner (EGC). Simulation results show that the *MIMO fusion* rules approach the optimal-LR and outperforms MRC and EGC at high signal to clutter ratio (SCR).

Index Terms : wireless sensor networks, radar, target fluctuation, clutter, MIMO, data fusion, Rayleigh, optimal likelihood, maximum ratio combiner, equal gain combiner

1 Introduction

Wireless sensor networks (WSN) have attracted growing interest in various applications, especially in the area of battlefield surveillance, health care and telemedicine, environmental and habitat monitoring. Radar as a powerful sensor system, has been employed for the detection and location of reflecting objects such as aircraft, ships, vehicles, people and natural environment. By radiating energy into space and detecting the echo signal reflected from an object or target, the radar system can determine the presence of a target. Furthermore, by comparing the received echo signal with the transmitted signal, the location of a target can be determined along with other target related information [1].

Conventional radar system operates as a pure independent entity. While in a resource-constrained WSN, such detached operation may lead to deteriorated performance and waste of limited resources. Collaborative signal and information processing over the network is a very promising area of research and is related to distributed information fusion [2]. Important technical issues include the degree of information sharing between sensors and how sensors fuse the information from other sensors. Processing data from more sensors generally results in better performance but also requires more communication resources. Similarly, less information is lost when communicating information at a low level (e.g., raw data), but requires more bandwidth. Therefore, it is a tradeoff between system performance and resource utilization in collaborative information processing and data fusion.

A lot of prior research in data fusion are based on the assumption of lossless communication, i.e., the information sent from local sensors is perfectly recovered at the fusion center. For example, in [3] and [4], Vashney *et. al* investigated the optimum fusion rules under the conditional independence assumption. Other papers [5, 6] addressed the problem of distributed detection with constrained system resources, most of which provided the solutions to optimize sensor selection. However, this lossless communication assumption is not practical for many WSNs where the transmitted data suffers from channel fading and multi-user interference. In another hand, decision fusion with non-ideal communication channels are studied at both fusion center level [7, 8] and at the sensor

level [9, 10]. In [8], Thomopoulos and Zhang derived the optimal thresholds by assuming a simple binary symmetric channel between sensors and the fusion center. Their method is quite simple but requires global knowledge of the entire system. In [7], channel-aware decision fusion rules have been developed using a canonical distributed detection system where binary decisions from multiple parallel sensors are transmitted through fading channels to a fusion center. Later, Lin *et. al* [11] have extended the channel aware decision fusion rules to more realistic WSN models that involve multi-hop transmissions. The above results, however, are mostly obtained based on one target or one event detection which is not applicable to multi-target situations. Furthermore, in a radar sensor system, when clutter, the unwanted echoes from the natural environment is much larger than the receiver noise, detection can be quite different from that when the noise is dominant.

The objective of this work is to derive the decision fusion rules of multiple fluctuating targets in multi-radar (MT-MR) sensor networks. We focus on the detection decision performance of fused data with the existence of clutter. The MT-MR decision fusion is modeled as a multi-input multi-output (MIMO) system. We present the theoretical formulation of the MIMO decision fusion problems. We make the assumption that the multiple targets are stationary targets embedded in clutter. Rayleigh target fluctuation model and Gaussian clutter are used in our first stage study. Particularly, we assume that the radar in our scenario, is a constant false alarm receiver (CFAR) when receiving. CFAR automatically raises the threshold level to keep clutter echoes and external noise from overloading, which performs as a good rejection of clutter.

The remainder of this paper is organized as follows. In the next section, we introduce the concept of clutter and target fluctuation model in radar sensor system. In Section 3, we briefly overview the previous work on fusion rules designed for a canonical parallel distributed detection system with single hop transmission between sensor nodes and fusion center. In Section 4, we present our MIMO decision fusion model for multi-target multi-radar sensor networks. Simulation and performance analysis are presented in Section 5. Section 6 concludes this paper.

2 Target Detection in Radar Sensor System

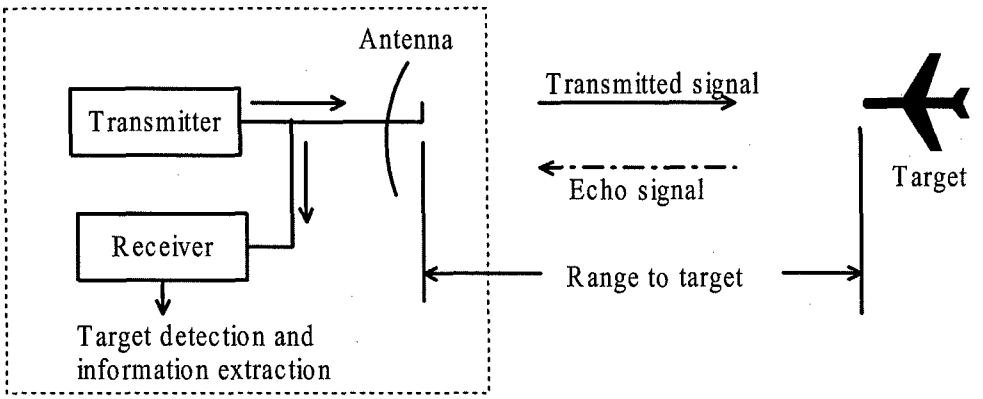

Figure 1: Basic Principle of Radar System

The basic principle of radar [1] is illustrated in Fig. 1. An electromagnetic signal is generated by the transmitter and is radiated into space by antenna. A portion of the transmitted energy is intercepted by the target and reradiated in various directions. The reradiation directed back towards the radar is collected by the radar antenna, which delivers it to a receiver. There it is processed to detect the presence of the target and determine its location. A single antenna is usually used on a time-shared basis for both transmitting and receiving when the radar waveform is a repetitive series of pulses. The range, or distance, to a target is found by measuring the time it takes for the radar signal to travel to the target and return back to the radar. The target's location in angle can be found from the direction the narrow-beamwidth radar antenna points when the received echo signal of maximum amplitude. If the target is in motion, there is a shift in the frequency of the echo signal due to the doppler effect. This frequency shift is proportional to the velocity of the target relative to the radar. The doppler frequency shift is widely used in radar as the basis for separating desired moving targets from fixed clutter echoes reflected from the natural environment such as land, sea or rain. Radar can also provide information about the nature of the target being observed.

In active radar sensor networks, the received data usually consists of three parts: white thermal noise, clutter scattered by the land environment, and if a target is present, a reflected or reradiated

version of the transmitted signal [12]. That is, we have

$$y^{(t)} = \alpha^{(t)} s^{(t)} + n^{(t)} + \omega^{(t)} \tag{1}$$

in which $s^{(t)}$ and $y^{(t)}$ are the transmitted and received signals, respectively. $\alpha^{(t)}$ is the target cross section or radar cross section (RCS). It is assumed that $n^{(t)}$ is additive noise and $\omega^{(t)}$ is the returned clutter, a distorted version of the transmitted signal $s^{(t)}$. In the work presented here, it is assumed that the received clutter is much larger than the white thermal noise, i.e $\omega^{(t)} >> n^{(t)}$. Thus (1) turns to

$$y^{(t)} \approx \alpha^{(t)} s^{(t)} + \omega^{(t)} \quad (when \;\; \omega^{(t)} >> n^{(t)}) \tag{2}$$

Classical radar equation takes target cross section or radar cross section (RCS) to determine the power density returned to the radar for a particular power density incident on the target. Nevertheless, the scattering of electromagnetic energy from a target is a rather complicated phenomenon, which depends on a number of factors such as target geometry, size, shape, aspect, altitude with respect to radar antenna etc. Therefore, it has been advantageous to model the target RCSs as a random variable. Some common fluctuation models are now available in the open literature, i.e. Swerling chi , lognormal, Rayleigh, Weibull as a compound Rayleigh distribution, Shadowed Rice target etc. In this work, we treat the target fluctuation as Rayleigh distribution which has the probability density function (pdf) as

$$f_\nu(\nu) = \frac{\nu}{\sigma_c^2} \exp\left(-\frac{\nu^2}{2\sigma_c^2}\right) \tag{3}$$

Where $2\sigma_c^2$ is the mean square value of the envelope ν.

Clutter is the unwanted echoes from the natural environment such as land, sea, rain, birds, insects etc. Clutter can be distributed in spatial extent in that it is much larger in physical size than the radar resolution cell. There are also point or discrete clutter echoes that produce large backscatter. Because of the highly variable nature of clutter echoes it is often described by a

probability density function. Some clutters have similar distributions as the target fluctuation model, e.g., Gaussian, Rayleigh, log-Normal and Weibull. Nevertheless, other distributions have been proposed to describe the special statistics of clutter including K-distribution, contaminated normal, gamma and log-Weibull. For the first stage of this work, we set the returned clutter follows Gaussian distribution with zero mean.

3 Review of Previous Decision Fusion Rules

In a single target, single hop sensor network, the typical parallel fusion structure in a flat fading channel is depicted in Fig. 2. The received signal at the fusion center from kth sensor is $y_k = h_k u_k + n_k$, where h_k is the channel fading envelope and n_k is the zero-mean additive Gaussian noise with variance σ^2. K sensors collect data generated according to either H_0 (there is no target present) or H_1 (there is target present) and transmit these decisions over fading and noisy channels to a fusion center. The fusion center tries to decide which hypothesis is true based on the received data y_k from all k.

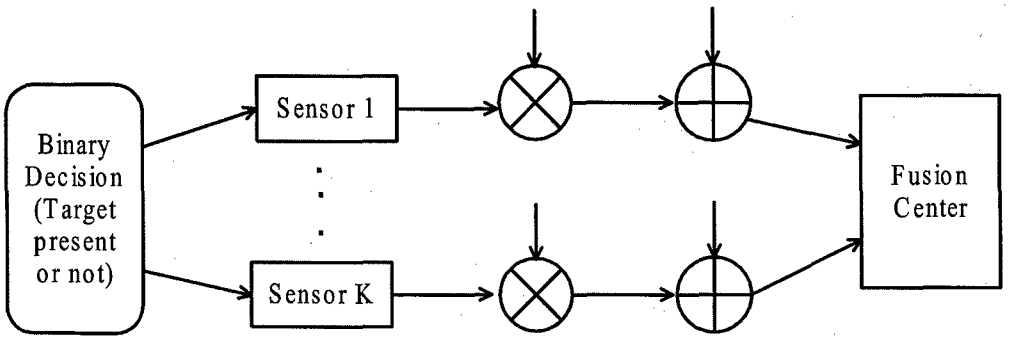

Figure 2: Single-target, single-hop decision fusion model

Assume that the kth local sensor makes a binary decision $u_k \in \{+1, -1\}$, with false alarm and detection probability P_{fk} and P_{dk} respectively. That is, we have $P_{fk} = P[u_k = 1|H_0]$ and $P_{dk} = P[u_k = 1|H_1]$. Several decision fusion rules have been developed based on the above model in [11]. Throughout this work, we use $\Lambda^{(s)}$ to denote the fusion statistics for the single hop, single

target transmission model.

- Optimal LR-based fusion statistic using complete prior knowledge. Assuming complete channel knowledge, the optimal LR-based fusion statistic was derived as

$$\Lambda_1^{(s)} = \prod_{k=1}^{K} \frac{P_{dk}\psi_k^{(+)} + (1 - P_{dk})\psi_k^{(-)}}{P_{fk}\psi_k^{(+)} + (1 - P_{fk})\psi_k^{(-)}} \tag{4}$$

where $Y = [y_1, ..., y_k]^T$ is a vector containing observations received from all K sensors, $\psi_k^{(+)} = e^{-((y_k - h_k)^2/2\sigma^2)}$ and $\psi_k^{(-)} = e^{-((y_k + h_k)^2/2\sigma^2)}$.

- LR-based fusion rules using only fading statistics for Rayleigh fading channel. Implementing the optimal LR test as in (4) requires that all a priori information, including the instantaneous channel gains. Under the Rayleigh fading model, the LR-based fusion statistic using only the fading parameter is summarized below

$$\Lambda_2^{(s)} = \prod_{k=1}^{K} \frac{P_{dk}\Psi_k^{(+)} + (1 - P_{dk})\Psi_k^{(-)}}{P_{fk}\Psi_k^{(+)} + (1 - P_{fk})\Psi_k^{(-)}} \tag{5}$$

where $\Psi_k^{(+)} = 1 + \sqrt{2\pi\gamma} y_k e^{(\gamma^2 y_k^2/2)} Q(-y_k\gamma)$, $\Psi_k^{(-)} = 1 - \sqrt{2\pi\gamma} y_k e^{(\gamma^2 y_k^2/2)} Q(y_k\gamma)$ and $\gamma = (\sigma_c/\sigma_n\sqrt{\sigma_c^2 + \sigma_n^2})$ with $2\sigma_c^2$ being the mean square value of the fading channel, σ_n^2 is the noise variance, and $Q(\cdot)$ is the complementary distribution function of a standard Gaussian random variable.

- A two-stage approximation using the Chair-Varshney fusion rule. A direct alternative to the above LR-based fusion rules is to consider the information transmission and decision fusion as a two-stage process: first y_k is used to infer about u_k: then, the estimation of u_k are employed in the optimum fusion rule. Given the model in Fig. 2, the maximum likelihood (ML) estimation for u_k is $\hat{u_k} = sign(y_k)$. Applying the fusion rule derived in [11], the Chair-Varshney fusion rule is obtained as

$$\Lambda_3^{(s)} = \sum_{y_k<0} \log\left(\frac{1-P_{dk}}{1-P_{fk}}\right) + \sum_{y_k>0} \log\left(\frac{P_{dk}}{P_{fk}}\right) \tag{6}$$

- Fusion statistics using a maximum ratio combiner (MRC). In the low SNR regime, if the local sensors are identical,i.e., P_{dk} and P_{fk} are the same for all ks, then $\Lambda_1^{(s)}$ reduces to a form analogous to an MRC

$$\Lambda_4^{(s)} = \frac{1}{K}\sum_{k=1}^{K} h_k y_k \tag{7}$$

- Fusion statistics using an equal gain combiner (EGC). At low SNR regime, if the local sensors are identical,i.e., P_{dk} and P_{fk} are the same for all ks, then $\Lambda_2^{(s)}$ reduces to a form analogous to an EGC

$$\Lambda_5^{(s)} = \frac{1}{K}\sum_{k=1}^{K} y_k \tag{8}$$

Among the above five fusion rules, $\Lambda_1^{(s)}$ requires complete channel knowledge and provides uniformly the most powerful detection performance. At low SNR, the MRC statistic provides the best performance among the three suboptimum fusion rules; while at high SNR, the Chair-Varshney fusion rule outperforms the MRC and the EGC statistics. The EGC statistic, however, provides better performance over a wide range of SNR than the MRC statistic and the Chair-Varshney fusion rule and requires the least amount of prior information.

4 MIMO decision fusion model for multi-target multi-radar sensor networks

In our scenario, it is assumed that there are multiple radar sensors and multiple stationary targets in the field. A radar detects the presence of a target and generates the decision data according to two hypothesis: H_0 : there is no target present and H_1 : there is target present. Each decision data is transmitted to the fusion center, normally a radar sensor as well. In a multi-hop radar sensor network, the decision data is relayed via several radars to reach the fusion center. When there are multiple radar sensors and multiple targets in the field, the data fusion problem can be roughly modeled as a Multi-Input Multi-Output (MIMO) fusion problem. In this paper, we assume the radar sensors are disparate, geographically dispersed in the field such that the radar observations or decisions are spatially independent. Fig. 3 illustrates an example of single-hop decision fusion problem.

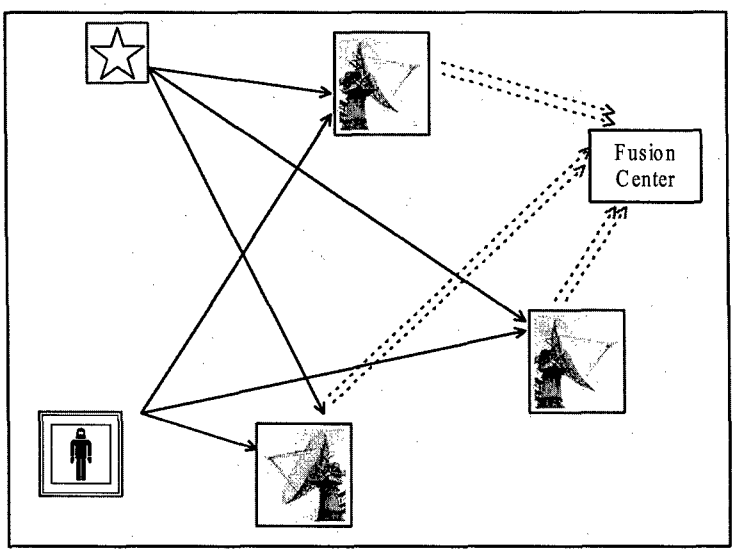

Figure 3: MIMO fusion model

Let M denote the number of radar sensors and N be the number of targets. The received signal $Y^{(t)}$ at the fusion center at time t is a $N \times M$ matrix.

$$\begin{bmatrix} y_{11}^{(t)} & \cdot & \cdot & \cdot & y_{M1}^{(t)} \\ \cdot & \cdot & \cdot & \cdot & \cdot \\ \cdot & \cdot & \cdot & \cdot & \cdot \\ \cdot & \cdot & \cdot & \cdot & \cdot \\ y_{1N}^{(t)} & \cdot & \cdot & \cdot & y_{MN}^{(t)} \end{bmatrix} \tag{9}$$

We assume that the radar sensors are geographically dispersed, detection decisions are made at each separate local radar. The element $y_{ij}^{(t)}$ of (9) is the decision (target present or absent) of the jth target from the ith radar sensor. $y_{ij}^{(t)}$ can be represented as

$$y_{ij}^{(t)} = \alpha_{ij}^{(t)} \cdot s_{ij}{}^{(t)} + \omega_{ij}^{(t)} \tag{10}$$

Observe that in [11], the researchers assume that both the false alarm P_f and probability of detection P_d are fixed and identical for all local sensors. Moreover there is no correlation between the false alarm P_f and probability of detection P_d. In radar system however, this assumption is very unpractical especially in the heavy clutter situation. One method to suppress the heavy clutter is to use *constant false alarm rate* (CFAR) receiver. CFAR automatically raises the threshold level to keep clutter echoes and external noise from overloading the automatic tracker with extraneous information. In our study, we assume the receivers of all radar sensors are CFAR which implies that though the false alarm rate is a constant, the probability of detection of each local radar sensor varies. We use P_f as the fixed false alarm rate and P_{di} to denote the distinct probability of detection at radar sensor i throughout this work.

We next derive the MIMO decision fusion rules for the multi-target radar sensor networks starting from the single-hop radar sensor networks.

4.1 Decision fusion rule in multi-target, single-hop radar sensor networks

- Assume we have complete knowledge of the target fluctuation coefficients, the optimal LR-based fusion rule for the jth target was derived as

$$\Lambda_j^{(1)} = \prod_{i=1}^{M} \frac{P_{di}\psi_{ij}^{(+)} + (1-P_{di})\psi_{ij}^{(-)}}{P_f\psi_{ij}^{(+)} + (1-P_f)\psi_{ij}^{(-)}} \quad j = 1, ..., N \tag{11}$$

Complete decision vector for N targets are denoted as $\underline{\Lambda}^{(1)} = [\Lambda_1, \Lambda_1, ..., \Lambda_N]^T$ and

$$\underline{\psi}_i^{(+)} = \begin{bmatrix} e^{-(y_{i1}-\alpha_{i1})^2/2\sigma^2} \\ e^{-(y_{i2}-\alpha_{i2})^2/2\sigma^2} \\ \cdot \\ \cdot \\ \cdot \\ e^{-(y_{iN}-\alpha_{iN})^2/2\sigma^2} \end{bmatrix} \quad i = 1, ..., M \tag{12}$$

$$\underline{\psi}_i^{(-)} = \begin{bmatrix} e^{-(y_{i1}+\alpha_{i1})^2/2\sigma^2} \\ e^{-(y_{i2}+\alpha_{i2})^2/2\sigma^2} \\ \cdot \\ \cdot \\ \cdot \\ e^{-(y_{iN}+\alpha_{iN})^2/2\sigma^2} \end{bmatrix} \quad i = 1, ..., M \tag{13}$$

- LR-based fusion rules using only target fluctuation statistics. Under the assumption of Gaussian clutter model and Rayleigh target fluctuation model, the LR-based fusion statistic using only the target fluctuation coefficients is summarized below

$$\Lambda_j^{(2)} = \prod_{i=1}^{M} \frac{P_{di}\Psi_{ij}^{(+)} + (1-P_{di})\Psi_{ij}^{(-)}}{P_f\Psi_{ij}^{(+)} + (1-P_f)\Psi_{ij}^{(-)}} \quad j = 1, ..., N \tag{14}$$

where $\gamma = (\sigma/\sigma_\omega\sqrt{\sigma^2 + \sigma_\omega^2})$ with $2\sigma^2$ being the mean square value of the target fluctuation model, σ_ω^2 is the clutter variance.

$$\underline{\Psi}_i^{(+)} = \begin{bmatrix} 1+\sqrt{2\pi\gamma}y_{i1}e^{(\gamma^2 y_{i1}^2/2)}Q(-y_{i1}\gamma) \\ 1+\sqrt{2\pi\gamma}y_{i2}e^{(\gamma^2 y_{i2}^2/2)}Q(-y_{i2}\gamma) \\ \cdot \\ \cdot \\ \cdot \\ 1+\sqrt{2\pi\gamma}y_{iN}e^{(\gamma^2 y_{iN}^2/2)}Q(-y_{iN}\gamma) \end{bmatrix} \qquad i = 1, ..., M \tag{15}$$

$$\underline{\Psi}_i^{(-)} = \begin{bmatrix} 1-\sqrt{2\pi\gamma}y_{i1}e^{(\gamma^2 y_{i1}^2/2)}Q(y_{i1}\gamma) \\ 1-\sqrt{2\pi\gamma}y_{i2}e^{(\gamma^2 y_{i2}^2/2)}Q(y_{i2}\gamma) \\ \cdot \\ \cdot \\ \cdot \\ 1-\sqrt{2\pi\gamma}y_{iN}e^{(\gamma^2 y_{iN}^2/2)}Q(y_{iN}\gamma) \end{bmatrix} \qquad i = 1, ..., M \tag{16}$$

- Fusion statistics using a maximum ratio combiner (MRC). In the low SNR regime, if the local radar sensors are identical,i.e., P_{di} and P_{fi} are the same for all is, then $\underline{\Lambda}^{(1)}$ reduces to a form analogous to an MRC

$$\Lambda_j^{(3)} = \frac{1}{M}\sum_{i=1}^{M}\alpha_{ij}y_{ij} \qquad j = 1, ..., N \tag{17}$$

- Fusion statistics using an equal gain combiner (EGC). At low SNR regime, if the local radar sensors are identical, i.e., P_{di} and P_{fi} are the same for all ks, then $\underline{\Lambda}^{(2)}$ reduces to a form analogous to an EGC

$$\Lambda_j^{(4)} = \frac{1}{M}\sum_{i=1}^{M}y_{ij} \qquad j = 1, ..., N \tag{18}$$

4.2 Decision fusion for multi-target multi-radar sensor networks

When considering a multi-hop radar sensor networks, decision fusion problem for multiple targets could be quite complicate. For simplicity, we follow the assumption in single-hop case and assume the relay radar sensors have no direct observation of all the targets. Comparing Fig. 3 with Fig. 4, the above assumption assures that the MIMO fusion problem for multi-hop remains the same dimension as the one in the single-hop case.

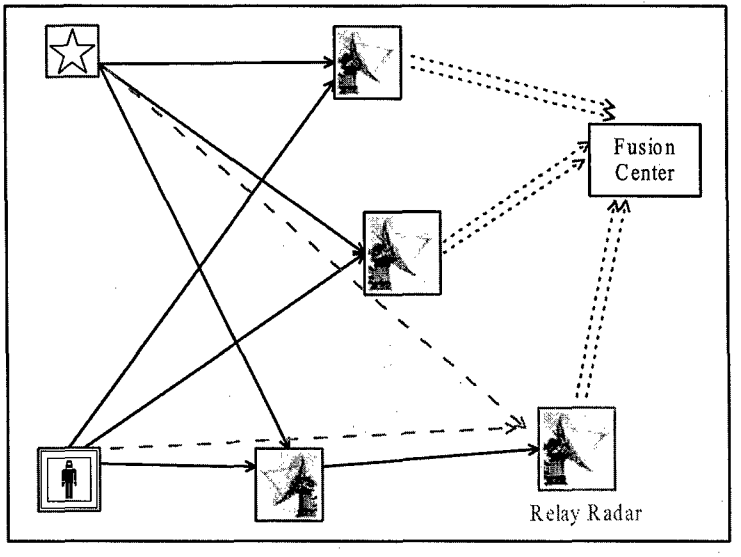

Figure 4: MIMO fusion model for multi-hop radar sensor networks

We make the further assumption that each relay radar makes a simple hard decision on the signal transmitted from its last hop radar. Therefore, given that the clutter is Gaussian, we have

$$s^k = sign(\alpha^{k-1} s^{k-1} + \omega^{k-1}) \tag{19}$$

Hence, the ultimate received signals at the fusion center transmitted from all the M last hop radars have the similar form as (9). We also assume that the Rayleigh RCS has unit power, i.e., $E[\alpha_{ij}^2] = 1$ and Gaussian clutter has variance σ^2 to facilitate SCR calculation later in the paper.

Implementing the decision rules for single target, multi-hop WSNs in [11] to our multi-target, multi-hop radar sensor networks, we get the decision fusion rules as follows.

- Optimal LR-based Fusion Rule

In multi-hop radar sensor network, we assume only the first hop radar sensors are CFAR with false alarm P_f^0 and probability of detection P_{di}^0. Let P_{di}^c be the probability of detection at the ith radar in the last relay, [11] has proved that for one given target detection, $P_{di}^c \approx P_{di}^0$ and $P_f^c = P_f^0$ at high signal to clutter ratio (SCR). At low SCR, P_{di}^c and P_f^ccan be approximated as

$$P_{di}^c \approx \frac{1}{2} + \frac{2^{M_i}(\prod_{k=0}^{M_{i-1}} \alpha_{ik})}{(\sqrt{2\pi}\sigma)^{M_i}} \left(P_{di}^0 - \frac{1}{2}\right) \tag{20}$$

$$P_f^c \approx \frac{1}{2} + \frac{2^{M_i}(\prod_{k=0}^{M_{i-1}} \alpha_{ik})}{(\sqrt{2\pi}\sigma)^{M_i}} \left(P_f^0 - \frac{1}{2}\right) \tag{21}$$

Assume there are M radar sensors in the last hop, M_i is the number of hops at the ith radar. α_{ik} is RCS value at the kth relay of radar i.

The optimum LR-based fusion rule for multi-target radar sensor networks can be written as

$$\Lambda_j^{(1)} = \prod_{i=1}^{M} \frac{P_{di}^c + (1 - P_{di}^c) \cdot \phi_{ij}}{P_f^c + (1 - P_f^c) \cdot \phi_{ij}} \quad j = 1, ..., N \tag{22}$$

where

$$\underline{\phi}_i = \begin{bmatrix} e^{-(2y_{i1}\alpha_{i1})^{M_i}/\sigma^2} \\ e^{-(2y_{i2}\alpha_{i2})^{M_i}/\sigma^2} \\ \cdot \\ \cdot \\ \cdot \\ e^{-(2y_{iN}\alpha_{iN})^{M_i}/\sigma^2} \end{bmatrix} \quad i = 1, ..., M \tag{23}$$

- Denote $\underline{\Lambda}^{(2)}$ as the LR rule that corresponds to the case when only the target RCS statistics are known. $\underline{\Lambda}^{(2)}$ can be derived for the multi-hop MT-MR sensor networks.

$$\Lambda_j^{(2)} = \prod_{i=1}^{M} \frac{1 + [P_{di}^c - Q(\gamma y_{ij})]\sqrt{2\pi}\gamma y_{ij} e^{(\gamma y_{ij})^2/2}}{1 + [P_f^c - Q(\gamma y_{ij})]\sqrt{2\pi}\gamma y_{ij} e^{(\gamma y_{ij})^2/2}} \quad j = 1, ..., N \tag{24}$$

where $\underline{y}_i = [y_{i1}, y_{i2}, ...y_{iN}]$ is a vector containing all N decision data from radar i. P_{di}^c and P_f^c are denoted as in (20) and (21).

- Decision fusion rules of Maximum ratio combiner (MRC) and equal gain combiner (EGC) have the identical format as the single hop case because for both of them, the decision fusion only depends on the last hop.

5 Simulation Results

In this section, we simulate the performance of the decision fusion rules derived for multi-target radar sensor networks. For ease of SCR calculation, we assume that all the target RCSs have unit power, i.e, $E[\alpha_{ij}^2] = 1$. Binary decisions are made at the local radar sensors and the relay radars. The target RCS are generated using the Rayleigh model.

For multi-target, single-hop radar sensor network and multi-target, multi-hop radar sensor network, we are interested to compare the four decision fusion rules:

- Optimal LR-based rule
- LR-based rule with target RCS statistics only
- MRC rule
- EGC rule

In all simulations, we assume the constant false alarm rate $P_f = 0.01$ (for multi-hop case, $P_f = 0.01$ is the one at the first hop). Under hypothesis H_0 when a target is detected as absent,

$P_f = Q(\frac{X_t}{\sigma})$. We then know the detection threshold $X_t = Q(P_f)^{-1}\sigma$. When a target is detected, i.e., hypothesis H_1, the probability of detection $P_{di} = Q(\frac{X_t - \alpha_i}{\sigma})$.

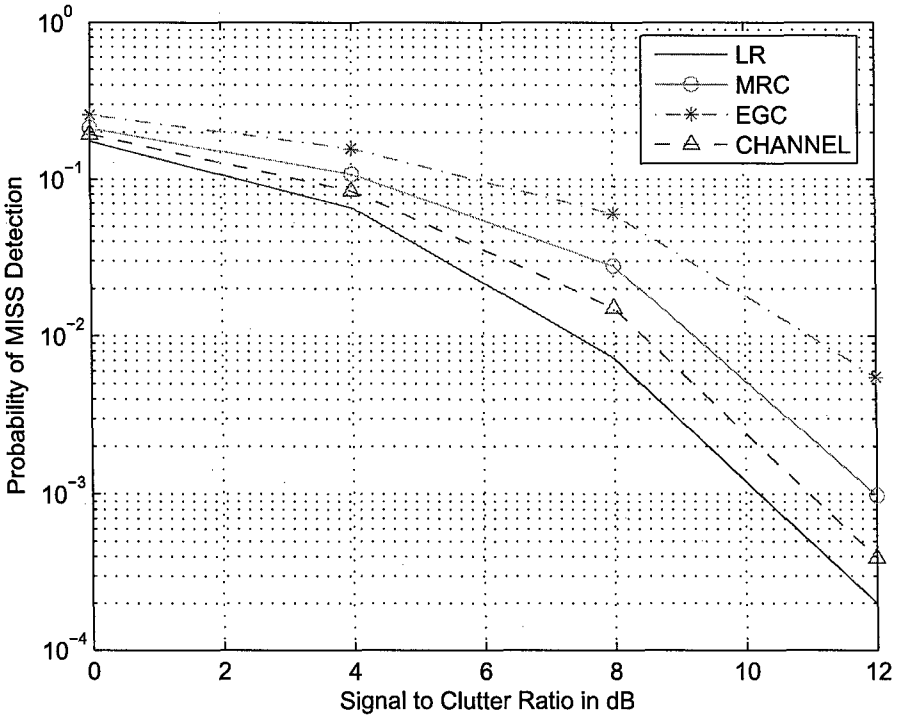

Figure 5: Single hop

Fig.5 gives the probability of miss detection vs. the SCR for multi-target, single-hop radar sensor network. There are total two stationary targets, three radar sensors in the field. The optimal LR- based fusion rule provides the most powerful detection performance but it requires complete target RCS knowledge. The LR-based rule with target RCS statistics approaches the optimal LR-based rule in low SCR and have about 1dB loss in higher SCR. MRC and EGC have similar performance. Both are little worse than the LR-based rule with target RCS statistics.

Fig.6 and Fig.7 are the performance for multi-target, multi-hop radar sensor networks. Fig.6 shows the probability of miss detection when each of the three radar sensors reaches the fusion center in two hops. Fig.7 shows the performance when the three radar sensors reach the fusion center in unequal hops. In our simulation, we assume that one radar sensor reaches the fusion

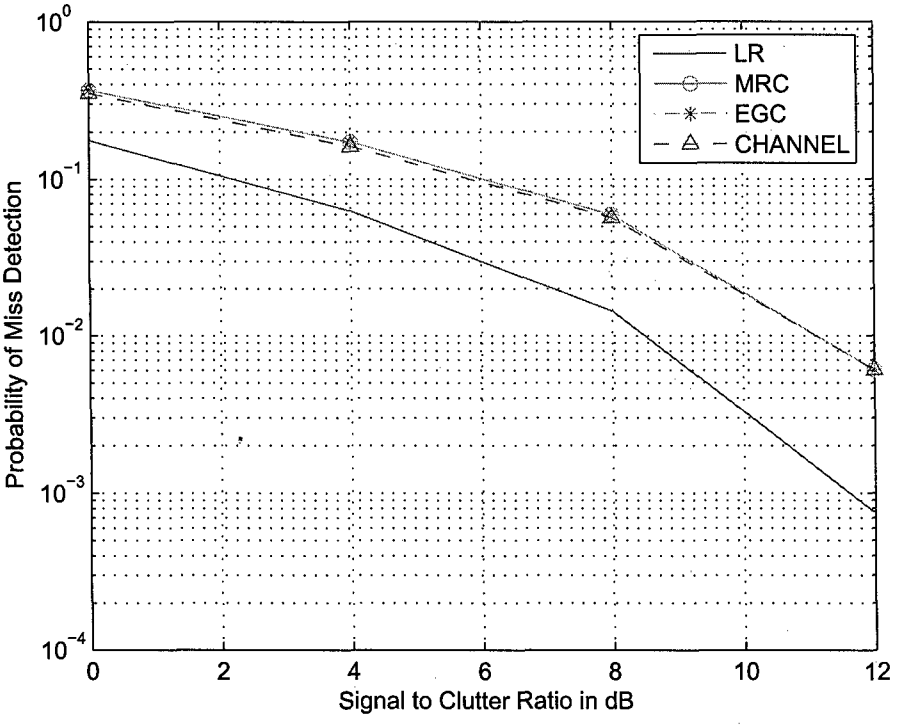

Figure 6: Multi-hop, equal hops

center in two hops while the others in single hop. As expected, the probability of detection for the single-hop case outperforms the one for multi-hop.

6 Conclusions

In this paper, we presented the MIMO decision fusion rules for multi-target, multi-hop radar sensor networks under the assumption that the target RCS is Rayleigh model and clutter echoes follow Gaussian. We derived the optimum LR-based fusion rule and a sub-optimal LR-based fusion rule with the target RCS statistics only. Simulation results show that the *MIMO fusion* rules approach the optimal-LR and outperforms MRC and EGC at high signal to clutter ratio (SCR).

In many cases, two or more local radars may share a common relay node on their way to the fusion center. Under this circumstances, the independent assumption made toward the target RCS may not be held. It is actually a very interesting space correlation issue. As the radar observations

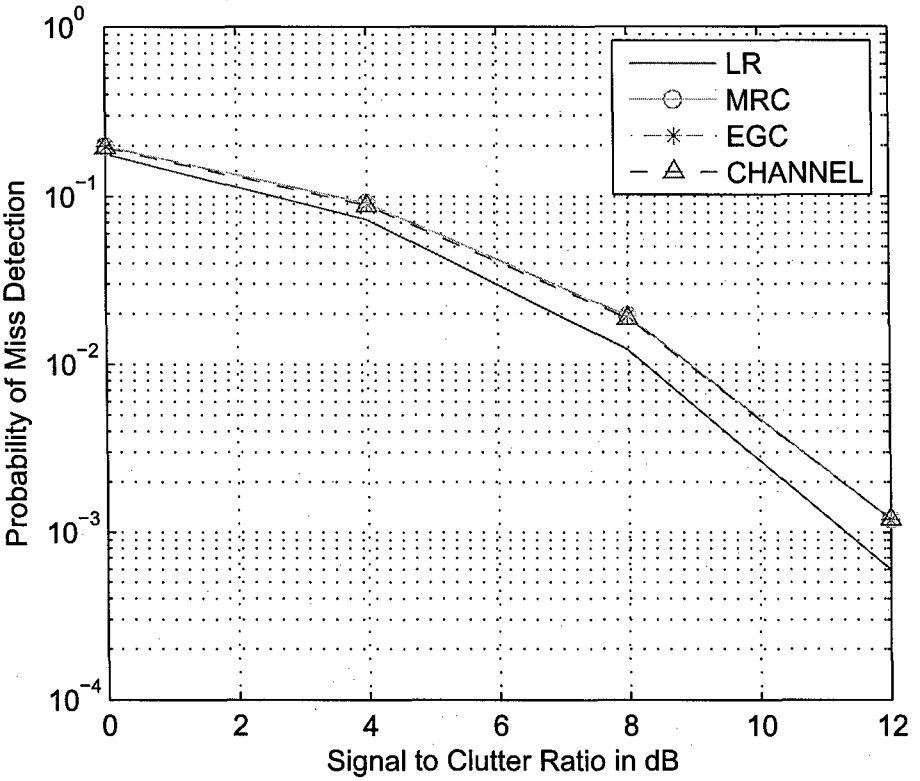

Figure 7: Multi-hop, unequal hops

always demonstrate time correlation, further research will be focused on this space-time correlation of radar sensor networks.

Acknowledgment

This work was supported by the Office of Naval Research (ONR) Young Investigator Award under Grant N00014-03-1-0466. The authors would like to thank Dr. Rabinder Madan for helpful discussion and suggestions on radar sensor networks.

References

[1] M. L. Skolnik "Introduction to Radar Systems" *TATA McGRAW HILL*, 10th reprint, 2004

[2] C-Y. Chong and S. P. Kumar "Sensor Networks: Evolution, Opportunities and Challenges" *Proceedings of The IEEE* vol. 91, No. 8, Aug. 2003

[3] Z. Chair and P. K. Varshney "Optimal data fusion in multiple sensor detection systems." *IEEE Transactions on Aerospace and Electronic Systems.*, AES-22, pp. 98-101, Jan. 1986.

[4] P. K. Varshney "Distributed Detection and Data Fusion" *New York: Springer*, 1997

[5] J. Hu and R. Blum "On the optimality of finite-level quantization for distributed signal detection" *IEEE Transactions on Information Theory*, vol. 47, pp. 1665 - 1671, May. 2001.

[6] J. Chamberland and V. V. Veeravalli "Decentralized detection in sensor networks" *IEEE Transactions on Signal Processing*, vol. 51, pp. 407 - 416, Feb. 2003

[7] R. Niu, B. Chen and P. K, Varshney "Decision fusion rules in wireless sensor networks using fading channel statistics" *In Proceedings of CISS 2003*, Baltimore, MD, Mar 2003

[8] S. C. A. Thomopoulos and L. Zhang "Distributed decision fusion with networking delays and channel errors" *Information Science*, vol. 66, pg. 91 - 118, Dec. 1992

[9] B. Chen and P. Willett "Channel optimized binary quantiers for distributed sensor networks" *In Proceedings of IEEE International Conference on Acoustics, Speech, and Signal Processing*, Montreal, Canada, May 2004

[10] B. Liu and B. Chen "Joint Source-Channel coding for distribute sensor networks" *In Proceedings of the 38th Annual Asilomar Conference on Signals, Systemss, and Computers, Pacific Grove*, CA, Nov. 2004

[11] Y. Lin, B. Chen and P. K. Varshney "Decision Fusion Rules in multi-hop wireless sensor networks" *IEEE Transactions on Aerospace and Electronic Systems*, vol.41, no.2,pp 475-488,Apr.2005

[12] Y. Sun, P. Willett and R. Lynch "Waveform Fusion in Sonar Signal Processing" *IEEE Transactions on Aerospace and Electronic Systems*, vol.40, no.2,pp 462-477,Apr.2004

UWB Sensor Networks in Hostile Environment: Interference Analysis and Performance Study

Lingming Wang and Qilian Liang

Department of Electrical Engineering

University of Texas at Arlington

Arlington, TX 76019-0016. USA

E-mail:wang@wcn.uta.edu. liang@uta.edu

Abstract

Interferences due to the hostile environment and the Multi-User Access are critical factors affecting performance of the Wireless Sensor Networks. There is clearly a need of a system that can survive from the severe interference. In this paper, we designed a hybrid Frequency Hopping/Time Hopping-Pulse Position Modulated (FH/TH-PPM) UWB system for Wireless Sensor Networks to confront the hostile environment. FH and TH are both used to get as much diversity gain as possible. An exact analysis is also derived for precisely calculating the bit error rates for both Additive White Gaussian Noise channel and path-loss channel in the presense of multitone/pulse (tone in frequency domain and pulse in time domain) interference and Multi-User Interference.

Index Terms : Time Hopping, Frequency Hoppoing, PPM, Wireless sensor networks, UWB, BER

1 Introduction

Wireless sensor networks are becoming more popular for an ever increasing range of applications with improvements in device size, power control, communications and computing technology. Since 2002 there has been great increasing popularity of commercial applications based on Ultra WideBand. This in turn has ignited interest in the use of this technology for sensor networks. Actually, UWB systems have potentially low complexity and low cost; have a very good time domain resolution, which facilitates location and tracking applications. So, UWB wireless sensor networks are promising.

One of the most important applications of WSN is in battle field, which means there exist hostile interferences. Frequency Hopping (FH) technology offers an improvement in performance when the communication systems is attacked by hostile interference and reduce the ability of a hostile observer to receive and demodulate the communication signal. This kind of inherent property finds it a potential position in the UWB sensor networks. Based on the UWB definition released by the FCC (FCC, 2002) that a signal is UWB if its bandwidth exceeds 500 MHz, the overall 7.5 GHz bandwidth, that is, frequencies in the range 3.1 GHz to 10.6 GHz as based on the FCC ruling, can be split into smaller frequency bands of at least 500 MHz each. This character inspired us to design a hybrid FH/TH-PPM UWB system.

Sensor Network communication systems have to be multi-user accessible, which means different users/sensor nodes are allowed to share the same physical medium for transmitting and receiving different data flows. In TH-UWB, the spectrum of the impulse radio signal is usually shaped by encoding data symbols using TH sequences, which are typically described as pseudorandom PN codes. These smae sequences can also serve as users' signatures and ensure access to the medium to multiple users. Therefore, this so called Time Hoppping Multiple Access (THMA) technology will be a reliable choice in this case. However, in a realistic scenario where systems cannot achieve ideal synchronization, multi-user interference

(MUI) will be another crucial factor besides the previous mentioned hostile interfence to affect the system performance. Clearly, the simple Signal-to-Noise-Ratio (SNR) is less than enough to give a comprehensive performance evaluation for sensor networks. Therefore, Signal-to-Interference-plus-Noise-Ratio (SINR) should be analyzed instead.

Several efforts have been made in the recent past for evaluating the effect of MUI on symbol error rate with single-user reception in an AWGN channel [7, 6]. However, hostile jammer are considered in none of them, which would be challenged in this paper. For example, a TH-UWB sensor network, which is set up in a hostile environment, it is feasible for the enemies to estimate the shape of a pulse. Therefore, a repeated-imitated-pulses intruder will be sent out to degrade the performance of the network. The main contribution of this paper, we put the hositle intereference along with the MUI into consideration, and through the precise analysis a closed-form performance analysis expression can be got.

The rest of this paper is organized as follows. The system models, including the transmission, channel and receiver, will be introduced in Section 2. The MUI and hostile interference will be studied in Section 3 and Section 4 respectively, and the SINR and closed-form BER will be derived as well. Numerical results and comparisons will be present in Section 5; and conclusions are made in Section 6.

2 System Models

In the proposed system, there are N_F non-overlapping FH bands, each with bandwidth B_h where B_h is the bandwidth required to transmit a TH-PPM signal in the absence of FH. Let $s^k(t)$ denotes the k-th user's signal at time t in this FH/TH-PPM UWB system with totally N_u users, and it takes the form

$$s^k(t) = \sqrt{\frac{E_b}{N_s}} \sum_{j=-\infty}^{+\infty} c_j^{fh}(k) p[t - jT_f - c_j^{th}(k)T_c - d_j(k)\delta]) \tag{1}$$

where $p(t)$is a chip waveform, which can take arbitrary time-limited pulse shapes proposed specifically for UWB communication systems, and is normalized to satisfy $\int_{-\infty}^{+\infty} p^2(t)dt = 1$. The notations and parameters are:

- N_s is the number of pulses used to transmit a single information bit. T_f is the time duration of a frame. In general case, $N_s \geq 1$ pulses carry the information of one bit. The bit duration T_b should satisfy, $T_b \geq T_f N_s$.
- E_b is the energy per information bit. $\sqrt{\frac{E_b}{N_s}}$ is the normalized energy in each symbol.
- $c_j^{th}(k)T_c$ is the time shift introduced by the TH code. T_c is the chip duration. $c_j^{th}(k)$ is the j-th coefficient of the TH sequence used by user k; it is pseudo-random with each element take an integral in the range $[0, N_h - 1]$, where N_h is the number of hops. $T_c \leq T_f/N_h$ should be satisfied.
- The $d_j(k)\delta$ term represents the time shift introduced by PPM modulation. In our system, 2PPM is only considered. Therefore, $d_j(k)$ represents the j-th binary data bit (0 or 1) transmitted by the k-th user; δ is the PPM shift.
- $c_j^{fh}(k) = \sqrt{(2)}cos(2\pi f_k j)$ is the k-th user's spreading code during j-th frame.

Notice that each symbol chooses one of the N_F sub-bands to transmit the signal, however, in each sub-band, the transmission is TH-2PPM.

In WSN, in order to save energy, sensor nodes choose to be idle for most of the time. The number of nodes who are actually in the status of communication is unknown. However, the total number of sensor nodes in the network and the access rate λ, i.e., the rate that a node in the communication status, for each node are easy to know. Therefore, the users of the communication system, N_u^T, is a Binomial random variable. Since the total number of nodes, N_U, is very large, we can approximate the Binomial distribution to a Gaussian random variable

with the mean $N_U\lambda$ and variance $N_U\lambda(1-\lambda)$, as

$$f_{N_u^T}(n_u^t) = \frac{1}{\sqrt{2\pi N_U\lambda(1-\lambda)}} e^{-(n_u^t - N_U\lambda)^2/2N_U\lambda(1-\lambda)} \tag{2}$$

For the N_u^T users, they randomly choose one of the sub-bands to transmit the signal according to $c_j^{fh}(k)$ symbol by symbol. It is also a Binomial random variable with the coefficient $1/N_F$. To simplify the problem, we assume that the users are distributed optimally, so the number of users share the same channel, N_u, should be expressed as

$$N_u = N_u^T/N_F. \tag{3}$$

Assume over one T_f, N_u users' signals are simultaneously transmitted over a channel with L_c paths [2], the composite waveform at the output of the receiver antenna maybe written as

$$r(t) = \sum_{k=1}^{N_u}\sum_{l=1}^{L_c} \alpha_l^{(k)} s_j^{(k)}(t - \tau_l^{(k)}) + n(t) + I(t) \tag{4}$$

where $n(t)$ is the additive Gaussian Noise withe two-sided power spectral density $N_0/2$, $I(t)$ is the hostile jammer interference, $\alpha_l^{(k)}$ and $\tau_l^{(k)}$ are the attenuation and the delay affecting replica of the k-th user's signal traveling through the l-th path. In writing (4), we have implicitly assumed a static channel, meaning the $\alpha_l^{(k)}$ and $\tau_l^{(k)}$ are either fixed or vary so slowly that they are practically constant over several bits.

Consider $s^{(1)}(t)$ to be the desired user, all the other $N_u - 1$ users signals are interference signals. We make assumptions

- The reference transmitter and receiver of a reference link are perfectly synchronized under the coherent detection hypothesis;
- A dominant path exists that conveys the major part of the desired user's energy [3];

the decision statistic over the 1-st user's j-th symbol is obtained as

$$z_j = \int_{jT_f}^{(j+1)T_f} r(t)v(t - \tau_1^{(1)} - jT_f - c_j^{(1)}T_c)dt, \tag{5}$$

where $v(t) = p(t) - p(t-\delta)$ is the correlation template waveform.

Afterwards, a simple hard decision of the information bit based on $z_j, j = 0, 1, \ldots, N_s - 1$ will be made by majority law.

3 Multi-User Interference Analysis

In this section, we will first focus on the analysis of MUI with the absence of hostile jammer interference. We assume there is no inter-channel-interference. Therefore, the received signal of 1-st user's j-th symbol can be expressed as::

$$r_j(t) = r_j^{(1)}(t) + r_{j,mui}(t) + n(t) \tag{6}$$

where $r_{j,mui}(t)$ is the MUI contribution at the receiver input. If the users are many and have comparable powers, we can approximate the MUI as a white Gaussian process by the central limit theorem [5] and, as such, it can be lumped into the additive Gaussian Noise,

$$w_{tot}(t) = r_{j,mui}(t) + n(t) \tag{7}$$

and $w_{tot}(t)$ is still a white Gaussian process. Correspondingly, the minimum error probability can be achieved by computing (5).

However, we still need to evaluate the energy of the MUI. Since the system is asynchronous, we need to consider all cases where a pulse originated by any of the transmitters but TX1, is detected by the receiver. First of all we need to analyze the noise provoked by the presence of one alien pulse at the output of the receiver by using the similar method as in[1]. ,

$$mui^{(k)}(\tau^{(k)}) = \sqrt{E_{RX}^{(k)}} \int_0^{T_c} p(t - \tau^{(k)}) v_t dt \tag{8}$$

where, $E_{RX}^{(k)} = \alpha^{(k)}(E_b/N_s)$, and here we suppose $\alpha^{(k)} = 1\ \forall k$.

Since $\tau^{(k)}$ is uniformly distributed over $[0, T_f)$, however, the region the MUI noise can affect to the desired user , is only at $[-T_p, T_c]$, with $T_c = 2T_p$[1]. Hence,

$$\sigma^2_{mui^{(k)}} = \frac{1}{T_f} \int_{-T_p}^{T_c} \left(\sqrt{E_{RX}^{(k)}} \int_0^{T_c} p(t - \tau^{(k)}) v(t) dt \right)^2 d\tau^{(k)} \tag{9}$$

and cumulate all the $N_u - 1$ interference sources, the total MUI energy is

$$\sigma_{mui}^2 = \frac{1}{T_f} \sum_{k=2}^{N_u} E_{RX}^{(k)} \left(\int_0^{T_f} \left(\int_0^{T_c} p(t - \tau^{(k)}) v(t) dt \right)^2 d\tau^{(k)} \right) \tag{10}$$

Since all the delays, τ, are identically distributed, and under the hypothesis of perfect power control, e.g., $E_{RX}^{(k)} = E_{RX}\ \forall k$,

$$\sigma_{mui}^2 = \frac{E_{RX}}{T_f} \sum_{k=2}^{N_u} \left(\int_0^{T_f} \left(\int_0^{T_c} p(t - \tau) v(t) dt \right)^2 d\tau \right) \tag{11}$$

Define σ_M^2 as

$$\begin{aligned} \sigma_M^2 &= \int_0^{T_f} \left(\int_0^{T_c} p(t - \tau) v(t) dt \right)^2 d\tau \\ &= \int_0^{T_f} \left(\int_0^{T_c} p(t - \tau) \left(p(t) - p(t - \delta) \right) dt \right)^2 d\tau \\ &= \int_{-T_p}^{T_f} \left(R_0(\tau) - R_0(\tau + \delta) \right)^2 d\tau \end{aligned} \tag{12}$$

and (10) becomes

$$\sigma_{mui}^2 = \frac{E_{RX}}{T_f} (N_u - 1) \sigma_M^2 \tag{13}$$

Therefore, the SIR_{mui} over one symbol can be expressed as:

$$SIR_{mui} = \frac{T_f}{(N_u - 1)\sigma_M^2}. \tag{14}$$

Let SNR_{ref} denotes the equivalent signal to noise and MUI ratio over one symbol, it can be written as

$$SNR_{ref} = (SNR_n^{-1} + SIR_{mui}^{-1})^{-1} \tag{15}$$

where SNR_n are the signal to noise ratio over one symbol.

Hence,

$$\begin{aligned} SNR_{ref} &= \left(\left(\frac{E_{RX}}{N_0} \right)^{-1} + \left(\frac{T_f}{(N_u - 1)\sigma_M^2} \right)^{-1} \right)^{-1} \\ &= \frac{T_f}{N_s T_f + (N_u - 1)\sigma_M^2 \left(\frac{E_b}{N_0} \right)} \left(\frac{E_b}{N_0} \right) \end{aligned} \tag{16}$$

where $E_b/N_0$is the system SNR.

We can also get the equivalent variance of $w_{tot}(n)$,

$$N_0' = N_0 + \frac{(N_u - 1)\sigma_M^2 E_b}{N_s T_f} \tag{17}$$

4 Performance Analysis with Multitone/pulse Interference

In this section, the SIR for the hostile interference part is obtained. As previously mentioned, in a hostile environment, which is a common case for sensor networks, it is feasible for an enemy to estimate/detect the pulse waveform, furthermore, send the imitational waveform to interfere the communication system. However, it is not economy or efficient for the interference to cover all the frequency bandwidth. So, what we study here is a multitone/pulse (tone in frequency domain; and pulse in time domain) interference, which implies that the jamming signal consists of one or more tones/sub-bands transmitted within the total bandwidth; and it has the same pulse shaper as the transmitted 2-PPM signal does.

We make the following assumptions:

- The multitone/pulse interference has a total power P_J, which is transmitted in a total of q equal power interfering tones spread randomly over the spread spectrum bandwidth;
- The time duration for the interference pulse is the same as the time duration of the transmitted signal pulse $p(t)$, which is denoted as T_p. To simplify the problem, we suppose $T_c = 2T_p$ and $\delta = T_p$. The hop period of the interference is also T_p, and each hop is independent.
- The multitone/pulse interference can catch the signal pulse with the perfect timing. We consider the scenario that there is at most one interference per FH sub-band. Hence, in one hop, the probability that a FH band contains an interference tone/pulse is q/N_F. Observe the transmitted signal as in (1), the signal hops both in the frequency domain

and in the time domain symbol by symbol. Therefore, our analysis will first focus on one symbol.

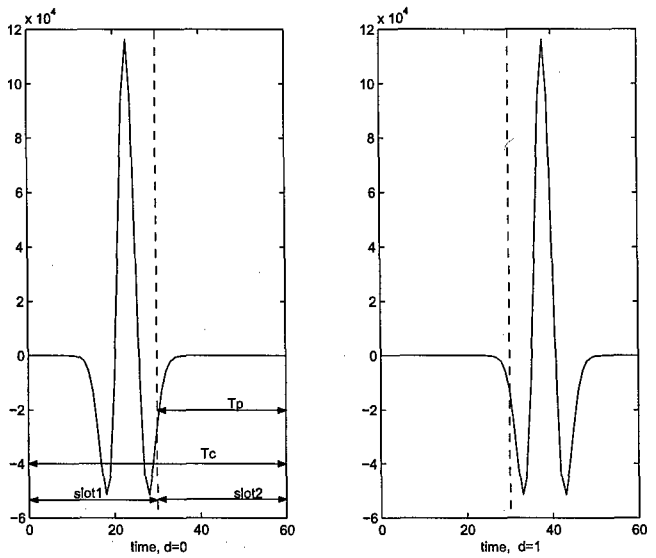

Figure 1: An example of the waveform of a 2-PPM signal.

For one symbol, no matter what $c_j^{fh}(k)$ and $c_j^{th}(k)$ are, it is a 2-PPM signal shown as in Fig 1. The left one is the waveform when $d_j(k) = 0$, and the right one is the waveform when $d_j(k) = 1$. We partition the symbol duration as two time slots, hence, for the multitone/pulse interference, there are two hops. And because in each hop, it is independently distributed, there should be totally four cases with regard to the jammer interference for each symbol:

1. *Case1.* There is no jammer interference in either of two slots, and the probability of case1 is

$$P\{case1\} = (1 - \frac{q}{N_F}) \cdot (1 - \frac{q}{N_F}). \tag{18}$$

2. *Case2.* There is jammer interference in each slot, and the probability of case2 is

$$P\{case2\} = \frac{q}{N_F} \cdot \frac{q}{N_F}. \tag{19}$$

3. *Case3.* There is one and only one jammer interference pulse, and it is at the same slot as the signal pulse. The probability of case3 is

$$P\{case3\} = (1 - \frac{q}{N_F}) \cdot \frac{q}{N_F}. \tag{20}$$

4. *Case4.* There is one and only one jammer interference pulse, and it is not at the same slot as the signal pulse. The probability of case4 is

$$P\{case4\} = (1 - \frac{q}{N_F}) \cdot \frac{q}{N_F}. \tag{21}$$

The received signal of the j-th symbol of 1-st user can be expressed as:

$$r'_j(t) = r^1_j(t) + I_{jammer}(t) + w_{tot}(t); \tag{22}$$

where $r^k_j(t)$ and $I_{jammer}(t)$ are the jammer interference contributions at the receiver input, and $w_{tot}(t)$ accounts for both the thermal and MUI noise contributions, and is still a white Gaussian process as proved in Section 3. Hence, a maximum a posteriori (MAP) approach can be adopted here to get the minimum error probability. For different cases of the jammer interference, the detection boundaries are shown in Fig. 2.

Hence, we can get the $SINR_{jammer}$ straightforwardly.

- For case1 and case2,

$$SINR_{jammer|case1,2} = \frac{E_{RX}}{N'_0}. \tag{23}$$

- For case 3,

$$SINR_{jammer|case3} = \frac{(\sqrt{E_{RX}} + \sqrt{\frac{P_J}{q}})^2}{N'_0}. \tag{24}$$

- For case 4,

$$SINR_{jammer|case4} = \frac{(\sqrt{E_{RX}} - \sqrt{\frac{P_J}{q}})^2}{N'_0}. \tag{25}$$

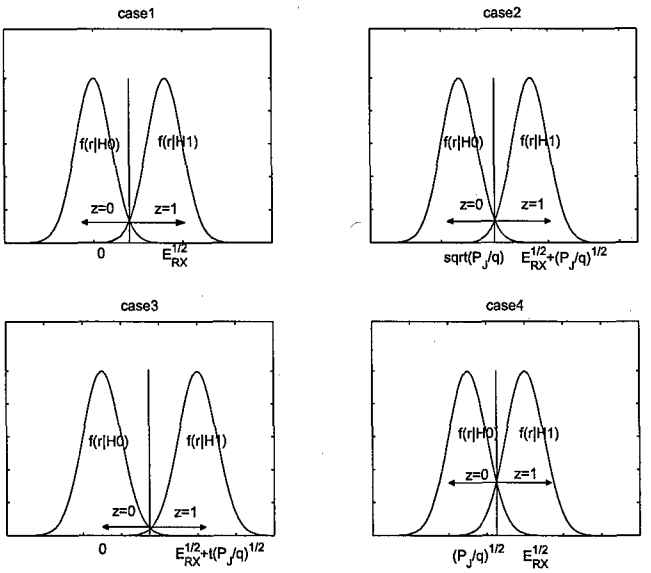

Figure 2: The MAP detection rule for all the cases.

For 2-PPM signal the error probability is [1],

$$Pr = Q(\sqrt{SNR_{spec}}). \tag{26}$$

Apply (17) and (23) to (25) into (26), we can derive,

- For case1 and case2,

$$pr_{s|c1,2} = Q(\sqrt{\left(\frac{\frac{E_b}{N_s}}{N_0'}\right)}); \tag{27}$$

- For case 3,

$$pr_{s|c3} = Q(\sqrt{\left(\frac{(\sqrt{\frac{E_b}{N_s}} + \sqrt{\frac{P_J}{q}})^2}{N_0'}\right)}); \tag{28}$$

- For case 4,

$$pr_{s|c4} = Q(\sqrt{\left(\frac{(\sqrt{\frac{E_b}{N_s}} - \sqrt{\frac{P_J}{q}})^2}{N_0'}\right)}). \tag{29}$$

Removing the conditioning on cases, we get

$$\begin{aligned} Pr'_s &= \left(\left(\frac{N_F-q}{N_F}\right)^2+\left(\frac{q}{N_F}\right)^2\right)Q(\sqrt{\left(\frac{\frac{E_b}{N_s}}{N'_0}\right)}) \\ &+ \left(\frac{N_F-q}{N_F}\right)\left(\frac{q}{N_F}\right)(Q(\sqrt{\left(\frac{(\sqrt{\frac{E_b}{N_s}}+\sqrt{\frac{P_J}{q}})^2}{N'_0}\right)}) \\ &+ Q(\sqrt{\left(\frac{(\sqrt{\frac{E_b}{N_s}}-\sqrt{\frac{P_J}{q}})^2}{N'_0}\right)})). \end{aligned} \tag{30}$$

Considering only N_u is a random variable, we should take (2) and (3) into (30),

$$Pr_s = \frac{1}{N_F\sqrt{2\pi N_U\lambda(1-\lambda)}}\int_1^{N_U} Pr'_s e^{-(n_u-N_U\lambda)^2/2N_U\lambda(1-\lambda)}dn_u \tag{31}$$

After we got the symbol error rate Pr_s, it is easy for us to obtain the bit error rate Pr_b by majority law.

$$Pr_b = \sum_{k=\lceil\frac{N_s}{2}\rceil}^{N_s} C_{Ns}^k Pr_s^k(1-Pr_s)^{N_s-k} \tag{32}$$

where $\lceil\ \rceil$ is the ceiling operation, and C_{Ns}^k is an N_s-choose-k Binomial coefficient, i.e., $C_{Ns}^k = \frac{k!(N_s-k)!}{N_s!}$.

5 Numerical Results and Comparisons

The parameters of the example UWB systems are listed in Table 1.

- The discussion on N_s;

  We fix $N_F = 20$, $q = 8$, $N_u = 10$ and the energy of the signal and jammer interference ratio $E_b/P_J = 5dB$, and compare the Symbol Error Rate (SER) and Bit Error Rate (BER) among $N_s = 1, 3, 5, 7$. The results are shown in Figure. 3 and Figure. 4 respectively. For SER, because, the more symbols used to transmit one bit, the energy for each symbol is less, SER is increasing when the N_s increases. However, BER is more

Table 1: Parameters of the example FH/TH-PPM UWB system

Parameter	Notation	2^{nd}-order mono-cycle
shaping factor for the pulse	ϵ	$0.25ns$
time shift introduced by PPM	δ	$0.5ns$
pulse duration	T_p	$0.5ns$
frame duration	T_f	$8ns$
chip duration	T_c	$1ns$
number of hops	N_h	6

meaningful here, and obviously, the more symbols we used to transmit one information bit, the better performance we can achieve. The curves drop quickly from $SNR = 0dB$ to $15dB$, however, after $15dB$, become flat, which caused by the jammer interference.

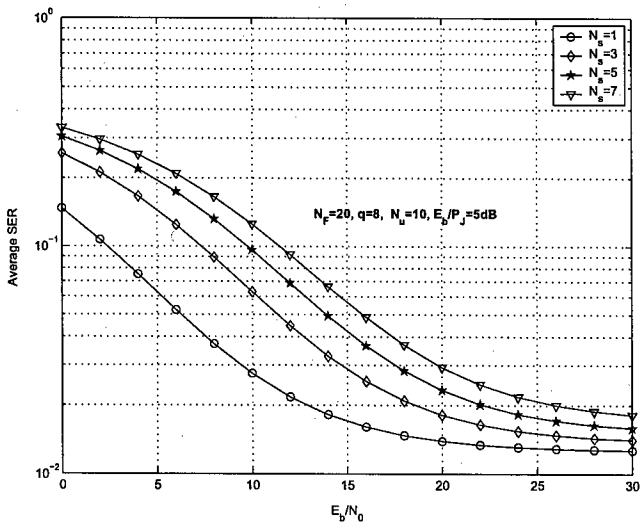

Figure 3: The average SER for different N_s.

- The discussion on E_b/P_J;

  We set $N_F = 20$, $N_s = 3$, $q = 8$, and $N_u = 10$, and compare the SER and BER among

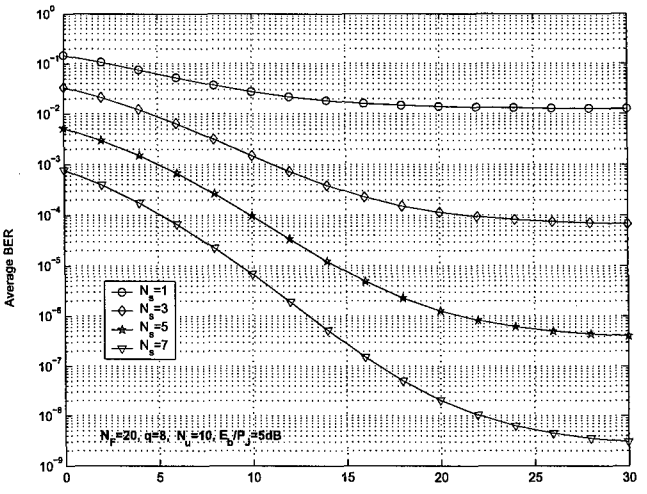

Figure 4: The average BER for different N_S.

$E_b/P_J = 0, 5, 10dB$. Figure. 5 and Figure 6 show the results. For both SER and BER, larger E_b/P_J can guarantee better performance. From $E_b/P_J = 5dB$ to $E_b/P_J = 10dB$, the performance gain is very limited, the reason of which is when E_b/P_J is higher than somebetter threshold, the jammer interference is too weak to give any impact to the system.

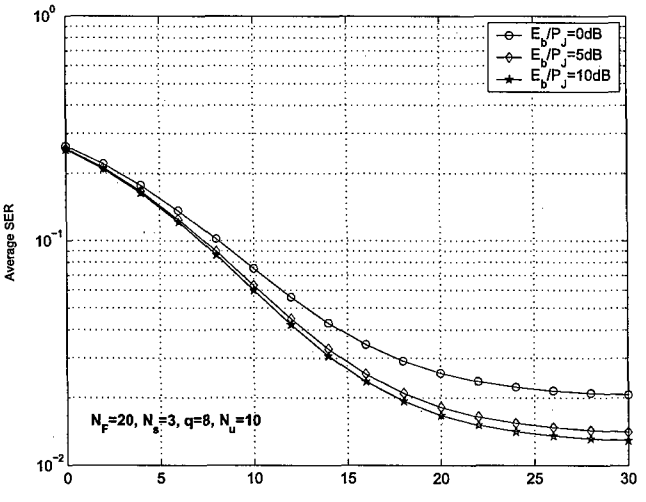

Figure 5: The average SER for different E_b/P_J.

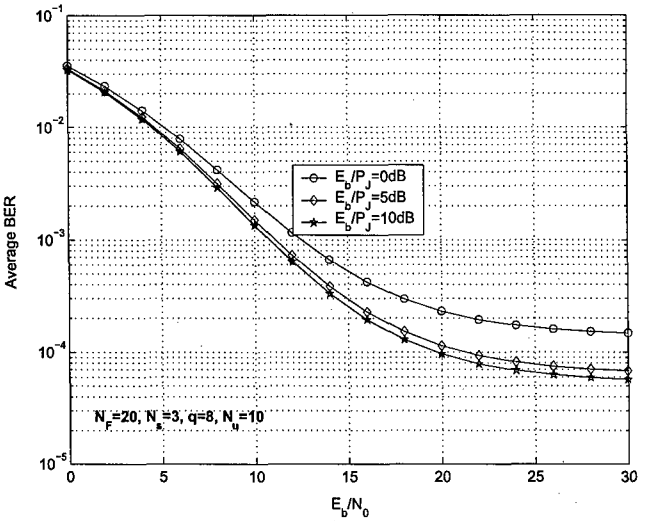

Figure 6: The average BER for different E_b/P_J.

- The discussion on q;

  N_F, N_s, N_u and E_b/P_J are fixed at 20, 5, 10 and $5dB$ respectively.We try to evaluate the performance for $q = 2, 8, 18$. At the first glance, larger q may be thought to yield worse performance, because large q means the probability that a jammer interference bumps the information signal is higher. However, we need to notice, high q also means the energy of the jammer interference for each sub-band is less, because the total jammer interference power is fixed. We can get the same conclusion in the Figure. 7 and Figure. 8. The worst and best performances are get at $q = 2$ and $q = 8$ respectively.

- The discussion on N_F;

  We evaluate the performance for $N_F = 1, 5, 10, 20$ when $N_s = 1$, and the number of users who are at communication status is 100. We need to evaluate how partitioning N_F can decrease the MUI, therefore, we set it as a jammer interference free channel. Obviously, Figure. 9 shows that we can get better performance when N_F is larger. Considering, more sub-bands partitioned means more cost, the N_F should be set at an appropriate value as long as the Quality of Sevice (Qos) is satisfying.

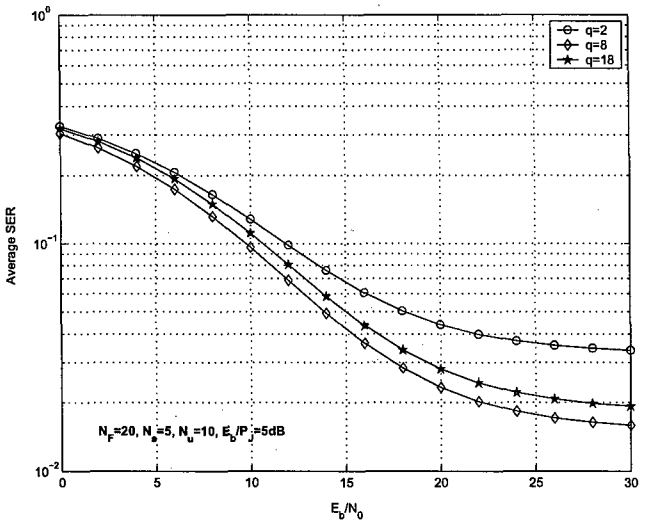

Figure 7: The average SER for different q.

- The discussion on N_u;

  We set $N_F = 20$, $q = 8$, $N_s = 5$ and $E_b/P_J = 5dB$. N_u is equal to $5, 10, 15, 20$ respectively to get different performance, which are shown in Figure. 10 and Figure. 11. At high SNR, the performance is degraded quickly when N_u becomes larger. That is because the MUI is related with E_b under the assumption that each user has comparable power.

- The discussion on λ;

  We proved in Section 2 that the N_u is approximately a Gaussian RV.With known N_U, the number of sensor nodes in the WSN, but unkonwn N_u, the number of users that would share the same sub-band, we need to calculate the SER as in (31). We set $N_U = 10,000$, N_F is set as 20 and we assume the users are optimally distributed. For different access rate, $\lambda = 0.01$ and $\lambda = 0.02$, the performances are shown in Figure 12 and Figure. 13, we can see though the N_U are the same, the difference in λ would yield totally different performance.

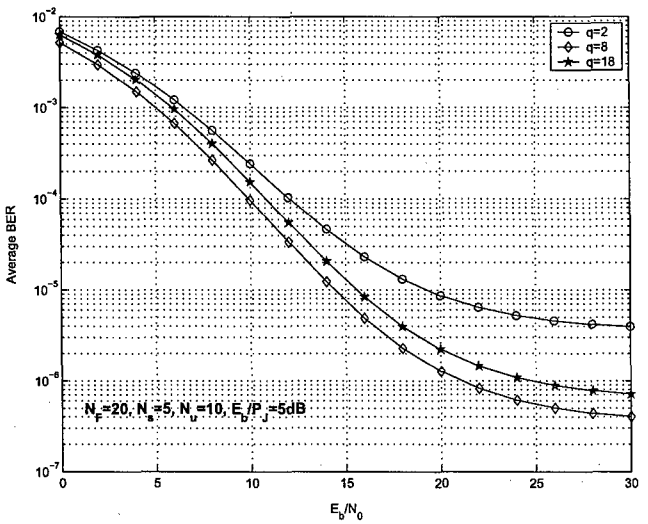

Figure 8: The average BER for different q.

6 Conclusions

In this paper, we make an performance analysis with the presence of the multi-tone/pulse jammer interference and multi-user interference based on the hybrid FH/TH-PPM-UWB system. We get an accurate expressions of SER and BER with the presence of MUI and hostile jammer interference. We evaluate the performances for different number of symbols to carrry one information bit N_s; the signal to jammer interference ratio E_b/P_J; the number of FH sub-bands N_F; the number of tones q of the jammer interference; the number of users sharing the same sub-band N_u; and the total number of users in the wireless sensor networks N_U, and the access rate for each sensor nodes λ, in terms of BER and SER so as to show how these parameters affect to the FH/TH-PPM UWB system.

Acknowledgement

This work was supported by the Office of Naval Research (ONR) Young Investigator Award under Grant N00014-03-1-0466, "Energy Efficient Wireless Sensor Networks for Future Combat

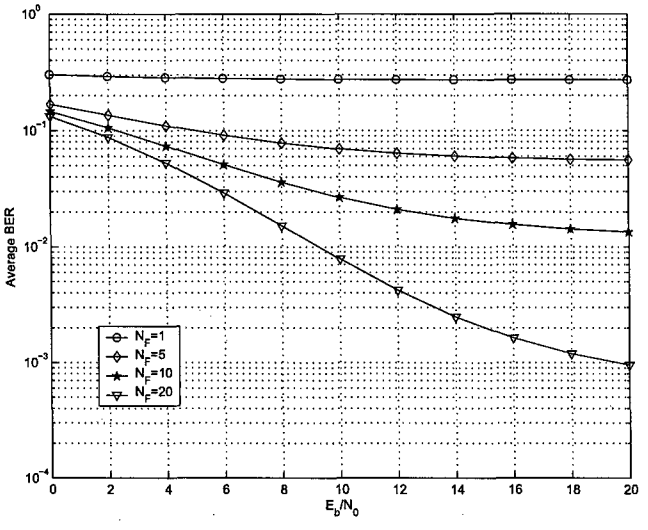

Figure 9: The average BER for different N_F.

System Using Fuzzy Logic."

References

[1] M.D. Benedetto and G. Giancola *Understanding Ultar Wide Band Radio Fundamentals*, Prentice Hall Technical Reference, NJ, USA, 2004

[2] J. Foerster (editor), "Channel Modeling Sub-committee Report Final," IEEE802.15-02/490 (see http://ieee802.org/15/.

[3] V. Lottici, A. D. Andrea and U. Mengali "Channel Estimation for Ultra-Wideband Communications," *IEEE Journal on Selected Areas in Communications*, vol. 20, No. 9, pp. 1638-1645, Dec 2002.

[4] R. A. Scholtz, "Multiple Access with Time-Hopping Impulse Modulation," *IEEE Militray Communication Conference*, vol. 2, pp. 447-450, Oct 1993.

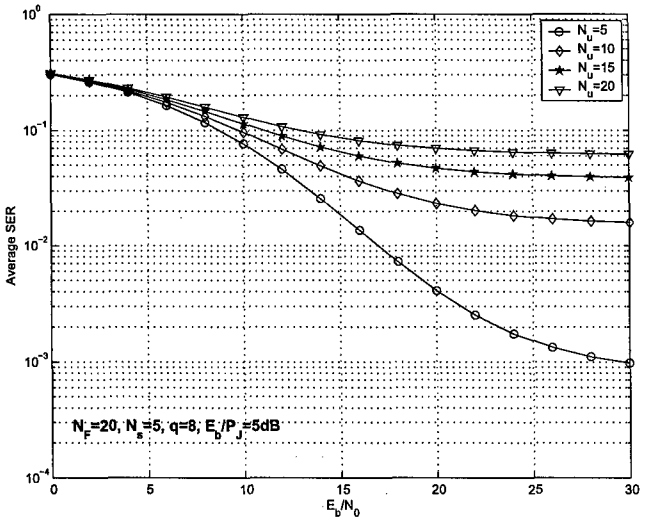

Figure 10: The average SER for different N_u.

[5] M. Z. Win and R. A. Scholtz, "Ultra-wide Bandwidth Time-Hopping Spread-Spectrum Impulse Radio for Wireless Multiple Access Communications," *IEEE Transactions on Communications*, vol. 48, Issue: 4, pp. 679-691, April 2000.

[6] B. Hu, and N. C. Beaulieu, " Accurate Performance Evaluation of Time-Hopping and Direct-Sequence UWB Systems in Multi-User Interference ," *IEEE Transactions on Communications*, Volume: 53, No. 6, pp. 1053-1062, June. 2005.

[7] L. Yang and G. B. Giannakis "A General Model and SINR Analysis of Low Duty-Cycle UWB Access Through Multipath With Narrowband Interference and Rake Reception," *IEEE Transactions on Communications*, Vol. 4, No. 4, pp. 1818-1833, July 2005.

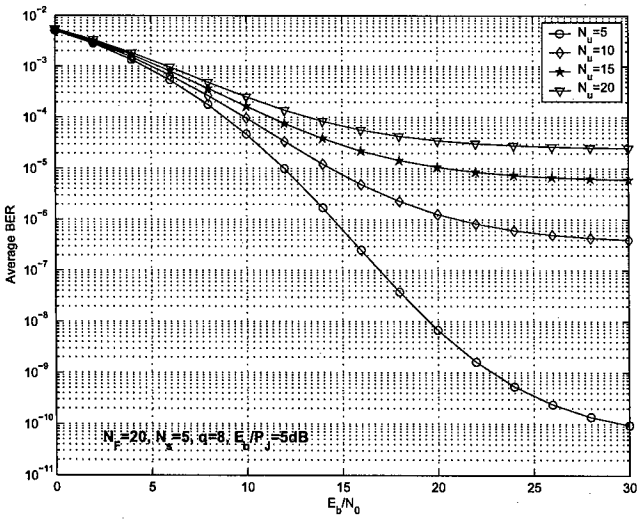

Figure 11: The average BER for different N_u.

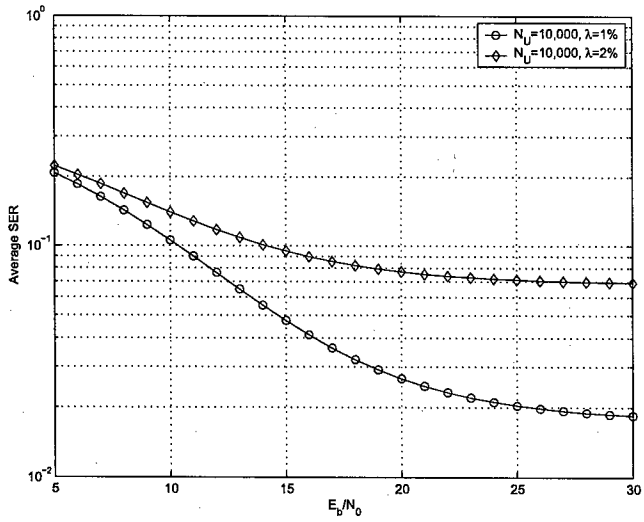

Figure 12: The average SER for different N_U.

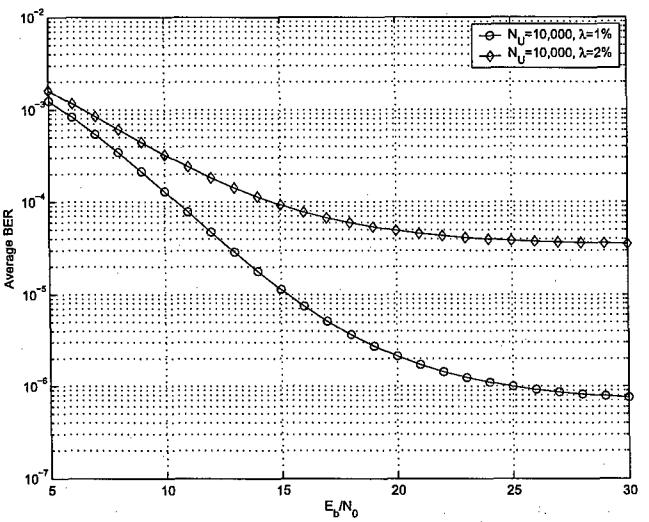

Figure 13: The average BER for different N_U.

Resource Allocation and Latency Estimation in Wireless Sensor Networks Using Maximum Likelihood Decision

Liang Zhao and Qilian Liang
Department of Electrical Engineering
University of Texas at Arlington
Arlington, TX 76010, USA
Email: zhao@wcn.uta.edu, liang@uta.edu

Abstract

In this paper, we address a fundamental problem in Wireless Sensor Networks, how many hops does it take for a packet to be relayed for a given distance? For a deterministic topology, this question reduces to a simple geometry problem. However, a statistical study is needed for randomly deployed WSNs. We propose a Maximum Likelihood decision based on the joint pdf of (H, n), which is also derived in this paper. Since the solution is not closed-form, we also propose an attenuated Gaussian approximation for the joint pdf. We show that the approximation visibly simplifies the decision process and the error analysis. The latency and energy consumption estimation are also included as application examples.

I. Introduction

The recent advances in MEMS, embedded systems and wireless communications enable the realization and deployment of wireless sensor networks (WSN), which consist of a large number of densely deployed and self-organized sensor nodes. The potential applications of WSN, such as environment monitor, often emphasize the importance of location information. Accordingly geographic routing [1] was proposed to handle such requirement. Most likely, a packet is not routed to a specific node, but a given location. An interesting question arises as "how many

hops does it take to reach a given location?" The prediction of the number of hops is important not only in itself but also in helping estimating the latency and energy cost, which are both important to the viability of WSN.

The question could become very simple if the sensor nodes are manually placed. For example, suppose sensor nodes are place in a square grid with separation of d. Obviously, the connectivity depends on the comparison of d and the transmission range R. Suppose $d < R < \sqrt{2}d$, this is simply a 4-connectivity network. For any node, the possible distance of its first-hop neighbors is $\{d\}$, the possible distances of its second-hop neighbors are $\{\sqrt{2}d, 2d\}$ and so on. Generally, the possible distances of its nth-hop neighbors are $\{\sqrt{(n-i)^2 + i^2}d, i = 0, 1, 2, \cdots, [n/2]\}$, where $[n/2]$ is the smallest integer not less than $n/2$. If we compare the given distance with these distances, the required number of hops can be easily found. For some given distance, there could be two solutions, such as $(8-1)^2 + 1^2 = (10-5)^2 + (10-5)^2 = 50$, then we have to select the number of hops with higher probability. For geographic approach, such conflicts can be easily solved with loss of accuracy. Thus, geographic approach is more efficient and accurate than statistical approach on deterministic topology.

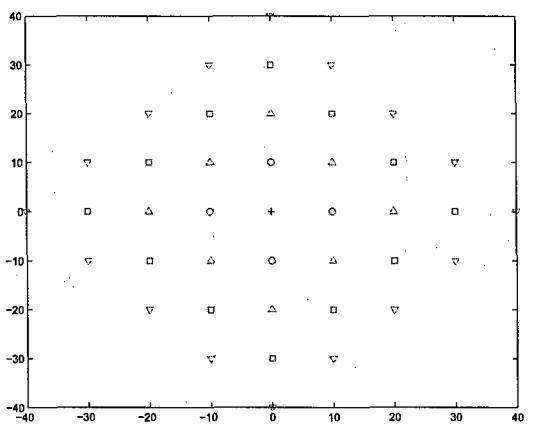

Fig. 1. The nodes in a square grid placement. Only nodes within 4 hops are shown.

However, if sensor nodes are deployed in a random fashion, which is the case for most potential application, the answer is beyond the reach of simple geometry. The stochastic nature of the random deployment calls for a statistical study. A natural and obvious estimation would be dividing the distance by the average inter-node distance (i.e., the average single-hop distance).

However, such estimation may be unable to provide the required accuracy. A probabilistic study is needed here, that is, finding $f(H|d)$, where H is the number of hops. Although the question raised here is not directly addressed before, a mirror problem, finding $f(d|h)$, has been well studied. In [2], Hou and Li studied the 2-D Poisson distribution to find a optimal transmission range. They found that the hop-distance distribution is determined not only by node density and transmission range but also by the routing strategy. They showed results for three routing strategies, Most Forward with Fixed Radius, Nearest with Forward Progress, and Most Forward with Variable Radius. Cheng and Robertazzi in [3] studied the one-dimension Poisson point and found the pdf of r_i as

$$f_{r_i}(r_i) = \frac{\lambda e^{-\lambda(R-r_i)}}{1 - e^{-\lambda(R-r_{e_{i-1}})}}, \tag{1}$$

where R is the transmission range, λ is the node density, r_i is the distance from the source to a ith-hop point and r_i is related to r_{e_i} by

$$r_{e_i} + r_i = R. \tag{2}$$

The pdf of r_{e_i} is also obtained,

$$f_{r_{e_i}}(r_{e_i}) = \frac{\lambda e^{-\lambda r_{e_i}}}{1 - e^{-\lambda(R-r_{e_{i-1}})}}. \tag{3}$$

Obviously, the distribution of r_i depends on previous r_j, $j < i$. They also pointed out the 2-D Poisson point distribution is analogous to the 1-D case, replacing the length of the segment by the area of the range.

Vural and Ekici reexamined the study under the sensor networks circumstances in [4], and gave the mean and variance of multi-hop distance. They also proposed to approximate the multi-hop distance using Gaussian.

The rest of this paper is organized as follows. We provide some preliminaries on skewness and kurtosis in Sectionsect:Preliminaries. The number of hops predication problem is addressed and solved in Section III. Since this problem has no closed-form solution, we propose an attenuated Gaussian approximation and show how to simplify the error analysis in Section IV. An application example is shown in Section V. Section VI concludes this paper.

II. Preliminaries :Skewness and Kurtosis

In this section, we provide some preliminaries on statistical methods [5]. Skewness is a measure of symmetry, or more precisely, the lack of symmetry. A distribution, or sample set, is symmetric if it looks the same to the left and right of the center point.

Definition 1: [5] For a given sample set X,

$$m_3 = \Sigma(X - \bar{X})^3/n, \tag{4}$$

$$m_2 = \Sigma(X - \bar{X})^2/n, \tag{5}$$

where $\bar{X}$ is the sample mean of X, and n is the size of X. Then a *sample estimate of skewness coefficient* is given by

$$g_1 = \frac{m_3}{m_2^{\frac{3}{2}}}. \tag{6}$$

Skewness is zero for a symmetric distribution. Positive skewness indicates right skewness and negative indicates left.

Kurtosis is a measure of whether the data are peaked or flat relative to a normal distribution.

Definition 2: [5] A sample estimate of kurtosis for a sample set X is given by

$$g_2 = m_4/m_2^2 - 3, \tag{7}$$

where $m_4 = \Sigma(X - \bar{X})^4/n$ is the fourth-order moment of $\bar{X}$ about its mean.

Skewness and kurtosis is useful in determining whether a sample set is normal. Note that the skewness and kurtosis of a normal distribution are both zero; significant skewness and kurtosis clearly indicate that data are not normal.

III. The Number of Hops Prediction

A. Problem Formulation

We make the following assumptions.

- The nodes are deployed at random on a plan, that is, the node distribution follows 2D Poisson random process. Thus, the probability of "there is no node in a given area A" is given by [6]

$$Pr(\text{No nodes in } A) = e^{-\lambda A}, \tag{8}$$

where λ is the density of nodes.

- The distance from the source to the destination d is known, which is common in geographic routing.
- Neither of the source and destination is close to the border. This assumption holds true for most of the nodes if the network size is large enough.

The problem of interest is to find the number of hops, denoted H needed to reach a specific destination r from a given source node. We can make a Maximum Likelihood (ML) decision,

$$H = \underset{max}{\arg} f(H|r), H = 1, 2, 3, \cdots . \tag{9}$$

Considering

$$f(H|r) = \frac{f(H,r)}{f(r)}, \tag{10}$$

the decision rule can be translated into

$$H = \underset{max}{\arg} f(H,r), \tag{11}$$

where $f(H,r)$ is also called objective function. In the next subsection, we are concerned with deriving $p(H,r)$.

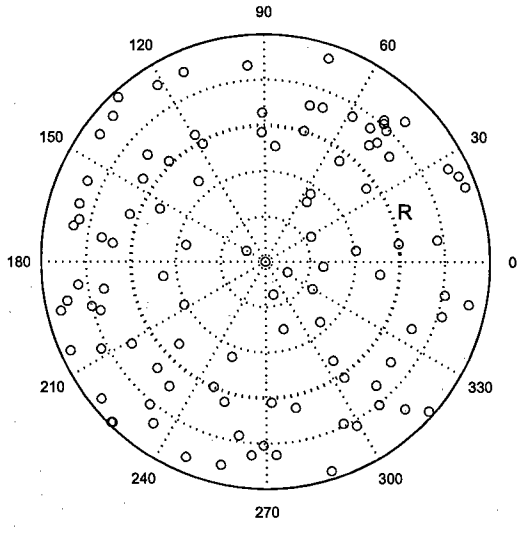

Fig. 2. Poisson node distribution.

B. Derivation of the Joint PDF $p(H, r)$

Let r denote the distance from the source to a node, the cdf of d is

$$F_r(r) = 1 - e^{-\lambda \pi r^2}. \tag{12}$$

And the pdf of d is

$$f_r(r) = \lambda 2\pi r e^{-\lambda \pi r^2}. \tag{13}$$

When $H = 1$, the joint cdf of (H, r_1)

$$p(H = 1, r_1) = \begin{cases} 1 - e^{-\lambda \pi r_1^2} & r_1 \leq R \\ 0 & r_1 > R \end{cases} \tag{14}$$

and the joint pdf is

$$f(H = 1, r_1) = \begin{cases} \lambda 2\pi r_1 e^{-\lambda \pi r_1^2} & r_1 \leq R \\ 0 & r_1 > R \end{cases} \tag{15}$$

Note that the conditional pdf of $H = 1$ given $r < R$ is unity for $r < R$, which is intuitively correct but simple, we are more interested in multi-hop distance. In the following, $r > R$ is assumed so that $H > 1$. The two-hop case is shown in Fig. 3, a second-hop node must satisfy

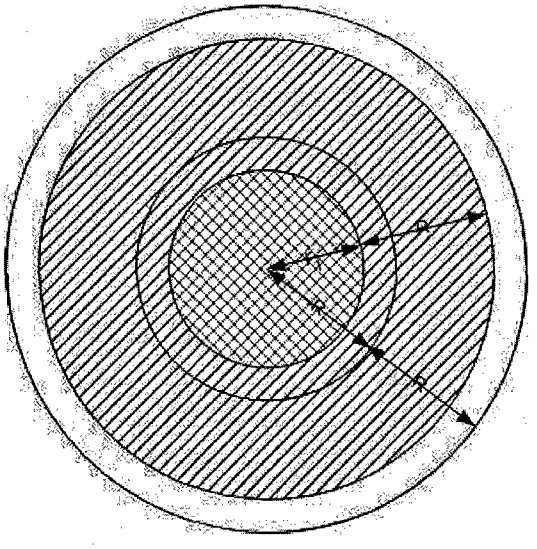

Fig. 3. The second-hop coverage.

$R < r_2 \leq 2R$. Furthermore, the farthest first-hop node is not necessarily at the maximum transmission range, which means, there is a gap r_{e_1} between R and r_1, i.e.,

$$r_{e_1} + r_1 = R. \tag{16}$$

Therefore, the joint pdf of (H_1, r_{e_1}) is

$$f(H=1, r_{e_1}) = \begin{cases} \lambda 2\pi (R - r_{e_1}) e^{-\lambda\pi(R-r_{e_1})^2} & r_{e_1} \leq R \\ 0 & O.W. \end{cases} \tag{17}$$

And accordingly, the joint cdf of (H_2, r_2) is

$$p(H=1, r_2|r_1) = \begin{cases} e^{-\lambda\pi[(R+r_1)^2-(r_2+r_1)^2]} - e^{-\lambda\pi[(R+r_1)^2-r_1^2]} & R < r \leq 2R \\ 0 & O.W. \end{cases} \tag{18}$$

Generally, for $H = n$ (shown in Fig.4), we have

$$p(H_n, r_n|r_1, r_2, \cdots, r_n - 1) = \begin{cases} e^{-\lambda\pi[(R+\sum_{i=1}^{n-1} r_i)^2-(\sum_{i=1}^{n} r_i)^2]} - e^{-\lambda\pi[(R+\sum_{i=1}^{n-1} r_i)^2-(\sum_{i=1}^{n-1} r_i^2]} & \\ & R < r \leq nR \\ 0 & O.W. \end{cases} \tag{19}$$

and

$$\begin{aligned} & p(H_n, r_n) = \\ & \int_R^{(n-1)R} \int_R^{(n-2)R} \cdots \int_0^R p(H_n, r_n|r_1, r_2, \cdots, r_n - 1) \\ & f(H_{n-1}, r_{n-1}|r_1, r_2, \cdots, r_n - 2) \cdots \\ & f(H_1, r_1) dr_1 \cdots dr_{n-2} dr_{n-1} \end{aligned} \tag{20}$$

Theoretically, we can take derivative of (20) with respect to r to obtain the objective function, use (11) to decide the most likely H given r and give the probability of error for such a decision. However, (20) is awkward to evaluate and the computational cost could limit the applicability of such a decision scheme.

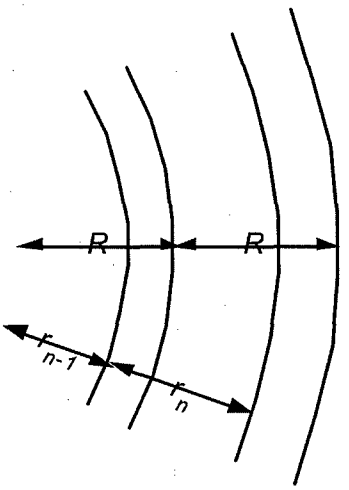

Fig. 4. The ith-hop coverage.

TABLE I

STATISTICS OF $f(H = n, r_n), n \geq 3$

Number of Hops	Mean	Std	Skewness	Kurtosis
1	19.991	7.0651	-0.57471	-0.58389
2	45.132	7.8365	-0.16958	-1.0763
3	72.01	8.2129	-0.10761	-1.0332
4	99.45	8.391	-0.07938	-0.97857
5	127.14	8.5323	-0.06445	-0.93104
6	154.96	8.6147	-0.05341	-0.9004
7	182.68	8.573	-0.07738	-0.91687

IV. ATTENUATED GAUSSIAN APPROXIMATION

Since (20) is awkward to evaluate even using numerical methods, we use histograms collected from Monte Carlo simulations as substitute to the joint pdf. All the simulation data are collected from such a scenario that N sensor nodes were uniformly distributed in a circular region of radius of 300 meters. For convenience, polar coordinates were used. The source node was placed at $(0, 0)$. The transmission range was set as R meters. For each setting of (N, R), we ran 300 simulations, in each of which all nodes are re-deployed at random. And the node density is

given by

$$\lambda = \frac{N}{\pi R^2} \tag{21}$$

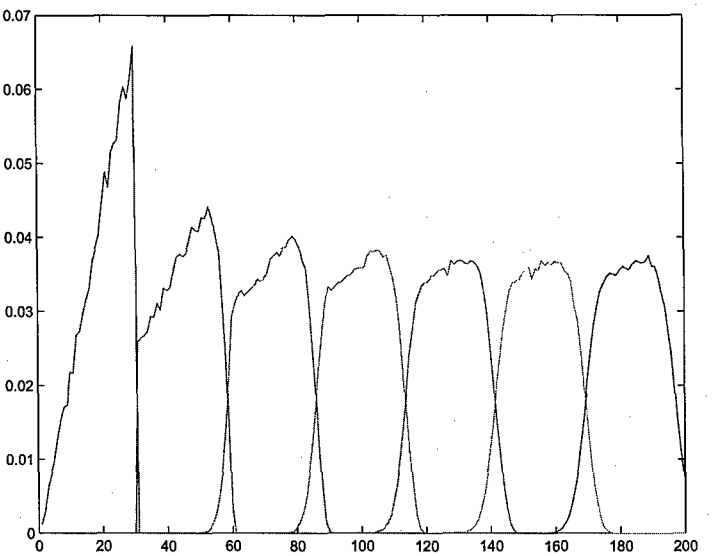

Fig. 5. Histograms of hop-distance joint distribution. ($R = 30$, $\lambda = 6.37(10)^{-3}$)

The histograms of $f(H, r)$ are plotted in Fig. 5, which clearly shows that the joint distribution of (H, r) approach the normal when H increases. Table I lists the first-, second-, third- and fourth-order statistics of $f(H, r)$. The skewness and kurtosis clearly satisfy the Gaussianity condition within tolerance of error. Thus, the objective function can be approximated by

$$\begin{aligned} f(H = n, r_n) &= \alpha^n \mathcal{N}(m_n, \sigma_n) \\ &= \frac{\alpha^n}{2\pi\sigma} e^{-\frac{(r-m_n)^2}{2\sigma_n^2}}, \end{aligned} \tag{22}$$

where α is the equivalent attenuation base, m_n and σ_n are the mean and standard deviation(std), respectively. The specific values of these parameters can be evaluated from (20) numerically or estimated from simulations. Observe Table I, for large n, the joint pdf of (H, r) has following properties,

1) $\sigma_n \approx \sigma_{n-1}$, which means the neighboring joint pdf's have similar spread.
2) $m_n - m_{n-1} \approx m_{n+1} - m_n$, which means the joint pdf's are evenly spaced.

3) $3 < \frac{m_n - m_{n-1}}{\sigma_n} < 5$, which means the overlap between the neighboring joint pdf's is small but not negligible. (As a rule of thumbs, $Q(3)$ is considered relatively small and $Q(5)$ is regarded negligible.)

4) $\frac{m_n - m_{n-2}}{\sigma_n} \gg 5$, which means the overlap between the non-neighboring joint pdf's is negligible.

5) $\alpha < 1$. For large density λ, $\alpha \to 1$. Along with Property 1, this tell us that the neighboring joint pdf's have nearly identical shape.

As shown in the following discussion, these properties largely simplify the decision rule and the error analysis. Another interesting observation, besides these properties, is that the following equations do not stand true.

$$m_n = nm_1 \tag{23}$$

$$m_n = nR \tag{24}$$

$$m_n = (n-1)R + R/2 \tag{25}$$

Although these equations sound plausible, they all give visible errors. The aforementioned estimator $[r/R] + 1$ for H, though widely used, is not good in the new light shed by this study. However, Property 2 does tell us the increment for m_n is constant, if denoted by Δ,

$$m_n = m_1 + (n-1)\Delta \tag{26}$$

We showed in [7] that $m_1 = 2/3R$, irrelevant to the node density. Although Δ is a function of λ and R, λ is often regarded constant for a specific application and R varies in a short range, thus, we can safely expect $\Delta = aR$, where a is a constant, for example, $a = 0.9$ for the data in Table I. In summary, the following empirical equation stands for most application for WSN.

$$m_n = R(\frac{2}{3} + (n-1)a) \tag{27}$$

The above results about the constant increment of mean hop-distance is used in Section V-B for energy consumption estimation.

A. Decision Boundaries

Following (11), we decide H given r using the following rule.

$$H = arg_{max} f(H, r) \tag{28}$$

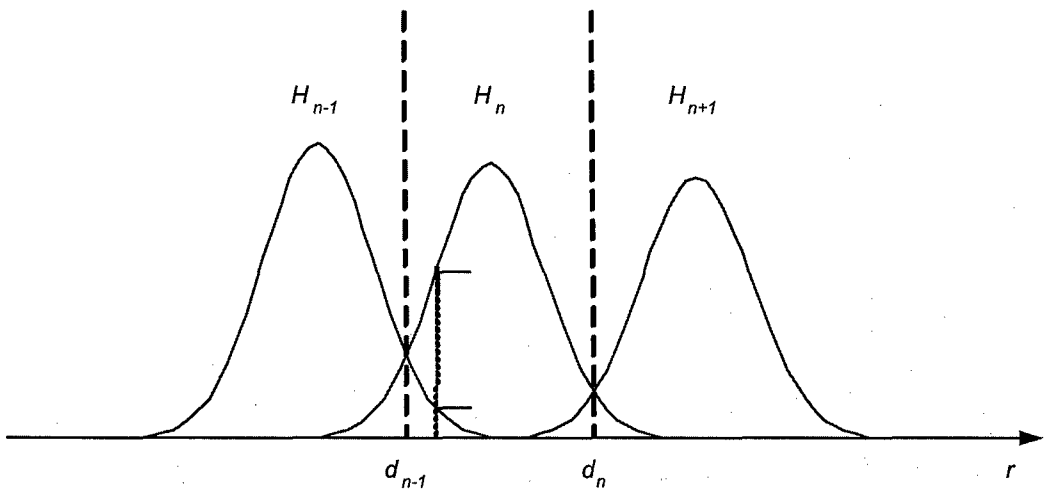

Fig. 6. Gaussian Approximation.

Observe the $f(H_n, r_n)$ in Fig. 6, the decision is needed only between neighboring H, that is,

$$f(H = n, r) \underset{n+1}{\overset{n}{\gtrless}} f(H = n + 1, r). \tag{29}$$

This is because, for a specific value of r, there are only two H_n with dominating $f(H = n+1, r)$, compared to which $f(H = n + 1, r)$ for other values of H_n is negligible. Substitute (22) into (29), we obtain the decision boundary d_n between the regions $H = n$ and $H = n + 1$.

$$\begin{aligned} d_n &= \frac{B + \sqrt{B^2 + AC)}}{A} \\ A &= \sigma_{n+1}^2 - \sigma_n^2 \\ B &= m_n\sigma_{n+1}^2 - m_{n+1}\sigma_n^2 \\ C &= m_n^2\sigma_{n+1}^2 - m_{n+1}^2\sigma_n^2 + 2\sigma_n^2\sigma_{n+1}^2 \ln\alpha \end{aligned} \tag{30}$$

Using Property 1,

$$d_n = \frac{m_{n+1}^2 - m_n^2 - 2\sigma_n^2 \ln\alpha}{2(m_{n+1} - m_n)} \tag{31}$$

For large density λ, Property 5 is applicable, (30) simplifies to

$$d_n = \frac{\sigma_n^2 m_{n+1} + \sigma_{n+1}^2 m_n}{\sigma_n^2 + \sigma_{n+1}^2} \tag{32}$$

Applying Property 1 to (32),

$$d_n = \frac{m_n + m_{n+1}}{2} \tag{33}$$

If we use the empirical equation (27),

$$d_n = \frac{2}{3}R + (n - \frac{1}{2})aR \tag{34}$$

No matter which approximate solution we choose for d_n, the decision rule is given by

$$r \underset{n}{\overset{n+1}{\gtrless}} d_n. \tag{35}$$

In other words,

$$\text{we decide } H = \hat{n} \text{ if } d_{\hat{n}-1} < r \leq d_{\hat{n}}, \tag{36}$$

which is equivalent to

$$n = [\frac{r - \frac{2}{3}R}{aR} + \frac{1}{2}] + 1. \tag{37}$$

B. Error Performance Analysis

For out decision rule, a decision error occurs when $H = n \neq \hat{n}$. Thus, the probability of error with a specific r is

$$p(\epsilon, r) = \sum_{n \neq \hat{n}} f(n, r). \tag{38}$$

The total probability of error is obtained by integrating (38) over all possible r.

$$p(\epsilon) = \int p(\epsilon, r) dr \tag{39}$$

According to Property 4, only $f(n-1, r)$ and $f(n+1, r)$ could have outstanding value over the decision region $[d_{n-1}, d_n]$.

$$\begin{aligned} p(\epsilon) &\approx \sum_{n=2}^{\infty} \int_{d_{n-1}}^{d_n} f(n-1, r) + f(n+1, r) dr \\ &= \sum_{n=2}^{\infty} \alpha^{n-1} [Q(\frac{d_{n-1} - m_{n-1}}{\sigma_{n-1}}) - Q(\frac{d_n - m_{n-1}}{\sigma_{n-1}})] \\ &\quad + \alpha^{n+1} [Q(\frac{m_{n+1} - d_n}{\sigma_{n+1}}) - Q(\frac{m_{n+1} - d_{n-1}}{\sigma_{n+1}})] \end{aligned} \tag{40}$$

Note that

$$\begin{aligned} & \frac{d_n - m_{n-1}}{\sigma_{n-1}} - \frac{d_{n-1} - m_{n-1}}{\sigma_{n-1}} \\ = \; & \frac{d_n - d_{n-1}}{\sigma_{n-1}} \gg 1, \end{aligned} \tag{41}$$

therefore, $Q(\frac{d_n - m_{n-1}}{\sigma_{n-1}})$ is negligible compared to $Q(\frac{d_{n-1} - m_{n-1}}{\sigma_{n-1}})$. Similarly, $Q(\frac{m_{n+1} - d_n}{\sigma_{n+1}})$ is negligible. (40) is approximated by

$$\begin{aligned} p(\epsilon) \; \approx \; & \alpha^3 Q(\frac{m_3 - d_2}{\sigma_3}) + \sum_{n=3}^{\infty} [\alpha^{n-1} Q(\frac{d_{n-1} - m_{n-1}}{\sigma_{n-1}}) \\ & + \alpha^{n+1} Q(\frac{m_{n+1} - d_n}{\sigma_{n+1}})] \\ = \; & \alpha^2 Q(\frac{d_2 - m_2}{\sigma_2}) + \sum_{n=3}^{\infty} \alpha^n [Q(\frac{m_n - d_{n-1}}{\sigma_n}) \\ & + Q(\frac{d_n - m_n}{\sigma_n})] \end{aligned} \tag{42}$$

Substituting an appropriate solution of d_n into (42) would give us the probability of error within required accuracy. For example, if we choose (33),

$$\begin{aligned} p(\epsilon) \; \approx \; & \alpha^2 Q(\frac{m_3 - m_2}{2\sigma_2}) + \sum_{n=3}^{\infty} \alpha^n [Q(\frac{m_n - m_{n-1}}{2\sigma_n}) \\ & + Q(\frac{m_{n+1} - m_n}{2\sigma_n})] \end{aligned} \tag{43}$$

V. Application Examples

A. Latency Estimation

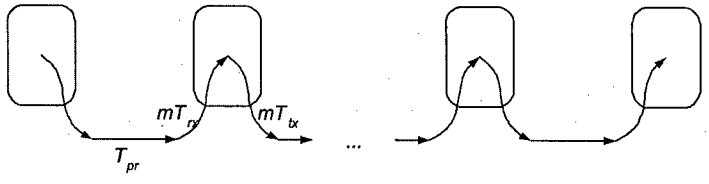

Fig. 7. Time model.

Suppose it takes T_{rx} for a sensor node to receive 1 bit of message and T_{tx} to transmit. Considering the transmission range in sensor networks is usually short compared to the light speed, the propagation time T_{pr} is negligible. Shown in Fig. 7, given the end-to-end distance r, we can find the required number of hops $H = \hat{n}$ according to (35), thus, a good estimator of the total latency of a l-bit message is

$$l[T_{tx} + (\hat{n} - 1)(T_{tx} + T_{rx}) + T_{rx}] \tag{44}$$

$$= l\hat{n}(T_{tx} + T_{rx}) \tag{45}$$

B. Energy Consumption Estimation

The following model is adopted from [8] where perfect power control is assumed. To transmit l bits over distance d, the sender's radio expends

$$E_{tx}(l, d) = \begin{cases} lE_{elec} + l\epsilon_{fs}d^2 & d < d_0 \\ lE_{elec} + l\epsilon_{mp}d^4 & d \geq d_0 \end{cases} \tag{46}$$

and the receiver's radio expends

$$E_{rx}(l, d) = lE_{elec}. \tag{47}$$

E_{elec} is the unit energy consumed by the electronics to process one bit of message, ϵ_{fs} and ϵ_{mp} are the amplifier factor for free-space and multi-path models, respectively, and d_0 is the reference distance to determine which model to use. The values of these communication energy parameters are set as in Table II.

TABLE II

ENERGY CONSUMPTON PARAMETERS

Name	Value
d_0	86.2m
E_{elec}	$50nJ/bit$
E_{DA}	$5nJ/bit$
ϵ_{fs}	$10pJ/bit/m^2$
ϵ_{mp}	$0.0013pJ/bit/m^4$

Let s_n denote the single-hop distance from the $(n-1)$th-hop to the nth-hop. Obviously, $s_n \leq R$. In our experimental setting, $R = 30m < d_0$ so that the free space model is always used. This agrees well with most applications, in which multi-hop short-range transmission is preferred to avoid the exponential increase in energy consumption for long-range transmission. Naturally, the end-to-end energy consumption for sending l bits over distance r is given by

$$\begin{aligned} E_{total}(l,r) &= \sum_{1}^{\hat{n}} \{E_{tx}(l,r) + E_{rx}(l)\} \\ &= l\sum_{1}^{\hat{n}} \{E_{elec} + \epsilon_{fs} s_n^2 + E_{elec}\}, \end{aligned} \tag{48}$$

where $\hat{n}$ is the decision result for given r. On the average,

$$\bar{E}_{total}(l,r) = 2\hat{n}lE_{elec} + \epsilon_{fs}\sum_{1}^{\hat{n}} E[s_n^2] \tag{49}$$

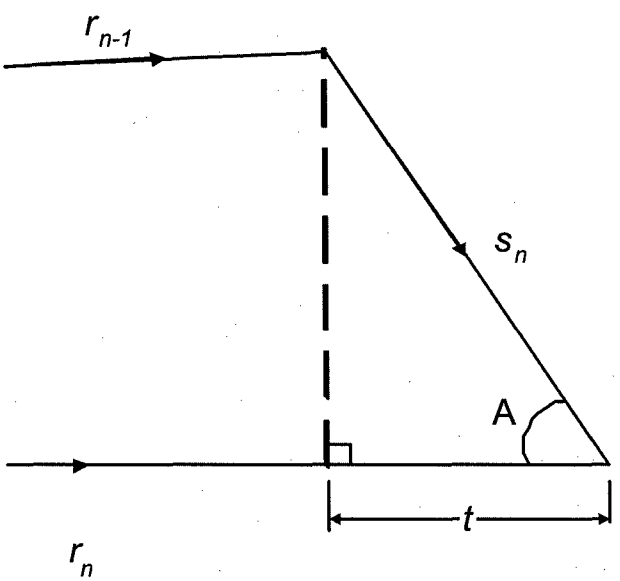

Fig. 8. The relationship between r_n, r_{n-1} and s_n.

The relationship between r_n, r_{n-1} and s_n is depicted in Fig.8.

$$\begin{aligned} t &= s_n \cos A \\ \cos A &= \frac{s_n^2 + r_n^2 - r_{n-1}^2}{2 s_n r_n} \\ \therefore s_n^2 &= r_{n-1}^2 - r_n^2 + 2 t r_n \end{aligned} \tag{50}$$

For large n, $r_n \gg s_n$ and $r_{n-1} \gg s_n$, therefore, $t \to \Delta$. According to Property 2, Δ can be treated as a constant.

$$\begin{aligned} E[s_n^2] &\approx E[r_{n-1}^2] - E[r_n^2] + 2\Delta E[r_n] \\ &= \sigma_{n-1}^2 - \sigma_n^2 + 2\Delta m_n \qquad (51) \\ (\because \text{Property 1}) &\approx 2\Delta m_n \qquad (52) \end{aligned}$$

Substitute (52) into (49),

$$\bar{E}_{total}(l, r) = 2\hat{n} l E_{elec} + 2\epsilon_{fs} \Delta \sum_{1}^{\hat{n}} m_n \tag{53}$$

VI. Conclusion

To predict the number of hops H needed to reach a given distance r in randomly deployed sensor networks, we proposed a ML decision based on the joint pdf of (H, n), which was also derived in this paper. Since the solution is not closed-form, we also proposed an attenuated Gaussian approximation for the joint pdf. We show that the approximation visibly simplifies the decision process and the error analysis. The latency and energy consumption estimation are also included as application examples.

Acknowledgment

This work was supported by the U.S. Office of Naval Research (ONR) Young Investigator Award under Grant N00014-03-1-0466.

References

[1] R. Jain, A. Puri, and R. Sengupta, "Geographical routing using partial information for wireless ad hoc networks," *IEEE Personal Communications*, vol. 8, pp. 48 – 57, Feb 2001.

[2] T.-C. Hou and V. Li, "Transmission range control in multihop packet radio networks," *Communications, IEEE Transactions on [legacy, pre - 1988]*, vol. 34, no. 1, pp. 38–44, 1986.

[3] Y.-C. Cheng and T. Robertazzi, "Critical connectivity phenomena in multihop radio models," *Communications, IEEE Transactions on*, vol. 37, no. 7, pp. 770–777, 1989.

[4] S. Vural and E. Ekici, "Analysis of hop-distance relationship in spatially random sensor networks," in *MobiHoc '05: Proceedings of the 6th ACM international symposium on Mobile ad hoc networking and computing*. New York, NY, USA: ACM Press, 2005, pp. 320–331.

[5] G. Snedecor and W. Cochran, *Statistical Methods*. Iowa State University Press / AMES, 1989.

[6] M. G. Kendall and P. A. P. Moran, *Geometrical Probability*. Charles Griffin & Co. Ltd., 1963.

[7] L. Zhao and Q. Liang, "Modeling end-to-end distance for given number of hops in wireless sensor networks," in *WCNC'06*, under review, 2006.

[8] W. B. Heinzelman, A. P. Chandrakasan, and H. Balakrishnan, "An application-specific protocol architecture for wireless microsensor networks," *IEEE Trans. Wireless Commun.*, vol. 1, no. 4, pp. 660 – 670, Oct. 2002.

Optimal Cluster Size for Underwater Acoustic Networks

Liang Zhao and Qilian Liang
Department of Electrical Engineering
University of Texas at Arlington
Arlington, TX 76010, USA
Email: zhao@wcn.uta.edu, liang@uta.edu

Abstract

In this paper, we are concerned with the optimal cluster size in Underwater Acoustic networks. Due to the sparse deployment and channel property, the clustering characteristics of UA is different from that of aerial sensor networks. We show that the optimal cluster size is also relevant to the working frequency of the acoustic transmission. Furthermore, we show that assigning working frequency to cluster members according to their distances to the cluster head could minimize the energy consumption.

I. Introduction and Motivation

An UnderWater Acoustic Sensor Network (UW-ASN) can be thought of as an *ad hoc* network consisting of sensors linked by an acoustic medium to perform distributed sensing tasks. To achieve this objective, sensors must self-organize into an autonomous network which can adapt to the characteristics of the underwater environment. UW-ASNs share many communication technologies with traditional *ad hoc* networks and terrestrial wireless sensor networks, but there are some vital differences such as limited energy and bandwidth constraint [1], thus the protocols developed for traditional wireless ad hoc networks are not necessarily well suited to the unique features of WSNs. When a wireless sensor may have to operate for a relatively long duration on a tiny battery, energy efficiency becomes a major concern.

Another issue in shallow water communications is that due to the limit of bandwidth in shallow water communications, multi-hop communication could introduce heavy interference

between cluster members, therefore, each sensor in a cluster communicate directly to its cluster head and intra-cluster communication should be coordinated by the cluster head in order to maximize the bandwidth usage.

The remainder of this paper is organized as follows.

II. Preliminaries

In this section, we provide some preliminaries needed for further discussion.

A. Underwater Acoustics Fundamentals

Based on the data and formulas in [2], Jurdak, Lopes and Baldi [3] derived the following model,

$$SL = TL + 85, \tag{1}$$

where SL is the source level and TL is the transmission loss. All the quantities in (1) are in $dB\ re\ \mu Pa$, where the reference value of 1 μPa amounts to $0.67 \times 10^{-22} Watts/cm^2$. For cylindrically spread signals, the transmission loss is approximated by [2],

$$TL = 10 \log d + \alpha d \times 10^{-}3, \tag{2}$$

where d is the distance betwen source and receiver in meters, α is the frequency dependent medium absorption coefficient. Fisher and Simmons [4] measured the medium absobtion in shallow seawater at temperatures at 4°C and 20°C. The average is obtained in [3],

$$\bar{\alpha} = \begin{cases} 0.0601 \times f^{0.8552} & 1 \leq f \leq 6 \\ 9.7888 \times f^{1.7885} \times 10^{-3} & 7 \leq f \leq 20 \\ 0.3026 \times f - 3.7933 & 20 \leq f \leq 35 \\ 0.504 \times f - 11.2 & 35 \leq f \leq 50. \end{cases} \tag{3}$$

To guarantee the reception quality, the required threshold of α, denoted by $\tilde{\alpha}$, might be chosen larger than $\bar{\alpha}$. However, we can generally expect $\tilde{\alpha}$ be a monotonically decreasing function of frequency f. To emphasize their relationship, $\tilde{\alpha}$ is written as $\tilde{\alpha}(f)$ in the rest of this paper. The transmitter power P_t required to achieve an intensity I_t at a reference distance of $1m$ is expressed as,

$$P_t = 2\pi \times 1m \times H \times I_t, \tag{4}$$

where I_t is related to SL by

$$I_t = 10^{SL/10} \times 0.67 \times 10^{-18}. \tag{5}$$

Summing up (1), (2), (4) and (5), we obtain

$$P_t = CHd10^{\alpha d10^{-3}}, \tag{6}$$

where C is a constant equaling $2\pi(0.67)10^{-9.5}$. Therefore, to transmit l bits over distance d, the sender's radio expends

$$E_{TX}(l,d) = lE_{elec} + lT_bP_t \tag{7}$$

and the receiver's radio expends

$$E_{RX}(l,d) = lE_{elec}, \tag{8}$$

where T_b the bit duration, E_{elec} is the unit energy consumed by the electronics to process one bit of message.

III. Optimal Clustering

In this section, we make data-centric analysis of energy consumption in UW-ASN.

A. Problem Formulation

Clustering has been widely used in pattern recognition, and we use it to obtain the energy-efficient organization for UW-ASN. Consider a heterogeneous UW-ASN, in which the low-capacity sensors serves as cluster members and are randomly distributed, and the high-capacity sensors serve as cluster heads and are manually positioned. If we obtain the optimal cluster size, then the required number of high-capacity sensors and their ideal positions can also be determined. all the sensor are the same and elect some from them to be cluster heads. If we assume the high-capacity sensors have virtually unlimited energy reserve compared to the low-capacity ones, only the energy consumption of the low-capacity sensors need to be counted. The energy cost for each bit of data collected by the ith member of the kth cluster is

$$E_{CM(ki)} = E_{elec} + T_bP_t(ki) \tag{9}$$

$$P_t(ki) = CHr_{ki}10^{\alpha r_{ki}10^{-3}} \tag{10}$$

where r_{ki} is the distance from the kth cluster head and its ith member.

Considering all c clusters, the overall cost is

$$E_{total} = \sum_{k=1}^{c} \sum_{i=1}^{M_k} E_{CM(ki)}, \tag{11}$$

where M_k is the number of non-head members in the k cluster.

Taking the expected value of the overall energy cost, we obtain $\bar{E_{total}}$ as the objective function. Minimizing the overall energy consumption is equivalent to minimizing

$$J = E[r10^{\alpha r}]. \tag{12}$$

B. Solution for Random Deployment

Suppose the low-capacity sensors are deployed at random, then their locations would follow the two-dimension Poisson distribution, i.e., the number of nodes N_A in area A is given by,

$$Pr(N_A) = (\lambda A)^{N_A} e^{-\lambda A}/N_A!, \tag{13}$$

where λ is the node density. A useful property of the Poisson process is that *if the number of nodes occurring in the area A is N, then the individual outcomes of N nodes are distributed independently and uniformly in the area A.* For the single-hop cluster, in which all cluster members can communicate with the cluster head directly, the distance r between any cluster member to the cluster head has the cdf given by

$$F(r) = \frac{\pi r^2}{\pi R^2}, \tag{14}$$

where R is the cluster size. Thus the pdf of r is

$$f(r) = \frac{2r}{R^2}. \tag{15}$$

Suppose the frequency allocation is irrelevant to r, which is the case for most applications in use, $\alpha(f)$ and r is independent. Substitute (15) into (12),

$$J = E[r10^{r}]10^{\alpha}. \tag{16}$$

$$\begin{aligned} E[r10^{r}] &= \int_0^R r10^{r}\frac{2r}{R^2}dr \\ &= [10^{r}(\frac{r^2}{\ln 10} - \frac{2r}{\ln^2 10} + \frac{2}{\ln^3 10})]_0^R \\ &= 10^{R}(\frac{R^2}{\ln 10} - \frac{2R}{\ln^2 10} + \frac{2}{\ln^3 10}) + 10\frac{2}{\ln^3 10} \end{aligned} \tag{17}$$

By setting the derivative of (17) to zero, we obtain

$$R_{opt} = \sqrt{2}/\ln 10. \tag{18}$$

IV. Conclusion

Although clustering has been well studied for the terrestrial WSN, the unique characteristics of the underwater acoustic communications call for a new study. Because the path loss is not only relevant to the distance, but also related to the working frequency, the optimal cluster size for UW-ASN shows different properties from the terrestrial WSN. Furthermore, we show that assigning working frequency to cluster members according to their distances to the cluster head could minimize the energy consumption.

Acknowledgment

This work was supported by the U.S. Office of Naval Research (ONR) Young Investigator Award under Grant N00014-03-1-0466.

References

[1] I. F. Akyildiz, D. Pompili, and T. Melodia, "Underwater acoustic sensor networks: Research challenges," *Ad Hoc Networks (Elsevier)*, vol. 3, no. 3, pp. 257–279, May 2005.

[2] R. Urick, *Principles of Underwater Sound.* Mcgraw-Hill, 1983.

[3] R. Jurdak, C. V. Lopes, and P. Baldi, "Battery lifetime estimation and optimization for underwater sensor networks," in *IEEE Sensor Network Operations*. IEEE Press, Winter 2004.

[4] F. Fisher and V. Simmons, "Sound absorption in sea water," *Journal of Acoustical Society of America*, vol. 62, p. 558, 1977.

A Distributed Query Processing Algorithm for Wireless Sensor Networks

Qingchun Ren and Qilian Liang
Department of Electrical Engineering
University of Texas at Arlington
Arlington, TX 76019-0016, USA
Email: ren@wcn.uta.edu, liang@uta.edu

Abstract— **Query processing methods have been studied extensively in traditional database systems. But few of them can be directly applied into sensor database systems due to the characteristics of sensor networks: decentralized nature of sensor networks, limited computational power, imperfect information recorded, and energy scarcity of individual sensor nodes. In this paper, we propose a quality-guaranteed and energy-efficient algorithm (QGEE) for sensor database systems. We employ an in-network query processing method to task sensor networks through declarative queries. Given a query, our QGEE will adaptively form an optimal query plan in terms of energy efficiency and query quality. The goal of our approach is to reduce interference coming from measurements with extreme errors and to minimize energy consumption by providing service that is considerably necessary and sufficient for the requirement of applications. Moreover, we employ probabilistic method to formulate the distribution of imperfect information sources in terms of probability distribution function (PDF), and acquire probabilistic query answers on uncertain data. The probability to an answer allows users to place appropriate confidence in it. The simulation results demonstrate that our algorithm can reduce resource usage and supply quality satisfied query answers to users.**

I. Introduction and Motivation

Recent developments in integrated circuit technology have allowed the construction of low-cost sensor nodes with signal processing and wireless communication capabilities. Wireless sensor networks (WSNs) are generally consisted of a large number of sensor nodes [2] operating under energy constraints in unattended mode, which are capable of limited computation, communication and sensing. WSNs are intended for a broad range of environmental sensing applications from weather data-collection to vehicle tracking and habitat monitoring [1] [3].

The widespread deployment of sensor nodes is transforming the physical world into a computing platform. Sensor nodes not only respond to physical signals to produce data, they also embed computing and communication capabilities. They are thus able to store, process locally and transfer the data they produce. From a data storage point of view, WSN can be regarded as a kind of database, distributed sensor database system (DSDS). DSDS, compared to traditional database systems, stores data within the network and allow queries to be injected anywhere through query processing operators in the network.

Existing query processing systems for WSNs, including Directed Diffusion [4], TinyDB [16], and Cougar [5], provide high-level interfaces that allow users to collect and process such continuous streams. Note that they are especially attractive as ways to efficiently implement monitoring applications without forcing users to write complex, low-level code for managing multihop network topologies or for acquiring samples from sensor nodes. TinyDB, Directed Diffusion and Cougar are relatively mature research prototypes that give some ideas on how future sensor network query processing systems will function. However, these future systems will be significantly more sophisticated than any of today's prototypes. To understand these requirements, queries may be classified along five dimensions- scope, volume, complexity, timeliness and quality-those dictate the design of networking mechanisms for query processing.

The goal of monitoring through sensor nodes is to infer information about objects from measurements made from remote locations. Since inference processes are always less than perfect, there is an element of uncertainty regarding the answers. When viewed from this perspective, the problem of uncertainty, which stands for the quality of query answers, is central to monitoring applications. Thus, to build useful information systems, it is necessary to learn how to represent and reason with imperfect information.

In this paper, we propose our solutions on query optimization and execution following acquisitional query processing (ACQP) approach [16]. Compared with typical methods, ACQP focuses on betaking the significant new query processing opportunity that arises in sensor networks: the fact that smart sensors have the capability to control over where, when, and how often data is physically acquired (i.e., sampled) and delivered to query processing operators. Motivated by these, we propose a quality-guaranteed and energy-efficient (QGEE) query processing algorithm for distributed and heterogenous WSNs. In the following sections, we outline QGEE paradigm, explain its key features, and describe in some detail using a particular example of environmental temperature monitoring. We specify local rules achieving, desired sensor nodes choosing, and query answers acquiring in terms of bounded probabilistic values. In doing so, we show how QGEE paradigm differs from existed query processing systems and qualitatively argue that this paradigm offering scaling,

robustness and energy efficiency benefits. We quantify some of these benefits via detailed packet-level simulations on QGEE.

The remainder of this paper is organized as follows: in Section II, we provide some preliminaries on vector space model and k-partial set cover problem; Section III formulates the problems we considered for our algorithm; Section IV presents our QGEE algorithm; simulation results are given in Section V; Section VI concludes this paper.

II. Preliminaries

A. Vector Space Model

Vector Space Model (VSM) [17] [18] is a way to represent documents through words that they contain. VSM has been widely used in the traditional information retrieval (IR) field [19] [20]. Most search engines also use similarity measures based on this model to rank Web documents. VSM creates a space in which both documents and queries are represented by vectors. For a fixed collection of documents, an m-dimensional vector is generated for each document and each query from sets of terms with associated weights. Then, a vector similarity function, such as the inner product, can be used to compute the similarity between a document and a query.

In VSM, weights associated with the terms are calculated based on the following two numbers:

- term frequency, f_{ij}, the number of occurrence of term y_i in document x_i; and
- inverse document frequency, $g_i = log(N/d_j)$, where N is the total number of documents in the collection and d_j is the number of documents containing term y_i.

The similarity $sim_{vs}(q, x_i)$ between a query q and a document x_i can be defined as an inner product of query vector Q and document vector X_i:

$$sim_{vs}(q, x_i) = Q \cdot X_i = \frac{\sum_{j=1}^{m} v_j \cdot w_{ij}}{\sqrt{\sum_{j=1}^{m}(v_j^2) \cdot \sum_{j=1}^{m}(w_{ij}^2)}} \quad (1)$$

where m_i is the number of unique terms in the document collection. Document weight $w_{i,j}$ and query weight v_j are

$$w_{ij} = f_{ij} w_{ij} = f_{ij} log(N/d_j) \quad and$$
$$v_j = \begin{cases} log(N/d_j) & y_j \, is \, a \, term \, in \, q \\ 0 & otherwise. \end{cases} \quad (2)$$

B. k-Partial Set Cover Problem

Covering problems are widely studied in discrete optimization. Basically, these problems involve picking a least-cost collection of sets to cover elements. Classical problems in this framework include general set cover problems and partial covering problems. k-partial set cover problem [21] as a partial covering problem is about how to choose a minimum number of sets to cover at least n elements, and which k elements should be chosen.

k-partial set cover problem can be formulated as an integer program as following.

MINIMIZE:

$$\sum_{j=1}^{m} c(S_j) \cdot x_j \quad (3)$$

SUBJECT TO:

$$y_i + \sum_{j:t_i \in S_j} x_j \geq 1 \qquad i = 1, 2, \ldots, n, \quad (4)$$

$$\sum_{i=1}^{n} y_i \leq n - k, \quad (5)$$

$$x_j \geq 0 \qquad j = 1, 2, \ldots, m, \quad (6)$$

$$y_i \geq 0 \qquad j = 1, 2, \ldots, n, \quad (7)$$

Where $x_i \in \{0,1\}$ corresponds to each $S_j \in S$. Iff set S_j belongs to the cover, then $x_j = 1$. Iff set t_j is not covered, then $y_i = 1$. $t_i \in \Gamma$.

III. Problem Formulation

As a motivation for our quality-guaranteed and energy-efficient query processing, we describe a scenario:

- A great multitude of temperature sensor nodes are randomly deployed in a region we interested. Individual sensor nodes (or in short, nodes) is connected to other nodes in its vicinity through a wireless communication interface, and it uses a multihop routing protocol to communicate with nodes that are spatially distant. All nodes are interconnected to at least one gateway directly or through intermedial nodes. Gateways are in charge of relaying data to a powered PC (front-end node) and, on the opposite direction, disseminating queries to related nodes. Within this sensor network, each node is provided with equal computing and sensing capability, but measurement quality may be different.

This scenario involves such a region-based query:

- *Environmental Temperature Monitoring:* With p confidence, tell the average temperature of nodes in the region defined by a rectangle (a,b,c,d).

Written in SQL-like language [15], this query is shown in Fig. 1.

```
SELECT          AVG(temp)
FROM            sensors
WHERE           loc in (a,b,c,d)  AND PROB>=p
SAMPLE PERIOD   100 seconds;
```

Fig. 1. Average Temperature Query in SQL Form

A. Source of Imperfect Information

Imperfect information is ubiquitous (almost all information that we have about the real world is not certain, complete or precise). In many occasions imperfect information can be classified into uncertainty, incompleteness, ambiguity and

imprecision proposed by Bonnissione, etc. [12], [14]. Incompleteness arises from the absence of values, imprecision from the existence of values which cannot be measured with suitable precision, ambiguity from vague statement, and uncertainty from the fact that an agent has constructed a subjective opinion about the truth of a fact which it does not know for certain.

In the context of our analyzing and understanding of query answer uncertainty, a significant challenge is how to understand the nature and the source of uncertainty well on temperature information derived from remote sensing. Image chain approach [6] is one of the most important and useful models for remote sensing processing. Image chain identifies steps in remote sensing process (or links in the chain) and illustrates that these steps are interrelated.

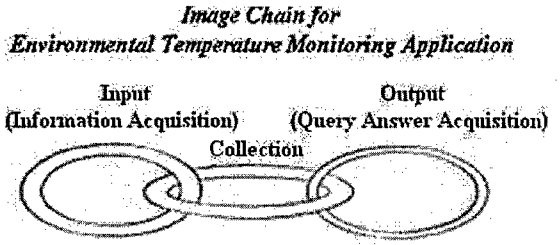

Fig. 2. Image Chain Model

Viewing the working process of our temperature monitoring application, there are three kinds of imperfect information source which contribute greatly to the uncertainty of query answers. They are measurement quality, point spread function (PSF) of nodes and link quality. Fig. 2 illustrates our image chain model. Links in the chain represent various steps in the remote sensing process from nodes collecting information related to environment (Input), flowing data records back to related front-end nodes (Collection) at run-time, to obtaining query answers through processing all collected information at front-end nodes (Output).

- *Measurement Quality of Nodes:* Measurement quality of nodes introduces uncertainty and imprecise information into query answers. As we know, the quality of nodes' sensing parts usually boils down to their measurement stabilities and measurement accuracies. In general, as measurement stability and accuracy increase, so do their power requirements and cost, which are all troublesome for general sensor nodes. Therefore, inaccurate measurements supplied by sensor nodes are very common phenomenons.
- *Point Spread Function (PSF) of Nodes:* PSF of nodes introduces ambiguity into query answers. Our temperature monitoring application is interested in the temperature over a region instead of one point in space. But considering operation feasibility, cost and speed, sampling method is widely used instead of completely measuring. In this aspect, another imperfect information source is raised: PSF of nodes. PSF is caused by nonuniform sensitivity within the region associated with nodes. Most nodes exhibit sensitivity variation similar to what is shown in Figure. 3. Note that, nodes are more sensitive to the the center of their regions than toward the edge.

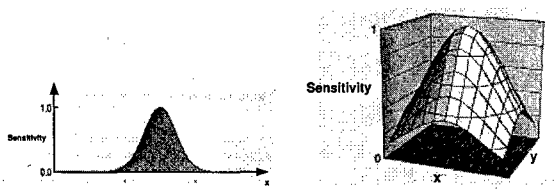

(a) (b)

Fig. 3. (a) 1-Dimension Gaussian model of a PSF and (b) 2-Dimension Gaussian model of a PSF

- *Link Quality:* Packets losing due to poor link quality introduces incompleteness into query answers. The dynamic and lossy nature of wireless communication pose major challenges to reliable, self-organizing WSNs. Packets transmission failures may happen during data transmission because of collision, node dying out (no battery), node being busy, or node's mobility. Moreover, in physical layer, sensor mobility generates channel fading during data transmission, which degrades the performance in terms of bit error rate (BER) and frame error rate.

Fixing other conditions, such as node density, communication range, sensing range and network coverage, we change measurement quality, PSF and link quality separately to evaluate the influences of those imperfect information sources on the correctness of query answers. The results are given in Table I. Note that with measurement errors, misrepresent errors, or missing information increased, the errors included in query answers are obviously increased and therefore the confidence of query answers is reduced.

TABLE I

USING ROOT MEAN SQUARE OF ERROR (RMSE) TO QUANTIFY THE ERRORS OF QUERY ANSWERS. LBR STANDS FOR LINK BREAK RATE.

RMSE	MeasureQuality		PSF (σ^2=1)		LinkQuality	
	σ=0.01	σ=0.1	r=1.65m	r=1.96m	LBR=0.1	LBR=0.5
MAX	0.2537	2.5618	22.882	25.17	0.2069	0.7132
MIN	0.2541	2.5416	22.905	25.195	0.1291	0.5895
AVG	0.0102	0.0944	3.0802	3.5202	0.0936	0.3127

B. Source of Energy Waste

Within a network, not all available nodes provide useful information that improves the accuracy of final results. Furthermore, some information might be redundant because nodes closing to each other would have similar data. From this prospect, collecting raw readings from all nodes to front-end nodes involves large amounts of raw readings which will lead to shorter lifetimes, especially for energy-limited WSNs.

For example, there is a WSN with n nodes. We assume that the lifetime for all nodes is T_{life} and queries submitted to the network are processed sequently. If there are ω queries (A_1, A_2, $\cdots$, and A_ω) relating to certain regions in this network ($\omega \leq n$), γ_1 nodes participate A_1 relating to area S_{A_1}, γ_2 nodes participate A_2 relating area S_{A_2}, $\cdots$, and γ_ω nodes participate A_ω relating to area S_{A_ω}. In this case, node density is $\frac{n}{\sum_{i=1}^{\omega} S_{A_i}}$ ($\gamma_1+\gamma_2+\cdots+\gamma_\omega=n$) and the lifetime of this network is $L_{t,w} = \omega T_{life}$. Note that, with the number of query ω decreasing, node density is increased ($\frac{n}{S_{A_1}} > \frac{n}{S_{A_1}+S_{A_2}} > \frac{n}{\sum_{i=1}^{\omega} S_{A_i}}$), and the lifetime of network is decreased ($L_{t,1} < L_{t,2} < L_{t,\omega}$).

For energy reservation issues on information collection, previous networking researches approach data aggregation [9] as an application specific technique to reduce the amount of data which is sent over the network. But where the aggregations should be carried out is a very essential and tough problem, which relates to the correctness and the effectiveness of operations.

IV. Quality-Guaranteed and Energy-Efficient (QGEE) Query Procession Algorithm Description and Discussion

Keeping these two problems: quality-required and power-limit in our mind, we propose a quality-guaranteed and energy-efficient (QGEE) query processing algorithm for WSNs. QGEE employs an in-network query processing method to task networks through declarative queries, which is critical for reducing network traffic when accessing and manipulating sensor data .

In QGEE algorithm, only a subset of nodes within a network will be chosen to acquire readings or samples corresponding to the fields or attributes referenced in queries. The goal of our approach is to reduce interference coming from measurements with extreme errors and to minimize energy consumption by providing service that is considerably necessary and sufficient for the needs of applications. Moreover, according to the analysis and classification on sources of imperfect information, we employ probabilistic method to formulate the distribution of them in terms of probability distribution function (PDF). Finally probabilistic query answers are acquired on uncertain data. The probability in a query answer allows users to place appropriate confidence in it as opposed to having an incorrect answer or no answer at all.

A. Confidence Control for Query Answers

1) Query Vector Space Model (VSM) Design and Active Nodes Selection: In information retrieval, VSM is a very efficient method to qualify the correlation between a query and all candidate documents. If we treat all sensor nodes as candidate documents for a query, the correlation between a query and nodes can be determined through the same principle used in information retrieval. Following factors are considered for our VSM vector design:

- Node Location
  Given a piece of region, the number and the location of nodes determine the observe proportion together. In order to employ as few as possible nodes to cover as large as possible region, we should select those nodes located at optimal locations. The detail on determining optimal locations is presented in Section IV-A.2.
- Measurement Quality
  Since the cost and the measurement quality of sensor nodes are related to each other, sensor nodes owning various quality levels are always deployed simultaneously in a WSN for economical reasons. Furthermore, through a query, database users supply not only what information they are interested in, but also the requirement on the quality of query answers, i.e., the confidence of query answers. In this case, we should select suitable nodes to response queries. In Table I, note that the RMSE of query answers are quite different under various measurement quality (in terms of different variance in that example).
- Remaining Battery Capacity
  Remaining battery capacity of sensor nodes is our third consideration factor. When the battery of a node is used up, data observed by this node will be missed, which will increase the uncertainty of query answer at some degree. This inspires us to select those nodes with high remaining battery capacity, so that all expected information can be collected.

In our algorithm, we employ VSM to combine all considering factors to select the most related nodes to participate query processing. The query vector (Υ) is designed as $\Upsilon = [R_l, A_d, B_m]$.

- R_l stands for location relativity. It is the indicator of the distance between the location of a sensor node at (x,y) and the optimal location at (x_0,y_0).

$$R_l = 1 - \frac{\sqrt{(x-x_0)^2+(y-y_0)^2}}{L} \tag{8}$$

  where L is a factor to ensure R_l to be a positive number and not larger than one. One way to design L is to let its value equal to the maximum distance of two nodes within a network.
- A_d stands for measurement quality. A_d equals to the confidence of measurement bias. For example, for speed detecting sensor nodes, CXM539 [10], the bias is $\pm$1mGauss and owns 0.95 confidence. In this case, $A_d = 0.95$.
- B_m stands for remaining battery capacity.

When a query submitted, the top-end node related fixes on optimal locations for this query and translates the query from SQL form into a query VSM vector Υ_0=$[1, A_{d,0}, B_{m,0}]$. For instance, Υ_0 is $[1, p, 5]$ according to the query given in Fig. 1. We assume the maximum battery capacity for nodes is $5J$. Υ_0 and information on optimal locations will be flooded over the whole network.

Nodes update their query VSM vectors ($\Upsilon_i = [R_{l,i}, A_{d,i}, B_{m,i}]$ (i=1,2,$\cdots$, n)) according to Υ_0 and

optimal locations. We assume that there are n nodes in this network. $R_{l,i}$ is defined as:

$$R_{l,i} = \max_j \{r_{l,i,j}\} \tag{9}$$

where $r_{l,i,j} = 1 - \frac{\sqrt{(x_i - x_{0,j})^2 + (y_i - y_{0,j})^2}}{L}$, (x_i, y_i) is the position of node i, and $(x_{0,j}, y_{0,j})$ is the position of jth optimal location.

We design a query correlation, which we refer to as ζ, to express the correlation between each node and a query. We formulate ζ in (10). Observe that, query correlation $\zeta_{\Upsilon_0,\Upsilon_i}$ is a function of query quality requirement and node's energy, measurement quality and location. Moreover, $\zeta_{\Upsilon_0,\Upsilon_i}$ is computed by nodes through a distributed way.

$$\begin{aligned} \zeta_{\Upsilon_0,\Upsilon_i} &= sim_{vs}(\Upsilon_0, \Upsilon_i) = \Upsilon_0 \cdot \Upsilon_i \\ &= \frac{1 \times R_{l,i} + A_{d,0} \times A_{d,i} + B_{m,0} \times B_{m,i}}{\sqrt{(1 + A_{d,0}^2 + B_{m,0}^2)(R_{l,i}^2 + A_{d,i}^2 + B_{m,i}^2)}} \end{aligned} \tag{10}$$

The higher ζ is, the higher the similarity between query and a node is. Inspired by this, we form our criteria for active nodes choosing: The decision-which nodes are active to respond queries-is based on their query correlation. That is, nodes with highest query correlation among their one-hop neighbors are chosen to participate in related query processing. In QGEE, active nodes are chosen locally leveraging cooperations among nodes. We assume that each node knows query correlations of its one-hop neighbors, which can be achieved by requiring each node to broadcast its query correlation initially.

2) Optimal Location Determination: We model the problem-determining optimal locations for a query, as a k-partial set cover problem. This problem is defined as follows: Let n be the number of all sensor nodes, n' be a given positive integer so that $n' \leq n$. If we have k same disks with radius r, the k-partial set cover problem tries to solve whether k disks can cover at least n' nodes. In this paper, we only consider sensor nodes in a plane (the dimension is 2). This kind of k-partial set cover problem is a NP problem.

At present, all known algorithm for NP problems require time that is exponential to the problem size. It is unknown whether there are any faster algorithms. Therefore, to solve a NP problem for any nontrivial problem size, one of the approaches is approximation algorithm, which can acquire the solution during polynomial time. SETCOVER algorithm [21] is a good approximation method to determine the value of k and the locations of these k disks on a plane. In QGEE, we choose centers of those k disks as our optimal locations. If we set these k disks can cover all sensor nodes (i.e., $n' = n$), those nodes locating at the centers of these disks can almost monitor the region completely interested by users.

In QGEE, considering the influence of PSF of nodes on uncertainty of query answers, we adaptively determine the value of the radius r of disks according to users' quality requirements instead of fixing it. We illustrate the process of calculating r with a simple example. We assume that PSF ($g(d)$) of nodes in a WSN is defined by (11) and confidence of query answer is required to be at least p as shown in the example in Fig. 1.

$$g(d) = \frac{1}{\sigma\sqrt{2\pi}} e^{-\frac{d^2}{2\sigma^2}} \tag{11}$$

where d is the distance between a point on the monitoring region and a specific node. σ^2 is the variance of d. $g(d)$ has the similar form as shown in Fig. 3(a).

Compared to other locations within a disk, measurements of active nodes own least sensitivity/confidence when they stand for the situation at the disk's edge. This nature inspires us to get the criteria to acquire suitable value for r. That is, if the sensitivity/confidence is equal to or higher than p at the edge of disks, we can ensure that the measurements of active nodes can represent the situation within this disk with p confidence. We drive equation (11) to determine r (see equation (12)).

$$r = -\sigma\sqrt{ln(2\pi\sigma^2 p^2)} \tag{12}$$

Note that r is a function of standard variance of PSF σ and query quality requirement p. If we fixed σ, r will decrease with the increase of p. That means, with higher query quality, smaller disks are used to search the optimum locations and more active nodes are needed for a query.

3) Sample Size Determination and Semi-Manufactured Query Answer Acquisition: We have picked up a set of nodes to respond a query. While, "How many measurements should be included in one sample?" is the question we will answer in this Section. Sample (any subset of a population) size determination refers to the process of determining exactly how many samples should be measured/observed in order that the sampling distribution of estimators meets users' pre-specified target precision [23].

Since nodes' readings are subject to many small and random errors which are caused by limitations of devices' hardware and environmental noise, uncertainty is inherent regarding to true values. Hence nodes reading (x) can be expressed as:

$$x = v + e_m + \eta \tag{13}$$

where v is the true value, e_m is the measurement error introduced by limitations of devices' hardware, and η is the environmental noise which is considered as white Gaussian noise in this paper and $\eta \sim N(0, \frac{N_0}{2})$. Based on central limit theorem [13], the probability distribution of measurement errors complies with a normal distribution. That is, $e_m \sim N(0, \sigma_e^2)$. Generally, in product's technical datasheet, manufactories supply the information on measurement errors. For example, as we mentioned above, the bias for CXM539 is $\pm$1Gauss with 0.95 confidence. That means for sensor nodes CXM593, $\sigma_e^2 = 0.1302$. For general cases, if we know the maximum bias Δx and its confidence p, we can obtain the general expression for σ_e^2. That is

$$\sigma_e^2 = \frac{\Delta x^2}{[Q^{-1}(\frac{1-p}{2})]^2} \tag{14}$$

where $Q(x)$ stands for Q-Function, defined as $Q(x) = \int_x^\infty \frac{1}{2\pi} e^{-\frac{y^2}{2}} dy$

Moreover, e_m and n_o are independent. Therefore, nodes reading also complies with a normal distribution with μ_x-mean and σ_x-standard derivation given in (15).

$$\mu_x = v \quad and \quad \sigma_x = \sqrt{\sigma_e^2 + \frac{N_0}{2}} \tag{15}$$

Therefore the PDF of nodes' reading $f_X(x)$ is

$$f_X(x) = \frac{1}{\sqrt{2\pi(\sigma_e^2 + \frac{N_0}{2})^2}} e^{-\frac{(x-v)^2}{2(\sigma_e^2 + \frac{N_0}{2})^2}} \tag{16}$$

Based on nodes reading, the estimator of the true value is defined as $\hat{x}_n = \frac{1}{n}\sum_{j=1}^{n} x_j$, thus the probability distribution function of $\hat{x}_n$ ($f_{\hat{X}_n}(\hat{x}_n)$) is similar to $f_X(x)$ with $\hat{\mu}_n = \mu_x$ and $\hat{\sigma}_n^2 = \frac{1}{n}\sigma_x^2$. That is

$$\begin{aligned} f_{\hat{X}_n}(\hat{x}_n) &= \frac{1}{\hat{\sigma}_n\sqrt{2\pi}} e^{-\frac{(\hat{x}_n - \hat{\mu}_n)^2}{2\hat{\sigma}_n^2}} \\ &= \frac{\sqrt{n}}{\sqrt{2\pi(\sigma_e^2 + \frac{N_0}{2})}} e^{-\frac{n(\hat{x}_n - v)^2}{2(\sigma_e^2 + \frac{N_0}{2})}} \end{aligned} \tag{17}$$

In QGEE, we let Δx as the margin of error between the estimator ($\hat{x}_n$) and the true value (v) to reflect the target precision of queries, as well as we specify our tolerance for making this error not smaller than p. The criteria for sample size determination is simply stated as:

$$P_r\{|\hat{x}_n - v| \le \Delta x\} \ge p \tag{18}$$

We have known the PDF of $\hat{x}_n$, hence the probability of the estimation error which not larger than d is

$$P_r\{|\hat{x}_n - v| \le \Delta x\} = 1 - 2Q(\frac{\Delta x}{\sqrt{\frac{\sigma_e^2 + \frac{N_0}{2}}{n}}}) \tag{19}$$

Solving (18) and (19) for n, we obtain

$$n \ge \frac{(\sigma_e^2 + \frac{N_0}{2})[Q^{-1}(\frac{1-p}{2})]^2}{\Delta x^2} \tag{20}$$

Since a statistic measurement on samples can rarely, if ever, be expected to be exactly equal to a parameter, it is important that an estimation is accompanied by a statement which describes the precision of this estimation. Confidence intervals [7] provide a method of stating both how close the value of a statistic being likely to be value of a parameter and the chance of being close. An confidence interval of an attribute, denoted by U_i is a interval $[l_i, h_i]$ such that l_i and h_i are real-valued, and that the condition $h_i \ge l_i$ holds.

Note that (18) is the same statement made when defining a $100 \times p\%$ confidence interval, and d is about half of the width of the confidence interval. Using the sample size defined by (20) to estimate the true value (v), we have

$$P_r\{\hat{x}_n - \Delta x < v < \hat{x}_n + \Delta x\} \ge p \tag{21}$$

With (21), we obtain a bounded value, i.e., $v \in [\hat{x_n} - \Delta x, \hat{x_n} + \Delta x]$, which owns p confidence. We call this kind of query answers from active nodes as "semi-manufactured" query answers.

Since heterogenous is one of natures of general WSNs, that is, measurement quality for each node may not be same, the sample size is given in (22) and confidence interval for node i is $v_i \in [\hat{x_{n,i}} - \Delta x_i, \hat{x_{n,i}} + \Delta x_i]$ with p_i confidence.

$$n_i \ge \frac{(\sigma_{e,i}^2 + \frac{N_0}{2})[Q^{-1}(\frac{1-p_i}{2})]^2}{\Delta x_i^2} \tag{22}$$

4) Information Collection: After active nodes are chosen, a data centric routing algorithm, EM-GMR [11] is employed by QGEE, which is a multipath, power-aware and mobility-aware routing scheme. EM-GMR is used to establish the route-tree from active nodes to front-end nodes for query answer return. EM-GMR uses reactive networking approach, in which it finds a route only when a message is to be delivered from source to destination.

EM-GMR scheme consists of route discovery phase, route reconstruction phase, and route deletion phase. In the route discovery phase, the source node uses a fuzzy logic system (FLS) [8] to evaluate all eligible nodes (closer to the destination location) in its communication range based on the parameters of each node: distance to the destination, remaining battery capacity, and degree of mobility. The source node chooses the top M nodes based on the degree of the possibility (output of FLS). The source node sends a Route Notification (RN) packet to each desired node, and each desired node will reply using a REPLY packet if it is available. If after a certain period of time, the source node did not receive REPLY from some desired node, it will pick the node with the $M + 1$st degree of selection possibility. In the second hop, selected nodes in each path will choose its next hop node uses a FLS.

Note that EM-GMR considers distance to the sensor node, remaining battery capacity, and mobility of each sensor node during route path setting up. This scheme could tremendously reduce the frame loss rate and link failure rate since mobility was considered, so that incompleteness information caused by poor link quality is reduced at certain degree.

B. Energy Consumption Control for Question Processing

In energy consumption control, we employ three strategies. They are active nodes number control, sample size control and link quality control.

First, in the query SVM design, node location is included besides measurement quality and remaining battery capacity, since it is directly related to the necessary number of active nodes to cover whole monitoring region. Through solving optimal location problem, we can employ as few as possible nodes to cover as large as possible monitoring region in order to carry out energy reservation task.

Second, in order to ensure the confidence of estimators satisfy users' requirements, we obtain (22) for determining the value of sample size. However, too large a sample implies a waste of resources, and too small a sample diminishes the

utility of the results. In our algorithm, we let (22) specify the value of sample size during information sensing. Therefore, we can acquire enough samples to met users' pre-specified target precision, at the same time reduce the energy consumption for data sensing.

Third, we tremendously reduce the frame loss rate and link failure rate through choosing more suitable nodes to set up route-tree for queries. With this improvement, we can reduce energy consumption for route-tree maintenance and information retransmission.

C. Final Query Answer Acquisition

After queries have been optimized and disseminated, the query processor begins to execute them-processing all semi-manufactured query answers to acquire the final query answers. Aggregation is required in many database applications, which is used in statistical queries that summarize information from database tuples. Common functions applied to collections of numeric values include SUM, AVERAGE, MAXIMUM, and MINIMUM. In this paper, our discuss on how to obtain final query answers focuses on those most often used aggregation operations: MAXIMUM, MINIMUM, and AVERAGE.

Returned semi-manufactured answers are confidence intervals, i.e., $[\hat{x_{n,i}} - \Delta x_i, \hat{x_{n,i}} + \Delta x_i]$ with p_i confidence ($i = 1, 2 \cdots, \psi$). For simplified reason, we let $l_i = \hat{x_{n,i}} - \Delta x_i$, $h_i = \hat{x_{n,i}} + \Delta x_i$. We assume there are ψ active nodes for a query.

1) MAXIMUM/MINIMUM Aggregation: We let $Z_{max} \doteq \max_i(x_i)$ and $Z_{min} \doteq \min_i(x_i)$ ($i = 1, 2, \cdots, \psi$). The cumulative distribution function (CDF) of $\hat{x}_{n,i}$ is given in (23) according to (17).

$$F_{\hat{X}_{n,i}}(\hat{x}_{n,i}) = Q(\frac{\sqrt{n_i}(\hat{x}_{n,i} - \hat{\mu}_{n_i,i})}{\hat{\sigma}_{n_i,i}}) \tag{23}$$

Since measurements from individual active nodes are independent with each other, the CDFs for Z_{max} and Z_{min} is given in (24) for MAXIMUM and in (25) for MINIMUM.

$$F_{Z_{max}}(z) = \prod_{i=1}^{\psi} F_{\hat{x}_{n_i,i}}(z) = \prod_{i=1}^{\psi} Q(\frac{\sqrt{n_i}(z - \hat{\mu}_{n_i,i})}{\hat{\sigma}_{n_i,i}}) \tag{24}$$

And

$$\begin{aligned} F_{Z_{min}}(z) &= 1 - \prod_{i=1}^{\psi}(1 - F_{\hat{x}_{n_i,i}}(z)) \\ &= 1 - \prod_{i=1}^{\psi}(1 - Q(\frac{\sqrt{n_i}(z - \hat{\mu}_{n_i,i})}{\hat{\sigma}_{n_i,i}})) \end{aligned} \tag{25}$$

For MAXIMUM aggregation, the final query answer is $Z_{max} \in [l'_{max}, h'_{max}]$ with p'_{max} confidence in bounded probability form. Where

$$l'_{max} = \max_i\{l_i\} \quad and \quad h'_{max} = \max_i\{h_i\} \tag{26}$$

$$p'_{max} = \frac{1}{\psi}\sum_{i=1}^{\psi} p_i \tag{27}$$

For MINIMUM aggregation, the final query answer is $Z_{min} \in [l'_{min}, h'_{min}]$ with p'_{min} confidence in bounded probability form. Where

$$l'_{min} = \min_i\{l_i\} \quad and \quad h'_{min} = \min_i\{h_i\} \tag{28}$$

$$p'_{min} = \frac{1}{\psi}\sum_{i=1}^{\psi} p_i \tag{29}$$

2) AVERAGE Aggregation: In this aggregation operation, a derivative value over a group of sensor nodes' data is returned. $Z_{avg} = \frac{1}{\psi}\sum_{j=1}^{\psi}\hat{x}_{n_j,j}$. The PDF for Z_{avg} ($f_{Z_{avg}(z)}$) has the similar distribution to $f_{\hat{X}_n}(\hat{x}_n)$. But the mean and variance are $\frac{1}{\psi}\Sigma_{j=1}^{\psi}\hat{\mu}_{n_j,j}$ and $\frac{1}{n\psi^2}\sum_{j=1}^{\psi}\hat{\sigma}^2_{n_j,j}$ individually.

For AVG aggregation, the final query answer is $Z_{avg} \in [l'_{avg}, h'_{avg}]$ with p'_{avg} confidence in bounded probability form. Where

$$l'_{avg} = \frac{1}{\psi}\sum_{j=1}^{\psi} l_i \quad and \quad h'_{avg} = \frac{1}{\psi}\sum_{j=1}^{\psi} h_i \tag{30}$$

$$p'_{avg} = \frac{1}{\psi}\sum_{i=1}^{\psi} p_i \tag{31}$$

V. Simulation and Performance Evaluation

Nodes are randomly deployed in an area of $10 \times 10m^2$, and sensing range is 1m. The initial energy of sensor nodes uniformly distributes within [0,5]J. We run Monte Carlo simulations to remove the randomicity of simulation results. We compare our QGEE against the query processing method without any query optimization.

The energy consumption model for data sensing is shown in (32).

$$E_q = E_{se} * S_t \tag{32}$$

where E_q is the energy consumed by processing a query. E_{se} is the energy consumed by data sensing. S_t is the sample period. In this simulation, we choose: $E_{se} = 5nJ/sample$.

We use the same energy consumption model as in [22] for the radio hardware. To transmit an l-symbol message for a distance d, the radio expends:

$$E_{Tx}(l,d) = E_{Tx-elec(l)} + T_{Tx-amp(l,d)} = l \times E_{elec} + l \times e_{fs} \times d^2 \tag{33}$$

and to receive this message, the radio expends:

$$E_{Rx} = l \times E_{elec} \tag{34}$$

The electronics energy, E_{elec}, as described in [22], depends on factors such as coding, modulation, pulse-shaping and matched filtering. The amplifier energy, $e_{fs} \times d^2$ depends on the distance to the receiver and the acceptable bit error rate. In this paper, we choose: $E_{elec} = 50nJ/syn$, $e_{fs} = 10pJ/sym/m^2$.

A. Active Nodes Selection Scheme Performance

In Fig. 4, we plot the query index versus the nodes dead time. We can see that after processing about 20 queries, all nodes, without query optimization, use up their energy. But for QGEE, the whole network is not down until 53 queries are completed. Therefore, QGEE can reserve 50% of energy on processing same number of queries.

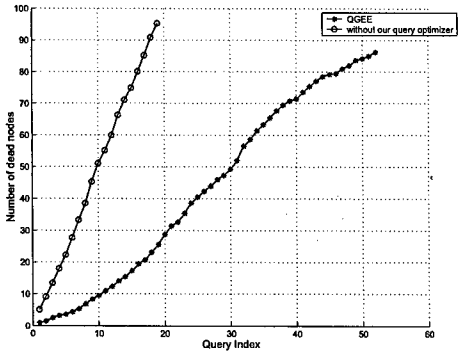

Fig. 4. Nodes Dead Time

In Fig. 5, we compare the observation covering rate of these two schemes. Observed that, QGEE employs $70 - 45 = 25$ less nodes to cover 90% area interested. This simulation result illustrates the reason why our QGEE can implement energy reservation. That is, about $\frac{25}{70} \times 100 = 35.71\%$ nodes switch to energy saving model during query processing.

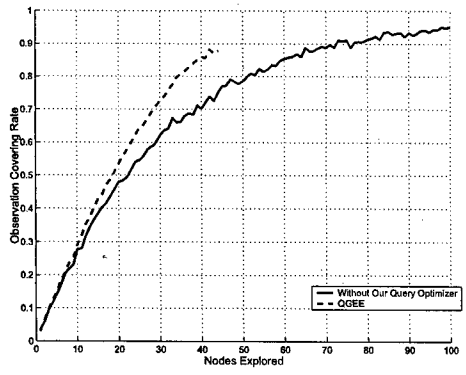

Fig. 5. Observation Coverage Rate

By employing our QGEE, the energy is saved and the lifetime of network is extended. But the cost to achieve this improvement is a certain degree of observation covering rate decreasing. Fig. 6 shows that the biggest decrease of observation covering rate is 16.6% for QGEE.

B. EM-GMR Performance

We compared our EM-GMR against the geographical multipath routing (GMR) scheme where only distance to the destination is considered. In Fig. 7, we plotted the simulation time versus the number of nodes dead. Observe that when

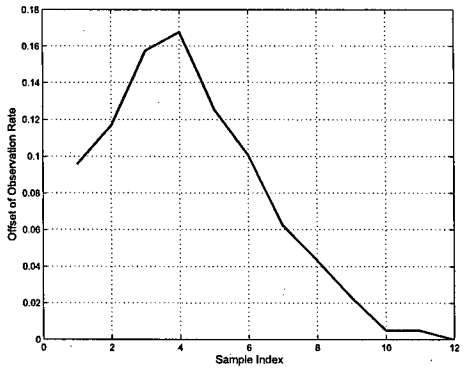

Fig. 6. Decrease of Observation Coverage Rate

50% nodes (30 nodes) die out, the network lifetime for EM-GMR has been extended about $\frac{175-125}{125} = 40\%$. In Fig. 8, we compared the frame loss rate of these two scheme. Observe that our EM-GMR outperforms the GMR for about 20% less frame loss. The average latency during transmission (end-to-end) is 419.68ms for our EMGMR and 407.5ms for GMR, and link failure rate for EMGMR is 5.68%, but for GMR it is 10.42%.

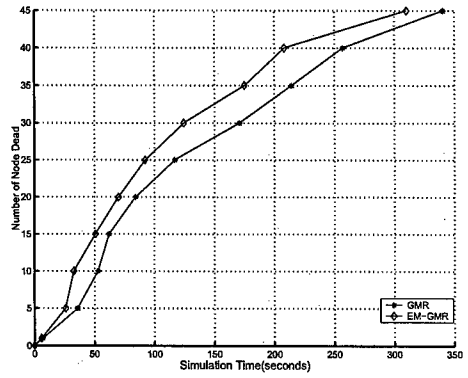

Fig. 7. Simulation time versus number of nodes dead

C. Probabilistic Answers Acquisition Scheme Performance

In this simulation, we give various query answer confidence requirement (i.e., various value for p). To simplify the simulation scenarios, we set there are enough nodes satisfying measurement quality requirements. For MAXIMUM, MINIMUM and AVERAGE aggregation operation, we check the probability of true values locating within the confidence intervals acquired at front-end nodes (see Table II). Note that, our QGEE can successfully obtain suitable confidence intervals to guarantee the true value of query answers locating within this interval with a probability (p_2), which is equal to or larger than the pre-specified probability (p_1) by users.

VI. Conclusions

In this paper, we propose a quality-guaranteed and energy-efficient algorithm (QGEE) for sensor database systems. Given

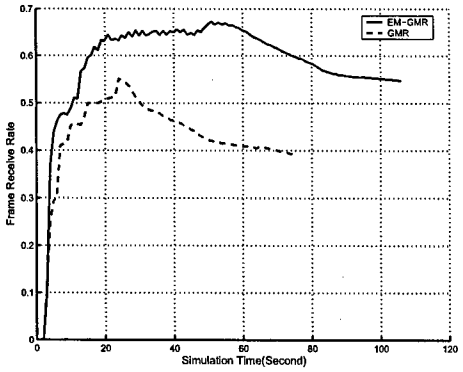

Fig. 8. Simulation time versus frame loss rate

TABLE II

CONFIDENCE FOR QUERY ANSWERS. p_1 IS THE PRE-SPECIFIED VALUE FOR p. p_2 IS THE ACQUIRED VALUE FOR p USING QGEE.

p_1	MAXIMUM	MINIMUM	AVERAGE
	p_2	p_2	p_2
0.8	0.8133	0.8133	0.8112
0.9	0.9139	0.9151	0.9144
0.9050	0.912	0.9122	0.9144
0.9246	0.93	0.9318	0.9301
0.9334	0.948	0.942	0.9428
0.95	0.958	0.9561	0.9551
0.99	0.9939	0.9924	0.9938

a query, our QGEE can adaptively form an optimal query plan in terms of energy efficiency and query quality. Our approach can reduce interference coming from measurements with extreme errors and minimize energy consumption by providing service that is considerably necessary and sufficient for the need of applications. Moreover, we employ probabilistic method to formulate the distribution of imperfect information sources in terms of probability distribution function (PDF), and acquire probabilistic query answers on uncertain data. The probabilities to an answer allow users to place appropriate confidence in it.

The simulation results demonstrate that our algorithm can reduce resource usage about 50%, the frame loss rate about 20% and supply quality satisfied query answers to users.

ACKNOWLEDGEMENT

This work was supported by the U.S. Office of Naval Research (ONR) Young Investigator Program Award under Grant N00014-03-1-0466.

REFERENCES

[1] J. Warrior, "Smart sensor networks of the future," *Sensor Magazine*, Mar. 1997.

[2] G. J. Pottie and W. J. Kaiser, "Wireless integrated network sensors," *Communications of the ACM*, vol. 43, no. 5, pp. 551-558, May 2000.

[3] A. Cerpa, J. Elson, M. Hamilton and J. Zhao, "Habitat monitoring: application driver for wireless communications technology," *2110 ACM SIGCOMM Workshop on Data Communications in Latin Amercia and the Caribbean*, Costa Rica, Apr. 2001.

[4] C. Intanagonwiwat, R. Govindan and D. Estrin, "Directed diffusion: A scalable and robust communication paradigm for sensor networks," *Proceedings of the 6th Annual International Conference on Mobile Computing and Networking (MobiCOM)*, Boston, Aug. 2000.

[5] Y. Yao and J. Gehrke, "Query processing in sensor networks," *Proceedings of the 1st Biennial Conference on Innovative Data Systems Research*, Asilomar, CA, Jan. 2003.

[6] J. R. Schott, *Remote Sensing: The Image Chain Approach, Oxford University Press*, 1997.

[7] J. D. Wilfrid and J. M. J. Frank, *Introduction to Statistical Analysis*, McGraw-Hill, NY, 1983.

[8] J. M. Mendel, *Uncertain Rule-Based Fuzzy Logic Systems: Introduction and New Directions*, Prentice Hall, NJ, 2001.

[9] F. Zhao and L. Guibas, *Wireless Sensor Networks: An Information Processing Approach*, Morgan Kaufmann, CA, 2004.

[10] Products Description, [On Line] WWW: http://xbow.com.

[11] Q. Liang and Q. Ren, "Energy and mobility aware geographical multipath routing for wireless sensor networks," *Proceedings of WCNC2005*, New Orleans, LA, Mar. 2005.

[12] P. P. Bonissone and R. M. Tong, "Editorial: reasoning with uncertainty in expert systems," *International J. Man Machine Studies*, vol. 22, pp. 241-250, 1985.

[13] A. Papoulis, *Probability, Random Variables, and Stochastic Processes*, McGraw-Hill, NY, 2002.

[14] P. Bosc and H. Prade, "An introduction to fuzzy set and possibility theory based approaches to the treatment of uncertainty and imprecision in database management systems," *Proceedings of the 2nd Workshop on Uncertainty Management in Information Systems: From Needs to Solustions*, Catalina, CA, 1993.

[15] J. R. Groff, P. N. Weinber and L. Wald, *SQL: The Complete Reference*, Berkeley, CA, McGraw-Hill/Osborne, 2002.

[16] S. R. Madden, M. J. Franklin, J. M. Hellerstein and W. Hong, "TinyDB: An acquisitional query processing system for sensor networks," *IEEE Trans. Database System*, vol. 30, no. 1, Mar. 2005.

[17] D. Chow and C. T. Yu, "On the construction of feedback queries," *ACM J. Computing Machinery*, vol. 29, no. 1, pp. 127-151, Jan. 1982.

[18] S. K. M. Wong, W. Ziarko, V. V. Raghavan and P. C. N. Wong, "On modeling of information retrieval concepts in vector spaces," *ACM Trans. Database Systems*, vol. 12, no. 2, 1987.

[19] L. Gravano, H. Garcia-Molina and A. Tomasic, "Gloss: Text-source discovery over the internet," *ACM Trans. Database Systems*, vol. 24, no. 2, Jun. 1999.

[20] D. Grossman, O. Frieder, D. Holmes and D. Roberts, "Integrating structured data and text: A relational approach," *J. of the American Society for Information Science*, vol. 48, no. 2, Feb. 1997.

[21] R. Gandhi, S. Khuller and A. Srinivasan, "Approximation algorithm for partial covering problems," *J. of Algorithms*, vol. 53, no. 1, pp. 55-84, Oct. 2004.

[22] W. B. Heinzelman, A. P. Chandrakasan and H. Balakrishnan, "An application-specific protocol architecture for wireless microsensor networks," *IEEE Trans. Wireless Communications*, vol. 1, no. 4, Oct. 2002.

[23] J. M. Mendel, Lessons in Estimation Theory for Signal Processing Communications, and Control, Prentice Hall, NJ, 1995.

Cross-Layer Optimization for Mobile Ad Hoc Networks Using Fuzzy Logic Systems

Xinsheng Xia and Qilian Liang

Department of Electrical Engineering

University of Texas at Arlington

Arlington, TX 76019-0016 USA

E-mail: xia@wcn.uta.edu, liang@uta.edu

Abstract

In this paper, we introduce a new method for packet transmission delay analysis and prediction in mobile ad hoc networks. We use fuzzy logic system (FLS) to coordinate physical layer and data link layer. We demonstrate that a type-2 fuzzy membership functions (MFs), i.e., the Gaussian MFs with uncertain variance is most appropriate to model BER and MAC layer service time. Two FLSs: a singleton type-1 FLS and an interval type-2 FLS are designed to predict the packet transmission delay based on the BER and MAC layer service time. Simulation result shows that the interval type-2 FLS performs better than the type-1 FLS. And we use the outcomes of FLS predictors to control the transmission powers. Simulation results illustrate us the performances of the energy consumption, average delay and throughput. They show that the interval type-2 FLS performs better than the type-1 FLS. And we use the actual transmission delay to get the performance bound.

Index Terms : wireless Ad Hoc networks, cross-layer design, fuzzy logic system, interval type-2 fuzzy sets, packet transmission delay analysis

1 Introduction

The demand for Quality of Service (QoS) in mobile ad hoc networks is growing in a rapid speed. To enhance the QoS, we consider the combination of physical layer and data-link layer together, a cross-layer approach. A strict layered design is not flexible enough to cope with the dynamics of the mobile ad hoc networks [1]. Cross-layer design could introduce the layer interdependencies to optimized overall network performance. The general methodology of cross-layer design is to maintain the layered architecture, capture the important information that influence other layers, exchange the information between layers and implement adaptive protocols and algorithms at each layer to optimize the performance.

Lots of previous works have focused on cross-layer design for QoS provision. Liu [2] combine the AMC at physical layer and ARQ at the data link layer. Ahn [3] use the info from MAC layer to do rate control at network layer for supporting real-time and best effort traffic. Akan [4] propose a new adaptive transport layer suite including adaptive transport protocol and adaptive rate control protocol based on the lower layer information.

However, cross-layer design can produce unintended interactions among protocols, such as an adaptation loops. It is hard to characterize the interaction at different layers and joint optimization across layers may lead to complex algorithm.

In this paper, we discuss one of the parameters for QOS: packet transmission delay. And our algorithm is quite different from all the previous works. We propose to use the Fuzzy Logic System (FLS) for packet transmission delay analysis and prediction. We apply both a singleton type-1 FLS and an interval type-2 FLS for the analysis and prediction.

We apply the transmission delay predictors to control the transmission power. The simulation achieves performance parameters of average delay, energy consumption and throughput. Assume we know the actual transmission delay, we also get these parameters as the performance bounds.

The remainder of this paper is structured as following. In section II, we introduce the preliminaries. In section III, we make an overview of fuzzy logic systems. In section IV, we apply the

FLS into the cross-layer design. Simulation results and discussions are presented in section V. In section VI, we conclude the paper.

2 Preliminaries

2.1 IEEE 802.11a OFDM PHY

The physical layer is the interface between the wireless medium and the MAC [5]. The principle of OFDM is to divide a high-speed binary signal to be transmitted over a number of low data-rate subcarriers. A key feature of the IEEE 802.11a PHY is to provide 8 PHY modes with different modulation schemes and coding rates, making the idea of link adaptation feasible and important.

2.2 IEEE 802.11 MAC

The 802.11 MAC uses Carrier-Sense Multiple Access with Collision Avoidance (CSMA/CA) to achieve automatic medium sharing between compatible stations. In CSMA/CA, a station senses the wireless medium to determine if it is idle before it starts transmission. If the medium appears to be idle, the transmission may proceed, else the station will wait until the end of the in-progress transmission. A station will ensure that the medium has been idle for the specified inter-frame interval before attempting to transmit.

Besides carrier sense and RTS/CTS mechanism, an acknowledgment (ACK) frame will be sent by the receiver upon successful reception of a data frame. Only after receiving an ACK frame correctly, the transmitter assumes successful delivery of the corresponding data frame. The sequence for a data transmission is: RTS-CTS-DATA-ACK.

A mobile node will retransmit the data packet when finding failing transmission. Retransmission of a signal packet can achieve a certain probability of delivery. There is a relationship between the probability of delivery p and retransmission times n [6]:

$$n = 1.451n\frac{1}{1-p} \tag{1}$$

The IEEE 802.11 standard requires that a data frame is discarded by the transmitter's MAC after certain number of unsuccessful transmission attempts. According to the requirement of probability of delivery, we choose the minimum number of retransmission.

When MAC layer acquires access to the channel, the nodes will exchange the RTS-CTS-DATA-ACK packets. After the transmitters receive an ACK packet, a packet is transmitted successfully. In this paper, we assume that there will be always best-effort traffic present that can be locally and rapidly rate controlled in an independent manner at each node to yield necessary low delays and stable throughputs.

2.3 Bit Error Rate

BER is the percentage of bits with errors divided by the total number of bits that have been transmitted, received or processed over a given time period. It is a measure of transmission quality. The high BER means high packets loss rate. Requests for resends will increase latency. For delay insensitive traffic requires a very low BER.

2.4 MAC Layer Service Time

There are three basic processes when the MAC layer transmits a packet [7]: the decrement process of the backoff timer, the successful packet transmission process that takes a time period of T_{suc} and the packet collision process that takes a time period of T_{col}. Here, T_{suc} is the random variable representing the period that the medium is sensed busy because of a successful transmission, and T_{col} is the random variable representing the period that the medium is sensed busy by each station due to collisions. The MAC layer service time is the time interval from the time instant that a packet becomes the head of the queue and starts to contend for transmission, to the time instant that either the packet is acknowledged for a successful transmission or the packet is dropped. This time is important when we examine the performance of higher protocol layers.

2.5 Packet Transmission Delay

The packet delay represents the time it took to send the packet between the transmitter and the next-hop receiver, including the deferred time and the time to fully acknowledge the packet. The packet transmission delay between the mobile nodes includes three parts: the wireless channel transmission delay, the Physical/MAC layer transmission delay, and the queuing delay [8].

Defining D as the distance between two nodes and C as the light speed, the wireless channel transmission delay as:

$$Delay_{ch} = \frac{D}{C} \tag{2}$$

The Physical/MAC layer transmission delay will be decided by interaction of the transmitter and the receive channel, the node density and the node traffic intensity etc.

The queuing delay is decided by the mobile node I/O system-processing rate, the subqueue length in the node.

In order to make the system "stable", the rate at which node transfers packets intended for its destination must satisfy all nodes that the queuing lengths will not be infinite and the average delays will be bounded.

2.6 Energy

A mobile node consumes significant energy when it transmits or receives a packet. But we will not consider the energy consumed when the mobile node is idle.

The distance between two nodes are variable in the mobile ad hoc networks and the power loss model is used. To send the packet, the sender consumes [9],

$$P_{tx} = P_{elec} + \epsilon_{fs} \cdot d^2 \tag{3}$$

and to receive the packet, the receiver consumes,

$$P_{rx} = P_{elec} \tag{4}$$

Where P_{elec} represents the power that is necessary for digital processing, modulation, and ϵ_{fs} represents the power dissipated in the amplifier for the free space distance d transmission.

2.7 One-step Markov Path Model

The mobile nodes are roaming independently with variable ground speed. The mobility model is called one-step Markov path model [10]. The probability of moving in the same direction as the previous move is higher than other directions in this model, which means this model has memory. Fig.1 shows the probability of the six directions.

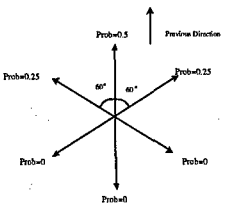

Figure 1: One-step Markov Path Model

3 Overview of Interval Type-2 Fuzzy Logic Systems

Figure 2 shows the structure of a type-2 FLS [11]. It is very similar to the structure of a type-1 FLS [12]. For a type-1 FLS, the *output processing* block only contains the defuzzifier. We assume that the reader is familiar with type-1 FLSs, so that here we focus only on the similarities and differences between the two FLSs.

The fuzzifier maps the crisp input into a fuzzy set. This fuzzy set can, in general, be a type-2 set.

In the type-1 case, we generally have "IF-THEN" rules, where the lth rule has the form "R^l : IF x_1 is F_1^l and x_2 is F_2^l and $\cdots$ and x_p is F_p^l, THEN y is G^l", where: x_is are inputs; F_i^ls are antecedent sets ($i = 1, \ldots, p$); y is the output; and G^ls are consequent sets. The distinction between type-1 and type-2 is associated with the nature of the membership functions, which is not important while

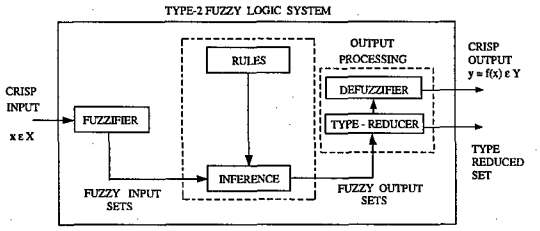

Figure 2: The structure of a type-2 FLS. In order to emphasize the importance of the type-reduced set, we have shown two outputs for the type-2 FLS, the type-reduced set and the crisp defuzzified value.

forming rules; hence, the structure of the rules remains exactly the same in the type-2 case, the only difference being that now some or all of the sets involved are of type-2; so, the lth rule in a type-2 FLS has the form "R^l : IF x_1 is $\tilde{\mathrm{F}}_1^l$ and x_2 is $\tilde{\mathrm{F}}_2^l$ and $\cdots$ and x_p is $\tilde{\mathrm{F}}_p^l$, THEN y is $\tilde{\mathrm{G}}^l$".

In the type-2 case, the inference process is very similar to that in type-1. The inference engine combines rules and gives a mapping from input type-2 fuzzy sets to output type-2 fuzzy sets. To do this, one needs to find unions and intersections of type-2 sets, as well as compositions of type-2 relations.

In a type-1 FLS, the defuzzifier produces a crisp output from the fuzzy set that is the output of the inference engine, i.e., a type-0 (crisp) output is obtained from a type-1 set. In the type-2 case, the output of the inference engine is a type-2 set; so, "extended versions" (using Zadeh's Extension Principle [13]) of type-1 defuzzification methods was developed in [11]. This extended defuzzification gives a type-1 fuzzy set. Since this operation takes us from the type-2 output sets of the FLS to a type-1 set, this operation was called "type-reduction" and the type-reduced set so obtained was called a "type-reduced set" [11]. To obtain a crisp output from a type-2 FLS, we can defuzzify the type-reduced set.

General type-2 FLSs are computationally intensive, because type-reduction is very intensive. Things simplify a lot when secondary membership functions (MFs) are interval sets (in this case, the secondary memberships are either 0 or 1). When the secondary MFs are interval sets, the type-2 FLSs were called "interval type-2 FLSs". In [14], Liang and Mendel proposed the theory and design

of interval type-2 fuzzy logic systems (FLSs). They proposed an efficient and simplified method to compute the input and antecedent operations for interval type-2 FLSs, one that is based on a general inference formula for them. They introduced the concept of upper and lower membership functions (MFs) and illustrate their efficient inference method for the case of Gaussian primary MFs. They also proposed a method for designing an interval type-2 FLS in which they tuned its parameters.

In an interval type-2 FLS with *singleton fuzzification* and meet under minimum or product t-norm, the result of the input and antecedent operations, F^l, is an interval type-1 set, i.e., $F^l = [\underline{f}^l, \overline{f}^l]$, where $\underline{f}^l$ and $\overline{f}^l$ simplify to

$$\underline{f}^l = \underline{\mu}_{\tilde{\mathrm{F}}_1^l}(x_1) \star \ldots \star \underline{\mu}_{\tilde{\mathrm{F}}_p^l}(x_p) \tag{5}$$

and

$$\overline{f}^l = \overline{\mu}_{\tilde{\mathrm{F}}_1^l}(x_1) \star \ldots \star \overline{\mu}_{\tilde{\mathrm{F}}_p^l}(x_p) \tag{6}$$

where x_i $(i = 1, \ldots, p)$ denotes the location of the singleton.

In this paper, we use center-of-sets type-reduction, which can be expressed as:

$$Y_{\cos}(Y^1, \cdots, Y^M, F^1, \cdots, F^M) = [y_l, y_r] = \int_{y^1} \cdots \int_{y^M} \int_{f^1} \cdots \int_{f^M} 1 \Big/ \frac{\sum_{i=1}^{M} f^i y^i}{\sum_{i=1}^{M} f^i} \tag{7}$$

where $Y_{\cos}$ is an interval set determined by two end points, y_l and y_r; $f^i \in F^i = [\underline{f}^i, \overline{f}^i]$; $y^i \in Y^i = [y_l^i, y_r^i]$, and Y^i is the centroid of the type-2 interval consequent set $\tilde{\mathrm{G}}^i$; and, $i = 1, \ldots, M$. Because $Y_{\cos}$ is an interval set, we defuzzify it using the average of y_l and y_r; hence, the defuzzified output of an interval type-2 FLS is

$$f(\mathbf{x}) = \frac{y_l + y_r}{2} \tag{8}$$

4 Modeling BER and MAC Layer service time with Gaussian Membership Function

4.1 Analyzing and Modelling BER

Let p be the probability that bit is error in any given time. So p can be described as a random variable with a known mean value E_a.

Now, at any given time the bit is error with probability p and the bit is correct with probability 1-p. Since the bit is either error or correct, the number of the bits it is error(E_b) for a fixed length transmission bits is binomial random variable. The length of the transmission bits is N_t, The probability that E_b takes any value x is :

$$P\{E_b = x\} = \mathrm{C}_x^{N_t}\mathrm{p}^x(\text{1-p})^{N_t-x} \tag{9}$$

As the number of the length of the transmission bits increase, the binomial distribution is approximated to a normal distribution, with mean $\mu = pN_t$ and variance $\sigma^2 = p(\text{1-}p)N_t$.

In this paper, we set up fine membership functions (MFs) for BER. From the original data of BER shown in Table I, we decomposed the whole data sets into ten segments and computed the mean m_i and std σ_i of the BER of the ith segment, $i = 1, 2, \cdots, 10$. We also computed the mean m and std σ of the entire BER. To see which value –m_i or σ_i– varies more, we normalized the mean and std of each segment using m_i/m, and σ_i/σ, and we then computed the std of their normalized values, σ_m and σ_{std}.

As we see from the last row of Tables I, $\sigma_m \ll \sigma_{std}$. We conclude, therefore, that if the BER of each segment (short range)are Gaussian with uncertain standard deviation. One example of type-2 Gaussian MF with uncertain standard deviation is shown in Fig.3.

Table 1: Mean and std values for ten segments and the entire BER, and their normalized std.

BER	mean	std
Segment 1	0.016613	0.033315
Segment 2	0.015618	0.027857
Segment 3	0.015528	0.017401
Segment 4	0.016206	0.02107
Segment 5	0.015721	0.017148
Segment 6	0.016298	0.029309
Segment 7	0.017062	0.037428
Segment 8	0.016253	0.022871
Segment 9	0.016448	0.023194
Segment 10	0.016237	0.020675
Entire Traffic	0.016198	0.025829
Normalized std	0.029161	0.26184

4.2 Analyzing and Modelling MAC Layer Service Time

Recent research by Zhai, kwon and Fang [7] discovered that the lognormal distribution could match for the MAC layer service time. i.e., if the MAC layer service time for the packet i is s_i, then

$$\log_{10} s_i \sim \mathcal{N}(\cdot; m, \sigma^2) \tag{10}$$

We, therefore, tried to model the logarithm of the MAC layer service time, to see if a Gaussian MF can match its nature. We decomposed the whole data sets into ten segments and computed the mean m_i and std σ_i of the logarithm of the MAC layer service time of the ith segment, $i = 1, 2, \cdots, 10$. We also computed the mean m and std σ of the entire logarithm of the MAC layer service time. To see which value –m_i or σ_i– varies more, we normalized the mean and std of each segment using m_i/m, and σ_i/σ, and we then computed the std of their normalized values, σ_m and

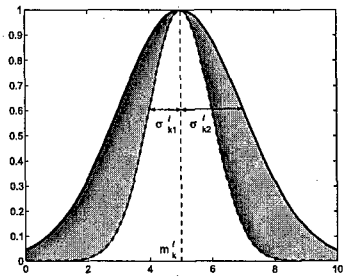

Figure 3: Type-2 Gaussian MF with uncertain standard deviation

σ_{std}.

As we see from the last row of Tables II, $\sigma_m \ll \sigma_{std}$. We conclude, therefore, that if the logarithm of MAC layer service time of each segment (short range)are Gaussian with uncertain standard deviation, as shown in Fig.3.

5 Cross-layer Design Using Interval Type-2 Fuzzy Logic System

As we introduce in the preliminaries, the high BER means high packets loss rate. Requests for resends will increase latency. For delay insensitive traffic requires a very low BER. And the MAC later service time is important when we examine the performance of higher protocol layers. So we could know BER and MAC layer service time will manage the packet transmission delay between the mobile nodes. We are now ready to evaluate the packet transmission delay using interval type-2 fuzzy logic systems.

We predict packet transmission delay based on the following two antecedents:

1. Antecedent 1. BER.

2. Antecedent 2. MAC layer service time.

The consequent is depicted as the packet transmission delay. The linguistic variables used to represent the BER and MAC layer service time were divided into three levels: *low*, *moderate*, and *high*. The consequents – the packet transmission delay were divided into 5 levels, *vert low*, *low*,

Table 2: Mean and std values for ten segments and the entire logarithm of MAC layer service time, and their normalized std.

MAC layer service time	mean	std
Segment 1	-1.1902	0.44295
Segment 2	-1.1929	0.44698
Segment 3	-1.1967	0.45237
Segment 4	-1.1959	0.44835
Segment 5	-1.1917	0.43598
Segment 6	-1.1924	0.44779
Segment 7	-1.1976	0.45687
Segment 8	-1.1996	0.45554
Segment 9	-1.1923	0.45068
Segment 10	-1.1997	0.462
Entire Traffic	-1.1949	0.44981
Normalized std	0.0028746	0.016421

moderate, high and very high.

We designed questions such as:

IF *BER* is *low* and *MAC layer service time* is *high*, THEN the packet transmission delay is _____.

So we need to set up $3^2 = 9$ (because every antecedent has 3 fuzzy sub-sets, and there are 2 antecedents) rules for this FLS. We summarized these rules in Table II.

We used Guassian membership functions (MFs) to represent the antecedents and the consequent.

Fig.4 show the FLS application for the cross-layer design.

Table 3: Fuzzy Rules and Consequent

Antecedent1	*Antecedent2*	*Consequent*
Low	*Low*	*VeryLow*
Low	*Moderate*	*Low*
Low	*High*	*Moderate*
Moderate	*Low*	*Low*
Moderate	*Moderate*	*Moderate*
Moderate	*High*	*High*
High	*Low*	*Moderate*
High	*Moderate*	*High*
High	*High*	*VeryHigh*

When a mobile node sends out a packet, it will first predict the packet transmission delay using the FLS algorithm. After that, the node could adjust the transmission power according to the predicted packet transmission delay. Therefore average delay, energy consumption and throughput performances will change.

6 Simulations

We implemented the simulation model using the OPNET modeler. The simulation region is 300×300 meters. There were 12 mobile nodes in the simulation model, and the nodes were roaming independently with variable ground speed between 0 to 10 meters per second. The mobility model was called one-step Markov path model. The movement would change the distance between mobile nodes. We assumed the collecting data distribution of the mobile node was exponential distribution and the arriving interval was 0.2 second and the length of the packet is 512 bits.

For type-1 FLS, We chose Gaussian membership function as antecedents; for interval type-2

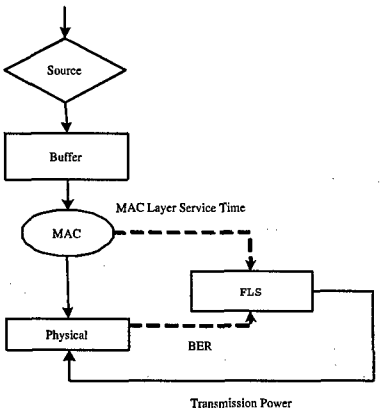

Figure 4: FLS application for cross-layer design

FLS, we used Gaussian primary MF's with fixed mean and uncertain std for the antecedents. The steepest decent algorithm was used to train all the parameters based on the 300 data sets. After training, the rules were fixed, and we tested the FLS based on the remaining 300 data sets.

In Fig.5, we summarized the root-mean-square-errors (RMSE) between the estimated packet transmission delay and the actual delay.

$$RMSE = \sqrt{\frac{1}{300}\sum_{i=301}^{600}[d(i) - f(i)]} \tag{11}$$

where d(i) was the actual packet transmission delay and f(i) was the estimated delay.

The simulation result shows that the interval type-2 FLS for packet transmission delay analysis and prediction outforms the type-1 FLS.

In the following performance analysis, we assume we could know the actual transmission delay. We just use it as a idea case and get the performance parameters as the bounds.

6.0.1 Average Latency

We used the average latency parameter to evaluate the network performance. Each packet was labeled a timestamp when it was generated by the source sensor node. When its destination sensor

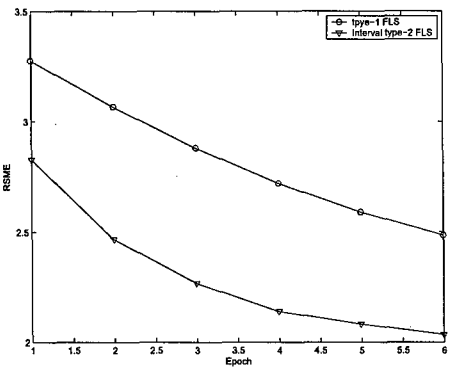

Figure 5: The RMSE of packet transmission delay prediction for two FLS approaches

node received it, the time interval was the transmission delay.

$$Average\,Latency = \frac{\sum_{i=1}^{K} D_i}{K} \tag{12}$$

Fig.6 showed the latency performance of the three algorithms. The type2 algorithm was better than the type1 algorithm. The type2 predictor could reduce the average delay by up to 20% than type1 predictor. And the idea case was the best performance among the three.

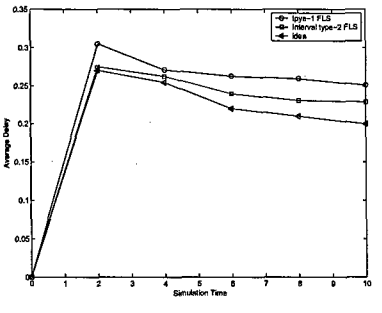

Figure 6: Average Delay for Three Algorithms

6.1 Energy Efficiency

It was not convenient to recharge the battery, so the energy efficiency was extremely important for mobile ad hoc networks. In the wireless mobile ad hoc networks, we used the parameter: the remaining energy to describe the energy efficiency.

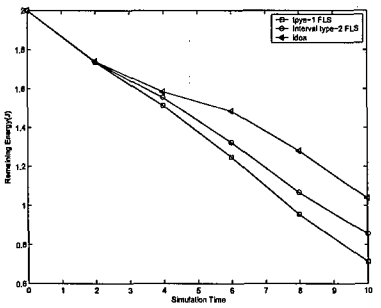

Figure 7: Remaining Energy for Three Algorithms

Fig.7 showed the remaining energy of the three algorithms. We assumed that the energy of each sensor is 2.0J and we adopted CSMA/CA protocol to solve the packets collision problem. If a sensor node transmitted Num_s packets (each packet cost 1 second) and receives Num_r packets (each packets also cost 1 second) and it was roaming in the network for T_m, we could get the remaining energy E_i of this sensor node:

$$E_i = 2.0 - (3 \times 10^{-5} \times T_m + 1.2 \times 10^{-3} \times 1 + 6 \times 10^{-4} \times 1) \tag{13}$$

Same as the average delay, for the performance of the energy consumption, the type2 algorithm was better than the type1 algorithm. The type2 predictor could reduce the energy consumption by up to 21% than the typ1 predictor. The idea case was set as the low bound.

6.2 Networks Efficiency

The mobile ad hoc networks were used to collect data and transfer packets. The throughput of packets transmitted was one of the parameters to evaluate the networks efficiency. In our simulation, we assumed the collecting data distribution of the mobile node was Poisson distribution and the arriving interval was 0.2 second.

Observing from Fig.8, the type2 algorithm was better than the type1 algorithm. The type2 predictor could increase the throughput by up to 45% than the typ1 predictor. And the idea case was set as the high bound.

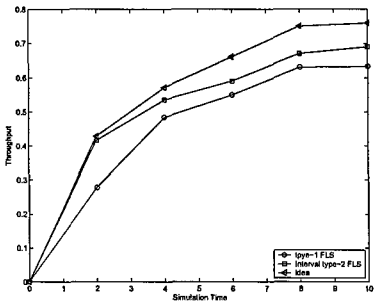

Figure 8: Throughput for Three Algorithms

We introduce the fuzzy logic system in the cross-layer design. Compare with other algorithms for cross-layer design, the fuzzy method could be flexible and simpler to implement. We could predict the packet transmission delay according to the information just from physical layer and mac layer. So we have potential application advantage. We use the FLSs as the predictors and we could control the transmission power according the outcomes of the predictors. Simulation results show that the type2 algorithm is better than the type1 algorithm. And we could set the idea case as the performance bounds.

7 Conclusion

Cross-layer design is a effective method to improve the performance of the mobile ad hoc network. We apply the fuzzy logic system to combine physical layer and data-link layer together. We select BER and MAC layer service time as antecedents to analyze and predict the packet transmission delay. And we apply a type-1 FLS and an interval type-2 FLS for the packet transmission delay analysis and prediction. Simulation result shows that the interval type-2 FLS for packet transmission delay analysis and prediction outform the type-1 FLS. We use the FLSs as the predictors and we could control the transmission power according the outcomes of the predictors. Simulation results show that the type2 algorithm is better than the type1 algorithm. And we could set the idea case as the performance bounds.

Acknowledgment

This work was supported by the U.S. Office of Naval Research (ONR) Young Investigator Award under Grant N00014-03-1-0466.

References

[1] A.J. Goldsmith and S.B. Wicker; " Design Challenges for Energy-Constrained Ad Hoc Wireless Networks, " *IEEE Wireless Comm.,* vol. 9, no. 4 , pp. 8-27, 2002.

[2] Q.Liu, S.Zhou and G.Giannakis; " Cross-Layer Combining of Adaptive Modulation and Coding with Truncated ARQ over Wireless Links ," *IEEE Transactions on Wireless Communications*, vol. 3 , no.5 , pp. 1746 - 1755, Sept. 2004.

[3] G. Ahn, A. Campbell, A. Veres and L. Sun; " Support Service Differentiation for Real-Time and Best-Effort Traffic in Stateless Wireless Ad Hoc Networks (SWAN),", *IEEE Transactions on Mobile Computing*, vol. 1, no. 3, pp. 192 - 207, July-Sept. 2002.

[4] O.B.Akan and I.F.Akyildiz; " ATL, An Adaptive Transport Layer Suite for Next Generation on Wireless Internet ,", *IEEE Journal on Selected Areas in Communcations*, June 2004.

[5] D.Qiao, S. Choi, and K.G. Shin " IEEE Trans. On Mobile Computing ,", *IEEE Transactions On Mobile Computing*, Oct. 2002.

[6] L. H. Bao, J. J. Garcia-Luna-Aceves, " Hybrid Channel Access Scheduling in Ad Hoc Networks", *IEEE Computer Society,* Washington, DC, USA.

[7] H. Zhai, Y. Kwon and Y. Fang, "Peformance analysis of IEEE 802.11 MAC protocols in wireless LANs," *Wireless Communication and Mobile Computing*, pp. 917-931, 2004.

[8] Xia, X.;Liang, Q.; "Latency-aware and energy efficiency tradeoffs for sensor networks", *15th IEEE PIMRC(Personal, Indoor and Mobile Radio Communications), 2004.*

[9] Heinzelman, W.B.; Chandrakasan, A.P.; Balakrishnan, H.; " An application-specific protocol architecture for wireless microsensor networks ," *IEEE Transactions on Wireless Communications*, Volume: 1 Issue: 4, Oct 2002

[10] Hou T. C., and Tsai T. J.; "Adaptive clustering in a hierarchical ad hoc network", *Proc. Int. Computer Symp.,Tainan, Taiwan,R.O.C.*, Dec. 1998, pp. 171-176.

[11] N. N. Karnik, J. M. Mendel, and Q. Liang, "Type-2 fuzzy logic systems," *IEEE Transactions On Fuzzy Systems*, vol. 7, no. 6, pp. 643-658, Dec. 1999.

[12] J. M. Mendel, "Fuzzy logic systems for engineering: a tutorial," *Proc. of the IEEE*, vol. 83, no. 3, pp. 345-377, March 1995.

[13] L. A. Zadeh, " The concept of a linguistic variable and its application to approximate reasoning - I," *Information Sciences*, vol. 8, pp. 199-249, 1975.

[14] Q. Liang and J. M. Mendel, "Interval type-2 fuzzy logic systems: theory and design," *IEEE Transactions on Fuzzy Systems*, vol. 8, no. 5, pp. 535-550, Oct 2000.

[15] Lu, C. et al; " RAP: a real-time communication architecture for large-scale wireless sensor networks ," *Proceeding of the eighth IEEE real-time and embedded technology and applications Symposium*, San Jose, California, pp. 55 - 66, Sept. 25 - 27, 2002.

An Asynchronous Energy-Efficient MAC Protocol for Ultra-Wideband Communications Over Wireless Sensor Networks

Qingchun Ren and Qilian Liang
Department of Electrical Engineering
University of Texas at Arlington
E-mail: ren@wcn.uta.edu, liang@uta.edu

Abstract— **Ultra wideband (UWB) technology offers unique advantages for wireless communications: precise location-timing capabilities, low power, low complexity, and low cost. No existing wireless network successfully takes advantage of those properties of this technology because of the lack of an efficient medium access control (MAC) technology. In this paper, we propose an energy-efficient MAC protocol: asynchronous MAC protocol for UWB communications (A-MAC-UWB). Basing on the characteristics of UWB communication, we utilize virtual MIMO technology to increase the data rate, and substitute space diversity for time diversity to improve system performance in terms of energy efficiency and bit error rate (BER). Also, we implement multiuser access through ALOHA scheme, instead of mutual exclusion method such as TDMA and random access. For multiuser interference, we set a model to adaptively adjust the data rate to ensure certain signal to noise ratio (SNR) at receiver side, since a Shanoncapacity of a multipath fading additive white Gaussian noise (AWGN) wideband channel is a linear function of SNR. For optimum design for power on/off phase duration, we consider the traffic whose arrival interval follows heavy tailed distribution, instead of Poisson distribution. Based on that, we acquire the probability density function (pdf) for power off phase duration for our algorithm. Compared with our previous work, we try to find a better method to trade off between data packet latency and energy reservation.**

I. Introduction

A wireless sensor network (WSN) can be thought as an *ad hoc* network consisting of sensor nodes linked by a wireless medium to perform distributed sensing tasks. Recent developments in integrated circuit technology have allowed the construction of low-cost small sensor nodes with signal processing and wireless communication capabilities. Distributed WSNs have increasing potential applications because they hold the potential to revolutionize many segments of our economy and life, from environmental monitoring and conservation, to manufacturing and business asset management, to automation in the transportation and health-care industries [1].

According to Federal Communications Commission (FCC), an ultra-wideband (UWB) system is defined as any radio system that has a 10-dB bandwidth larger than 20 percent of its center frequency, or has a 10-dB bandwidth equal to or larger than 500 MHz [2]. To enable the deployment of UWB systems, FCC allocated an unlicensed frequency band 3.1.10.6 GHz for indoor or hand-held UWB communication systems [2]. UWB is an attractive technology for WSNs due to its high data rate, low radiated power, and accurate ranging capability. Two different UWB communications systems - impulse-based systems and multi-carrier systems - have been pursued recently. For low cost and low power applications, impulse UWB (I-UWB) has several advantages over multi-carrier systems including robustness to Rayleigh fading and simple, low power hardware.

Multiantenna systems have been studied intensively in recent years due to their potential to dramatically increase the channel capacity in fading channels [3]. It has been shown [3] that multi-input-multi-output (MIMO) systems can support higher data rates under the same transmit power budget and bit-error-rate performance requirements as a single-input single-output (SISO) system. An alternative view is that for the same throughput requirement, MIMO systems require less transmission energy than SISO systems. However, direct application of multiantenna techniques to sensor node impractical due to the limited physical size of a sensor node which typically can only support a single antenna. In resent years, virtual MIMO conception have been proposed by Cui [4] and Jayaweera [5], which allow individual single-antenna nodes to cooperate on information transmission and/or reception. A cooperative MIMO system can be constructed such that energy-efficient MIMO schemes can be deployed.

In this paper, we propose an energy-efficient MAC protocol: asynchronous MAC protocol for UWB communications (A-MAC-UWB). Basing on the characteristics of UWB communication, we utilize virtual MIMO technology to increase the data rate, and substitute space diversity for time diversity to improve system performance. The structure of corresponding transmitter and receiver are given in this paper. Also, we implement multiuser access through ALOHA scheme, instead of mutual exclusion method such as TDMA and random access. For multiuser interference, we set a model to adaptively adjust the data rate to ensure certain SNR at receiver side, since a Shanoncapacity of a multipath fading additive white Gaussian noise (AWGN) wideband channel is a linear function of SNR. For optimum design for power on/off phase duration, we consider the traffic whose arrival interval follows heavy tailed distribution, instead of Poisson distribution. Based on that, we acquire the probability density function (pdf) for power off phase duration for our algorithm. Compared with

our previous work, we try to find a better method to trade off between data packet latency and energy reservation.

The remainder of this paper is organized as follows. In next section (Section III) we make a formulation on the problems covered in this paper. Assumption and modelling related to our algorithm is given in Section IV. Section V describe our A-MAC-UWB algorithm.

II. Related Work

In contrast to typical WLAN protocols, MAC protocols designed for WSNs usually trade off performance (latency, throughput, fairness) for cost (energy efficiency, reduced algorithmic complexity). The main idea of energy-efficient MAC protocols for narrowband systems is that sensor nodes intelligently power off users that are not actively transmitting or receiving packets. The goal is implementing information exchange, as well as reducing energy consumption to extend the lifetime of networks. Narrowband energy-efficient MAC protocols for WSNs can be classified into three main categories according to the strategies applied for channel access:

- *Contention-Based Protocols:* 802.11 [6] standard is based on carrier sensing (CSMA) and collision detection (through acknowledgements).
- *Slotted Protocols:* traffic-adaptive medium access (TRAMA) [7] employs a traffic adaptive and distributed election scheme to allocate the system time among sensor nodes. Other TDMA-based energy-efficient MAC protocols like EMACS, bit-map-assisted (BMA) and GANGS MAC protocols are described in [8], [9], [10].
- *TDMA-Based Protocols:* S-MAC [11] is a low power RTS-CTS protocol for WSNs inspired by PAMAS [12] and 802.11. T-MAC [13] improves on S-MAC's energy usage by using a very short listening window at the beginning of each active period. B-MAC [14] provides a flexible interface to obtain ultra low power operation, effective collision avoidance, and high channel utilization.

Multiple access communications employing pulsed UWB technologies has drawn significant research interest. The MAC should be specifically conceived for the UWB radio physical layer, and as such foresee and eventually optimize strategies for power sharing and management. Various multiple access schemes and their performance have been reported in the literature [15] [16]. Time hopping (TH) has been found to be a good multiple access technique for pulsed UWB systems [16]. Direct sequence (DS) spreading is also an attractive method for multiple access in UWB systems. F. Cuomo et al. [17] outlined key issues to design a multi access scheme based on UWB. They selected a distributed mechanism to handle radio resource sharing, and presented a general framework of radio resource sharing to the UWB wireless ad hoc network systems. J. Ding et al [18] studied the impact of the channel acquisition time with different MAC protocols: a centralized TDMA and a distributed CSMA/CA.

Information-theoretic results in [19] and [20] show that a Shannoncapacity of a multipath fading AWGN wideband channel is a linear function of signal to noise ratio (SNR). That is:

$$R = K \times SNR \tag{1}$$

Thus, for a given desired bit-error rate on the link, an efficient wideband physical layer implementation should have a linear rate function within the operational interval of SNRs. Moreover UWB is flexible in the reconfiguration process of data rate and power, due to the availability of a number of transmission parameters which can be tuned to better match the requirements of a data flow. Therefore, UWB systems can support multiple access much better than narrowband systems.

III. Problem Formulation

The biggest challenge for designers of WSNs is to develop systems that will run unattended for years. This calls for not only robust hardware and software, but also lasting energy resources. However, the current generation of sensor nodes is battery powered, whose available energy is limited, and replacing or recharging batteries, in many cases, may be impractical or uneconomical. Lifetime is a major constraint. Even though, future generations can be powered by ambient energy sources (sunlight, vibrations, etc.) [21], the current provided is very low. Energy consumption is heavily constrained. From both perspectives, protocols and applications designed for WSNs should be highly efficient and optimized in terms of energy.

Energy-efficient communication techniques typically focus minimizing the transmission energy only, which is reasonable in long-range applications where the transmission energy dominant in the total energy consumption. However, in short-range applications such as WSNs where the circuit energy consumption is comparable to or even dominates the transmission energy [4]. And Cui [4] claims that the traditional belief that MIMO systems are more energy-efficient than SISO system in Rayleigh-fading channel is misleading when both the transmission energy and the circuit energy consumption are considered in short-range applications, except that constellation size is optimized.

In UWB WSNs, if using multiple access instead of mutual exclusion access methods, one main energy wasting source is idle for waiting for next arrival data packet, we call it inter-packet idle listening, which is caused by burst traffic. Besides this, we found that there is another kind of idle listening for UWB systems, we call it inter-symbol idle listening. As shown in Section IV-B, each bit is repeated N_s times, during each frame duration (T_f) only one pulse is sent and the left time is idle for waiting for next pulse, and there are N_h bins during one frame time. In this case, for one information bit, the ratio of actual transmission/receiption time to one bit duration is $\frac{T_c}{T_f}$, and the ratio of inter-symbol idle time to one bit duration is $\frac{(N_h-1)T_c}{T_f}$. The typical values for those key parameters are: $T_f = 100ns$, $T_c = 0.75ns$, $N_s = 100$, and $N_h = 100$. Note that there is about 74.25% time is idle for one information bit transmission.

Furthermore, compared with narrowband communication systems, UWB is low power consumption. The research in

[10] points out that a bit rat of $100Kpbs$ over 5 meters with no more than 1 mW power consumption. Therefore, saving energy on circuit part is one of the most effective methods for UWB system than for narrowband system. Hence, how to extend the superiority of virtual MIMO systems in terms of energy efficiency down to very short distance for UWB systems is one of objects of this paper.

IV. Assumption and Modelling

A. Network Model

A commonly encountered distributed wireless sensor network model consists of a lead-sensor and a set of data collection nodes. In this model, a number of low-end data collection sensors are connected with a high-end data gathering node which may act as lead-sensor or a fusion center over a wireless link. In such networks, the data collection sensors are typically subjected to strict energy constraints while the data gathering node is not. The data collection nodes collect data on a physical phenomenon that is of interest and communicate them to the data gathering node over a wireless link which performs required joint processing. Suppose a set of data collection nodes (N_T) (possibly close to each other) has data to be sent to the data gathering node. All these sensors transmit their data simultaneously to the data gathering node as in a conventional VBLAST system[22]. Which sets of nodes can transmit simultaneously will be designed next section. We assume that there are $N_R - 1$ number of local sensors surrounding the data gathering node which are willing to assist it in realizing a virtual receiver antenna array of size N_R (including the data gathering node itself). Each of these N_R sensor nodes receive transmissions. The $N_R - 1$ assisting nodes quantize their received signal samples and re-transmit these bits to the data gathering node.

B. Physical Layer Model

The UWB physical model of the network on which the design of our protocol is based is discussed in this section. The most common and traditional way of emitting an UWB signal is by radiating pulses that are very short in time. IR transmits extremely short pulses giving rise to wide spectral occupation in the frequency domain (bandwidth from near dc to a few gigahertz). The way by which the information data symbols modulate the pulses may vary. Pulse Position Modulation (PPM) and Pulse Amplitude Modulation (PAM) are commonly adopted modulation schemes [24] [25]. In addition to modulation and in order to shape the spectrum of the generated signal, the data symbols are encoded using pseudorandom or pseudonise (PN) codes. Fig. 1 reports an example of transmission by two users, each characterized by a TH code word.

where T_f is the frame duration. T_c is the bin duration.

The output x^n $(n = 1, 2, \cdots, N_T)$ at $n - th$ user's output can be expressed as follows:

$$x^{(n)}(t) = \sqrt{E_{TX}^{(n)}} p(t - c^{(n)} T_c - a^{(n)} \varepsilon) \qquad (2)$$

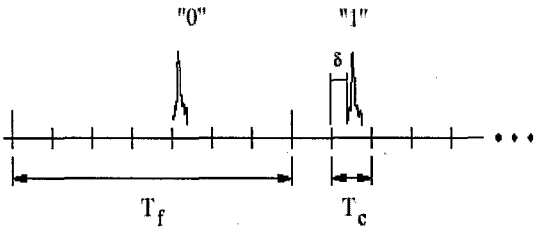

Fig. 1. UWB physical layer with PPM, the model of Win-Scholtz [16]

where $E_{TX}^{(n)}$ is the transmitted energy per pulse for $n - th$ user at transmitter antenna. Note that the bit interval, or the bit duration, that is, the time used to transmit one bit T_b is: $T_b = T_s$. Compared with generic TH-PPM UWB signal transmitters, such as the one used in Win-Scholtz physical model [16], in which $T_b = N_s T_s$ if also introducing N_s redundancy, our MIMO TH-PPM UWB transmitter improves the data rate N_s times, which is one of advantages introduced by utilizing MIMO technology.

The signal received by $i - th$ $(i = 1, 2, \cdots, N_R)$ user's antennas is $z^{(i)}(t)$ at time t, written as follows:

$$z^{(i)}(t) = \sum_{j=1}^{N_T} \alpha_j^{(i)}(t) x^{(j)}(t - \tau_j^{(i)}) + \omega^i(t) + n^{(i)}(t) \qquad (3)$$

where $\alpha_j^{(i)}(t)$ is the channel coefficient for the $j - th$ transmitter at $i - th$ receiver. $\tau_j^{(i)}$ is the delay of the $j - th$ transmitter at $i - th$ receiver. $\omega^i(t)$ is the multiuser interference. $n_i^{(n)}(t)$ is AWGN noise.

Combining (2) and (3), we drive that:

$$z^{(i)}(t) = \sum_{j=1}^{N_T} \sqrt{E_{TX}^{(j)}} \alpha_j^{(i)}(t) p(t - c^{(j)} T_c - a^{(j)} \varepsilon - \tau_j^{(i)}) + n^{(i)}(t) \qquad (4)$$

V. Proposed Asynchronous MAC Protocol for UWB Communications (A-MAC-UWB) Design

A-MAC-UWB divides system time into four phases: *T*RFR-*P*hase, *S*chedule-*P*hase, *O*n-*P*hase and *O*ff-*P*hase (Fig. 2).

- *T*RFR-*P*hase is preserved for normal nodes to exchange Traffic-Rate & Failure-Rate (TRFR) messages and data packets;
- *S*chedule-*P*hase is preserved for cluster heads to locally broadcast phase-switching schedules;
- *O*ff-*P*hase is preserved for all normal nodes to power off their radios. In this phase, there is no communication, but data storing and sensing may happen;
- *O*n-*P*hase is preserved for all normal nodes to power on their radios to carry on communication.

In A-MAC-UWB, according to information collected from normal nodes, cluster heads estimate the influence of clock drifts on communications and the capacity to buffer packets

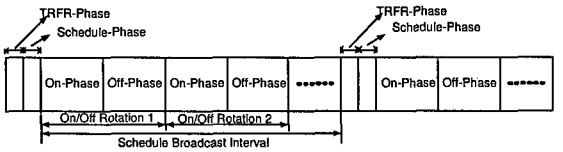

Fig. 2. Time Scheme Structure for A-MAC-UWB

within their region. Then cluster heads choose the power on/off duration and the interval for schedule broadcast. Finally, nodes set up their own phase-switching schedules to power on their radios for carrying on communication and to power off their radios for saving energy alternately.

A. Essential Parameter Design

1) Off-Phase Duration (T_f): It is now recognized [26] [27] that traffic in wired and wireless communication networks is better described by heavy-tailed distributions than by Poisson, Gaussian or other classical distributions with exponentially decreasing tails. In this paper, we model network arrivals as Pareto distribution, a heavy-tailed distribution, instead of Poisson distribution as in [28] did. The probability mass function is given in (5).

$$f(x) = \alpha k^{\alpha} x^{-\alpha-1}, \quad 1 < \alpha < 2, \quad k > 0, \quad x \geq k \tag{5}$$

and its cumulative distribution function is given by:

$$F(x) = 1 - (\frac{k}{x})^{\alpha} \tag{6}$$

where k represents the smallest value the random variable can take.

In this case, we establish an embedded-Markov chain to express the packet arrive process for each user. $N(t)$ is the number of data packets in buffer at time t. N_n^- stands for the queue length when the $n-th$ data packet arrival (the current arrival data packet not included). Even though the queue length of each user does not own Markov property any more, $N_n^-, n \geq 0$ forms a Markov chain, an embeded-Markov chain. The average arrival interval ($\frac{1}{\lambda}$) is given:

$$\frac{1}{\lambda} = \int_k^{\infty} x dF(x) = \frac{\alpha k}{\alpha - 1} \tag{7}$$

During *O*ff-*P*hase, there are about ($T_{f,i} \times \lambda_i$) data packets arrived at node i. We assume the buffer size for node i is B_s. Then the duration, denoted by t_i, within which node i's buffer can be fully filled with arrived data packets is given by $t_i = \frac{B_s}{\lambda_i}$. Considering the first criteria, $T_{f,i}$ for node i should not longer than t_i. In this algorithm, we let

$$T_{f,i} = t_i = \frac{B_s}{\lambda_i} = B_s(\frac{\alpha_i k_i}{\alpha_i - 1}) \tag{8}$$

We assume B_s is a constant, $\alpha_i = \alpha$ for all users. While k_i follows a uniform distribution at range [0, k*]. Note that, the cumulative density function for $T_{f,i}$ is given:

$$F_{T_{f,i}}(t_{f,i}) = P\{T_{f,i} \leq t_{f,i}\} = F_K(\frac{t_{f,i}(\alpha-1)}{\alpha B_s}) \tag{9}$$

Since

$$F_K(k) = \frac{k}{k^*} \tag{10}$$

then

$$F_{T_{f,i}}(t_{f,i}) = \frac{t_{f,i}(\alpha-1)}{\alpha k^* B_s} \tag{11}$$

Since, within a cluster, there are multiple nodes which have various traffic arrival rate, the duration for all nodes will not be equal. If we let the *O*ff-*P*hase duration for a whole cluster $T_{f,tot}$ equal to $i-th$ user, that is $T_{f,tot} = T_{f,i}$. Moreover, since a new arrival to an idle system, rather than going into service immediately, waits for the end of the vacation period, and arrivals are served following a first-come-first-in order. Therefore, the longer $T_{f,tot}$ is, the longer for data packets waiting at buffer for transmission is. We leverage the $GI^*/G/1$ with vacation modelto model our system. Through analysis, we try to get the relationship between average waiting time ($\bar{W}_j$) for $j-th$ user and $T(f,tot)$, that is $\bar{W}_j = f_j(T_{f,tot})$.

Based on this conclusion, we try to get the probability (p_j) for data packets out of date for $j-th$ when *O*ff-*P*hase duration equals to $T_{f,tot}$ is given in (13).

$$p_j = P\{\bar{W}_j \geq W_{max}\} = 1 - F_{T_{f,tot}}(f_j^{-1}(W_{max})) \tag{12}$$

Since $T_{f,tot} = T_{f,i}$, (13) is rewritten as follows:

$$p_{ij} = P\{\bar{W}_{ij} \geq W_{max}\} = 1 - F_{T_{f,i}}(f_j^{-1}(W_{max})) \tag{13}$$

where p_{ij} is the data packets out of date probability for $j-th$ user when letting $i-th$ user's *O*ff-*P*hase duration for the whole cluster.

For a system with a *O*ff-*P*hase duration $T_{f,i}$ and total data packets out of date probability $\Sigma_j p_j$, we represent its objective function as

$$arg\max_i \quad J(T_{f,i}) = arg\max_i \{\beta T_{f,i} - \gamma \sum_j p_{ij}\} \tag{14}$$

where β and γ are systems parameters that respectively represent the "latency constant" and the "penalty constant" and can be tuned to achieve the desired trade-off between maximizing energy reservation period and minimizing buffer overflowing rate.

2) On-Phase Duration (T_n): During *O*n-*P*hase, normal nodes start to send data packets through competition. Users, who have data packets to send, access the channel to make communication. Competing sources are allowed to send concurrently. Our A-MAC-UWB protocol does not use mutual exclusion (as is commonly done by random access or TDMA protocols) but, in contrast, allows interference to occur and adapt to it. The detail on working process will be discussed in the next part. One of the advantages for our algorithm is removing the overhead of control packets for carrier sensing for avoiding collision, such as RTS/CTS for CSMA/CA scheme, but also ensuring successful transmission.

Based on our transmitter and receiver design, each information bit will be received out by N_R nodes almost concurrently

during period T_s, the transmitted signal is given in (2). And the estimation on receiving signals are done by combining all received signal on N_R receiver nodes. The received signal at $i-th$ user has be given in (4). In that equation, besides the desired user's signal part, $w^{(i)}(t)$ represents the multiple access interference (MAI) caused by other users, and $n^{(i)}(t)$ is the AWGN noise.

Our physical layer design scheme takes the advantages both of virtual MIMO and UWB technologies. Through using MIMO, we substitutes space diversity for time diversity which is commonly used for traditional TH-PPM-UWB signal generation, to carry out performance improvement task. Moreover, the diversity is increased from N_s to $N_T \times N_R$. This modification is inspired by the close dependence on high time synchronization among users. In that case, common timescale should be set up among user to guarantee signal orthogonal among users, which is utilized to mitigate MAI for the source and destination nodes. While for our algorithm, each user just focuses on the working sequence of its transmitter antennas without being aware of the time difference with other users.

The optimum detection strategy for this multiple-access system leads to a multiuser receiver which, however, is too complex to implement and power-consumed. More feasible schemes are of interest. The simplest suboptimal receiver is obtained making two approximations. First, the MAI is thought of as a white Gaussian process [16]. The Gaussian approximation is justified by the central limit theorem if the users are many and have comparable powers. Second, a dominant path exists that conveys the major part of the desired user's energy.

We try to formulate the relationship between P_{rb} and SNIR, expressed as $P_{rb} = f(SNIR)$. Since SNIR is related with those parameters, such as T_s, N_s, we can implement the task of adaptively adjusting data rate R_b with various value of P_{rb} since $R_b = \frac{1}{T_s}$. Considering that longer T_s and bigger N_s mean more energy needed to achieve expected system performance, i.e., data successful transmission rate.

If we let the duration for *O*n-*P*hase of nodes be $T_{n,tot}$, the total number of data packets (N_i) arrived is given in (15), since the traffic arrival process is independent with the data transmission process. Generally, there are two parts for N_i: one is the data packets arrived during *O*ff-*P*hase, denoted by $N_{f,i}$; the other is the data packets arrived during *O*n-*P*hase, denoted by $N_{n,i}$.

$$N_i = N_{f,i} + N_{n,i} = \lambda_i(T_{f,tot} + T_{n,tot}) \tag{15}$$

In our *O*n-*P*hase duration and *O*ff-*P*hase duration designing, we not only try to extend the power off time to reserve energy (through more idle listening avoided), but also need to ensure data packets up to date. Keeping this in our mind, the criteria for active duration is that the active duration ($T_{n,i}$) should be long enough for all received data packets to be sent out. Then we have

$$R_{b,i}T_{n,i} = \lambda_i(T_{n,tot} + T_{f,tot}) \tag{16}$$

Solving (16) for $R_{b,i}$ we get

$$R_{b,i} = \frac{\lambda_i(T_{f,tot} + T_{n,tot})}{T_{n,tot}} \tag{17}$$

From other aspect of obtaining satisfied data successful transmission rate to acquire data rate, that is $\hat{R}_{b,i}$ for node i, we get $\hat{R}_{b,i} = K \times f^{-1}(P_{rb})$. We define the objective function for T_f design is:

$$U(T_{n,tot}) = \sum_i |R_{b,i} - \hat{R}_{b,i}| \tag{18}$$

Then the optimum task is shown in follows:

$$arg\min U(T_{n,tot}) \tag{19}$$

ACKNOWLEDGEMENT

This work was supported by the U.S. Office of Naval Research (ONR) Young Investigator Program Award under Grant N00014-03-1-0466.

REFERENCES

[1] D. Culler, D. Estin, and M. Srivastava, "Overview of sensor networks," in *IEEE Computer Society*, Aug. 2004, pp. 41–49.

[2] "First report and order in the matter of revision of part 15 of the commissions rules regarding ultra-wideband transmission systems, federal communications commission (fcc 02-48)," in *Std., ET Docket 98-153*, Apr. 2002.

[3] A. Paulraj, R. Nabar, and D. Gore, *Introduction to Space-Time Wireless Communications*. Cambridge Univ. Press.

[4] S. Cui, A. J. Goldsmith, and A. Bahai, "Energy-efficiency of mimo and cooperative mimo techniques in sensor networks," *IEEE J. Select. Areas Commun.*, vol. 22, no. 6, pp. 1089–1098, Aug. 2004.

[5] S. K. Jayaweera, "An energy-efficient virtual mimo communications architecture based on v-blast processing for distributed wireless sensor networks," in *IEEE SENCOM 2004*, Oct. 2004, pp. 299–308.

[6] M. M. Carvalho and J. J. Garcia-Luna-Aceves, "Delay analysis of ieee 802.11 in single-hop networks," in *11th IEEE International Conference on Network Protocols (ICNP'03)*, Nov. 2003, pp. 146–155.

[7] V. Rajendran, K. Obraczka, J. Juslin, and O. Koukousoula, "Energy-efficient, collision-free medium access control for wireless sensor networks," in *SenSys'03*, Nov. 2003, pp. 181–192.

[8] L. F. W. van Hoesel, H. J. Kip, and P. J. M. Havinga, "Advantages of a tdma based, energy-efficient, self-organizing mac protocol for wsns," in *IEEE VTC*, May 2004, pp. 1598–1602.

[9] J. Li and G. Y. Lazarou, "A bit-map-assisted energy-efficient mac scheme for wireless sensor networks," in *IPSN'04*, Apr. 2004, pp. 55–60.

[10] S. Biaz and Y. D. Barowski, "Gangs: an energy efficient mac protocol for sensor networks," in *ACMSE'04*, Apr. 2004, pp. 82–87.

[11] W. Ye, J. Herdemann, and D. Estin, "An energy-efficient mac protocol for wireless sensor networks," in *IEEE INFOCOM'02*, June 2002, pp. 1567–1576.

[12] S. Singh and C. Raghavendra, "Pamas: power aware multi-access protocol with signaling for ad hoc networks," in *ACM SIGCOMM Computer Communication Review*, July 1998, pp. 5–26.

[13] T. V. Dam and K. Langendoen, "Adaptive energy-efficient mac protocol for wireless sensor networks," in *SenSys'03*, Nov. 2003, pp. 171–180.

[14] J. Polastre, J. Hillm, and D. Culler, "Versatile low power media access for wireless sensor networks," in *SenSys'04*, Nov. 2004, pp. 95–107.

[15] J. R. Foerster, "The performance of a direct-sequence spread spectrum ultra-wideband system in the presence of multipath, narrowband interference and multiuser interference," in *2002 IEEE Conf. UWB Sys. and Tech.*, May 2002, pp. 87–91.

[16] M. Z. Win and R. Scholtz, "Ultra-wide bandwidth timehopping spread spectrum impulse radio for wireless multiple-access communications," *IEEE Trans. Commun.*, vol. 48, no. 2, pp. 679–689, Apr. 2000.

[17] F. Cuomo, C. Martello, A. Baiocchi, and F. Capriotti, "Radio resource sharing for ad hoc networking with uwb," *IEEE J. Select. Areas Commun.*, vol. 20, no. 9, pp. 1722–1732, Dec. 2002.

[18] J. Ding, L. Zhao, S. R. Medidi, and K. M. Sivalingam, "Mac protocols for ultra-wide-band (uwb) wireless networks: impact of channel acquisition time," in *SPIE ITCOM*, July 2002, pp. 97–106.

[19] I. E. Teletar and D. N. C. Tse, "Capacity and mutual information of wideband multipath fading channels," *IEEE Trans. Inform. Theory*, vol. 46, no. 4, pp. 1384–1400, July 2000.

[20] S. Verdu, "Spectral efficiency in the wideband regime," *IEEE Trans. Commun.*, vol. 48, no. 6, pp. 1319–1343, June 2002.

[21] F. Zhao and L. Guibas, *Wireless Sensor Networks: An Information Processing Approach*. Morgan Kaufmann, 2004.

[22] P. W. Wolniansky, G. J. Foschini, G. D. Golden, and R. A. Valenzuela, "V-blast: An architecture for realizing very high data rates over the rich-scattering wireless channel," in *ISSSE*, Sept. 1998, pp. 295–300.

[23] L. Zhao, X. Hong, and Q. Liang, "Energy-efficient self-organization for wireless sensor networks: a fully distributed approach," in *IEEE Globecom*, Nov. 2004, pp. 2726–2732.

[24] M. L. Welborn, "System considerations for ultrawideband wireless networks," in *IEEE Radio and Wireless Conference*, Aug. 2001, pp. 628–634.

[25] I. Guvenc and H. Arslan, "On the modulation options for uwb systems," in *IEEE MILCOM'03*, Oct. 2003, pp. 892–897.

[26] K. Park and W. Willinger, *Self-Similar Network Traffic and Performance Evaluation*. Wiley, 2000.

[27] G. Anandalingam and S. Raghavan, *Telecommunications Network Design and Management*. Kluwer Academic, 2002.

[28] Q. Ren and Q. Liang, "Asynchronous energy-efficient mac protocols for wireless," in *IEEE Military Communications Conference, (MILCOM'05)*, Oct. 2005.

[29] J. A. Nathaniel, J. L. Hyung, and S. H. Dong, "Pulse sense: a method to detect a busy medium in pulse-based ultra wideband (uwb) networks," in *IEEE Conference on Ultra Wideband Systems and Technologies*, May 2004, pp. 366–370.

Cross-Layer Optimization for Mobile Ad Hoc Networks Using Fuzzy Logic Systems

Xinsheng Xia and Qilian Liang
Department of Electrical Engineering
The University of Texas at Arlington
416 Yates Street, Rm 518
Arlington, TX 76010-0016
Email: xia@wcn.uta.edu, liang@uta.edu

Abstract—**In this paper, we introduce a new method for packet transmission delay analysis and prediction in mobile ad hoc networks. We use fuzzy logic system (FLS) to coordinate physical layer and data link layer. We demonstrate that a type-2 fuzzy membership functions (MFs), i.e., the Gaussian MFs with uncertain variance is most appropriate to model BER and MAC layer service time. Two FLSs: a singleton type-1 FLS and an interval type-2 FLS are designed to predict the packet transmission delay based on the BER and MAC layer service time. Simulation result shows that the interval type-2 FLS performs better than the type-1 FLS.**

I. Introduction

The demand for Quality of Service (QoS) in mobile ad hoc networks is growing in a rapid speed. To enhance the QoS, we consider the combination of physical layer and data-link layer together, a cross-layer approach. A strict layered design is not flexible enough to cope with the dynamics of the mobile ad hoc networks [1]. Cross-layer design could introduce the layer interdependencies to optimized overall network performance. The general methodology of cross-layer design is to maintain the layered architecture, capture the important information that influence other layers, exchange the information between layers and implement adaptive protocols and algorithms at each layer to optimize the performance.

Lots of previous works have focused on cross-layer design for QoS provision. Liu [2] combine the AMC at physical layer and ARQ at the data link layer. Ahn [3] use the info from MAC layer to do rate control at network layer for supporting real-time and best effort traffic. Akan [4] propose a new adaptive transport layer suite including adaptive transport protocol and adaptive rate control protocol based on the lower layer information.

However, cross-layer design can produce unintended interactions among protocols, such as an adaptation loops. It is hard to characterize the interaction at different layers and joint optimization across layers may lead to complex algorithm.

In this paper, we discuss one of the parameters for QOS: packet transmission delay. And our algorithm is quite different from all the previous works. We propose to use the Fuzzy Logic System (FLS) for packet transmission delay analysis and prediction. We apply both a singleton type-1 FLS and an interval type-2 FLS for the analysis and prediction.

The remainder of this paper is structured as following. In section II, we introduce the preliminaries. In section III, we make a overview of fuzzy logic systems. In section IV, we apply the FLS into the cross-layer design. Simulation results and discussions are presented in section V. In section VI, we conclude the paper.

II. Preliminaries

A. IEEE 802.11a OFDM PHY

The physical layer is the interface between the wireless medium and the MAC [5]. The principle of OFDM is to divide a high-speed binary signal to be transmitted over a number of low data-rate subcarriers. A key feature of the IEEE 802.11a PHY is to provide 8 PHY modes with different modulation schemes and coding rates, making the idea of link adaptation feasible and important.

B. IEEE 802.11 MAC

The 802.11 MAC uses Carrier-Sense Multiple Access with Collision Avoidance (CSMA/CA) to achieve automatic medium sharing between compatible stations. In CSMA/CA, a station senses the wireless medium to determine if it is idle before it starts transmission. If the medium appears to be idle, the transmission may proceed, else the station will wait until the end of

the in-progress transmission. A station will ensure that the medium has been idle for the specified inter-frame interval before attempting to transmit.

Besides carrier sense and RTS/CTS mechanism, an acknowledgment (ACK) frame will be sent by the receiver upon successful reception of a data frame. Only after receiving an ACK frame correctly, the transmitter assumes successful delivery of the corresponding data frame. The sequence for a data transmission is: RTS-CTS-DATA-ACK.

A mobile node will retransmit the data packet when finding failing transmission. Retransmission of a signal packet can achieve a certain probability of delivery. There is a relationship between the probability of delivery p and retransmission times n [6]:

$$n = 1.451n\frac{1}{1-p} \tag{1}$$

The IEEE 802.11 standard requires that a data frame is discarded by the transmitter's MAC after certain number of unsuccessful transmission attempts. According to the requirement of probability of delivery, we choose the minimum number of retransmission.

When MAC layer acquires access to the channel, the nodes will exchange the RTS-CTS-DATA-ACK packets. After the transmitters receive an ACK packet, a packet is transmitted successfully. In this paper, we assume that there will be always best-effort traffic present that can be locally and rapidly rate controlled in an independent manner at each node to yield necessary low delays and stable throughputs.

C. Bit Error Rate

BER is the percentage of bits with errors divided by the total number of bits that have been transmitted, received or processed over a given time period. It is a measure of transmission quality. The high BER means high packets loss rate. Requests for resends will increase latency. For delay insensitive traffic requiring a very low BER.

D. MAC Layer Service Time

There are three basic processes when the MAC layer transmits a packet [7]: the decrement process of the backoff timer, the successful packet transmission process that takes a time period of T_{suc} and the packet collision process that takes a time period of T_{col}. Here, T_{suc} is the random variable representing the period that the medium is sensed busy because of a successful transmission, and T_{col} is the random variable representing the period that the medium is sensed busy by each station due to collisions. The MAC layer service time is the time interval from the time instant that a packet becomes the head of the queue and starts to contend for transmission, to the time instant that either the packet is acknowledged for a successful transmission or the packet is dropped. This time is important when we examine the performance of higher protocol layers.

E. Packet Transmission Delay

The packet delay represents the time it took to send the packet between the transmitter and the next-hop receiver, including the deferred time and the time to fully acknowledge the packet. The packet transmission delay between the mobile nodes includes three parts: the wireless channel transmission delay, the Physical/MAC layer transmission delay, and the queuing delay [8].

Defining D as the distance between two nodes and C as the light speed, the wireless channel transmission delay as:

$$Delay_{ch} = \frac{D}{C} \tag{2}$$

The Physical/MAC layer transmission delay will be decided by interaction of the transmitter and the receive channel, the node density and the node traffic intensity etc.

The queuing delay is decided by the mobile node I/O system-processing rate, the subqueue length in the node.

In order to make the system"stable", the rate at which node transfers packets intended for its destination must satisfy all nodes that the queuing lengths will not be infinite and the average delays will be bounded.

F. One-step Markov Path Model

The mobile nodes are roaming independently with variable ground speed. The mobility model is called one-step Markov path model [9]. The probability of moving in the same direction as the previous move is higher than other directions in this model, which means this model has memory. Fig.1 shows the probability of the six directions.

III. Overview of Interval Type-2 Fuzzy Logic Systems

Figure 2 shows the structure of a type-2 FLS [10]. It is very similar to the structure of a type-1 FLS [11]. For a type-1 FLS, the *output processing* block only contains the defuzzifier. We assume that the reader is familiar with type-1 FLSs, so that here we focus only on the similarities and differences between the two FLSs.

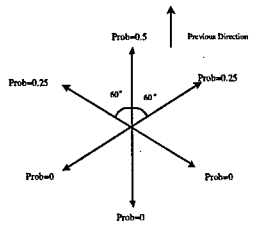

Fig. 1. One-step Markov Path Model

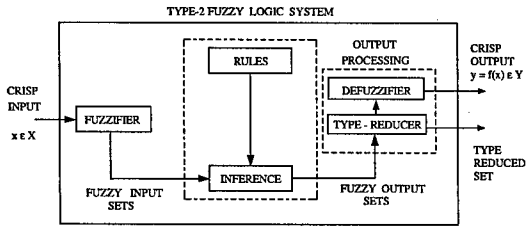

Fig. 2. The structure of a type-2 FLS. In order to emphasize the importance of the type-reduced set, we have shown two outputs for the type-2 FLS, the type-reduced set and the crisp defuzzified value.

The fuzzifier maps the crisp input into a fuzzy set. This fuzzy set can, in general, be a type-2 set.

In the type-1 case, we generally have "IF-THEN" rules, where the lth rule has the form "R^l : IF x_1 is F_1^l and x_2 is F_2^l and $\cdots$ and x_p is F_p^l, THEN y is G^l", where: x_is are inputs; F_i^ls are antecedent sets ($i = 1, \ldots, p$); y is the output; and G^ls are consequent sets. The distinction between type-1 and type-2 is associated with the nature of the membership functions, which is not important while forming rules; hence, the structure of the rules remains exactly the same in the type-2 case, the only difference being that now some or all of the sets involved are of type-2; so, the lth rule in a type-2 FLS has the form "R^l : IF x_1 is $\tilde{\mathrm{F}}_1^l$ and x_2 is $\tilde{\mathrm{F}}_2^l$ and $\cdots$ and x_p is $\tilde{\mathrm{F}}_p^l$, THEN y is $\tilde{\mathrm{G}}^l$".

In the type-2 case, the inference process is very similar to that in type-1. The inference engine combines rules and gives a mapping from input type-2 fuzzy sets to output type-2 fuzzy sets. To do this, one needs to find unions and intersections of type-2 sets, as well as compositions of type-2 relations.

In a type-1 FLS, the defuzzifier produces a crisp output from the fuzzy set that is the output of the inference engine, i.e., a type-0 (crisp) output is obtained from a type-1 set. In the type-2 case, the output of the inference engine is a type-2 set; so, "extended versions" (using Zadeh's Extension Principle [12]) of type-1 defuzzification methods was developed in [10]. This extended defuzzification gives a type-1 fuzzy set. Since this operation takes us from the type-2 output sets of the FLS to a type-1 set, this operation was called "type-reduction" and the type-reduced set so obtained was called a "type-reduced set" [10]. To obtain a crisp output from a type-2 FLS, we can defuzzify the type-reduced set.

General type-2 FLSs are computationally intensive, because type-reduction is very intensive. Things simplify a lot when secondary membership functions (MFs) are interval sets (in this case, the secondary memberships are either 0 or 1). When the secondary MFs are interval sets, the type-2 FLSs were called "interval type-2 FLSs". In [13], Liang and Mendel proposed the theory and design of interval type-2 fuzzy logic systems (FLSs). They proposed an efficient and simplified method to compute the input and antecedent operations for interval type-2 FLSs, one that is based on a general inference formula for them. They introduced the concept of upper and lower membership functions (MFs) and illustrate their efficient inference method for the case of Gaussian primary MFs. They also proposed a method for designing an interval type-2 FLS in which they tuned its parameters.

In an interval type-2 FLS with *singleton fuzzification* and meet under minimum or product t-norm, the result of the input and antecedent operations, F^l, is an interval type-1 set, i.e., $F^l = [\underline{f}^l, \overline{f}^l]$, where $\underline{f}^l$ and $\overline{f}^l$ simplify to

$$\underline{f}^l = \underline{\mu}_{\tilde{\mathrm{F}}_1^l}(x_1) \star \ldots \star \underline{\mu}_{\tilde{\mathrm{F}}_p^l}(x_p) \qquad (3)$$

and

$$\overline{f}^l = \overline{\mu}_{\tilde{\mathrm{F}}_1^l}(x_1) \star \ldots \star \overline{\mu}_{\tilde{\mathrm{F}}_p^l}(x_p) \qquad (4)$$

where x_i ($i = 1, \ldots, p$) denotes the location of the singleton.

In this paper, we use center-of-sets type-reduction, which can be expressed as:

$$Y_{\cos}(Y^1, \cdots, Y^M, F^1, \cdots, F^M) = [y_l, y_r] = \int_{y^1} \cdots \int_{y^M} \int_{f^1} \cdots \qquad (5)$$

where $Y_{\cos}$ is an interval set determined by two end points, y_l and y_r; $f^i \in F^i = [\underline{f}^i, \overline{f}^i]$; $y^i \in Y^i = [y_l^i, y_r^i]$, and Y^i is the centroid of the type-2 interval consequent set $\tilde{\mathrm{G}}^i$; and, $i = 1, \ldots, M$. Because $Y_{\cos}$ is an interval set, we defuzzify it using the average of y_l and y_r; hence, the defuzzified output of an interval type-2 FLS is

$$f(\mathbf{x}) = \frac{y_l + y_r}{2} \qquad (6)$$

IV. Modeling BER and MAC Layer service time with Gaussian Membership Function

A. Analyzing and Modelling BER

Let p be the probability that bit is error in any given time. So p can be described as a random variable with a known mean value E_a.

Now, at any given time the bit is error with probability p and the bit is correct with probability 1-p. Since the bit is either error or correct, the number of the bits it is error(E_b) for a fixed length transmission bits is binomial random variable. The length of the transmission bits is N_t, The probability that E_b takes any value x is :

$$P\{E_b = x\} = \mathrm{C}_x^{N_t}\mathrm{p}^x(1\text{-p})^{N_t - x} \quad (7)$$

As the number of the length of the transmission bits increase, the binomial distribution is approximated to a normal distribution, with mean $\mu = pN_t$ and variance $\sigma^2 = p(1\text{-}p)N_t$.

In this paper, we set up fine membership functions(MFs) for BER. From the original data of BER shown in Table I, we decomposed the whole data sets into ten segments and computed the mean m_i and std σ_i of the BER of the ith segment, $i = 1, 2, \cdots, 10$. We also computed the mean m and std σ of the entire BER. To see which value –m_i or σ_i– varies more, we normalized the mean and std of each segment using m_i/m, and σ_i/σ, and we then computed the std of their normalized values, σ_m and σ_{std}.

TABLE I

MEAN AND STD VALUES FOR TEN SEGMENTS AND THE ENTIRE BER, AND THEIR NORMALIZED STD.

BER	mean	std
Segment 1	0.016613	0.033315
Segment 2	0.015618	0.027857
Segment 3	0.015528	0.017401
Segment 4	0.016206	0.02107
Segment 5	0.015721	0.017148
Segment 6	0.016298	0.029309
Segment 7	0.017062	0.037428
Segment 8	0.016253	0.022871
Segment 9	0.016448	0.023194
Segment 10	0.016237	0.020675
Entire Traffic	0.016198	0.025829
Normalized std	0.029161	0.26184

As we see from the last row of Tables I, $\sigma_m \ll \sigma_{std}$. We conclude, therefore, that if the BER of each segment (short range)are Gaussian with uncertain standard deviation. One example of type-2 Gaussian MF with uncertain standard deviation is shown in Fig.3.

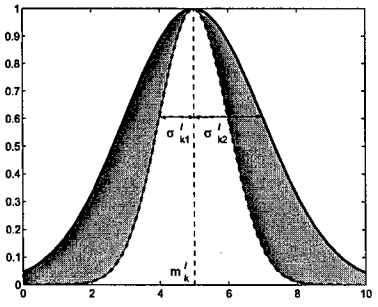

Fig. 3. Type-2 Gaussian MF with uncertain standard deviation

B. Analyzing and Modelling MAC Layer Service Time

Recent research by Zhai, kwon and Fang [7] discovered that the lognormal distribution could match for the MAC layer service time. i.e., if the MAC layer service time for the packet i is s_i, then

$$\log_{10} s_i \sim \mathcal{N}(\cdot; m, \sigma^2) \quad (8)$$

We, therefore, tried to model the logarithm of the MAC layer service time, to see if a Gaussian MF can match its nature. We decomposed the whole data sets into ten segments and computed the mean m_i and std σ_i of the logarithm of the MAC layer service time of the ith segment, $i = 1, 2, \cdots, 10$. We also computed the mean m and std σ of the entire logarithm of the MAC layer service time. To see which value –m_i or σ_i– varies more, we normalized the mean and std of each segment using m_i/m, and σ_i/σ, and we then computed the std of their normalized values, σ_m and σ_{std}.

TABLE II

MEAN AND STD VALUES FOR TEN SEGMENTS AND THE ENTIRE LOGARITHM OF MAC LAYER SERVICE TIME, AND THEIR NORMALIZED STD.

MAC layer service time	mean	std
Segment 1	-1.1902	0.44295
Segment 2	-1.1929	0.44698
Segment 3	-1.1967	0.45237
Segment 4	-1.1959	0.44835
Segment 5	-1.1917	0.43598
Segment 6	-1.1924	0.44779
Segment 7	-1.1976	0.45687
Segment 8	-1.1996	0.45554
Segment 9	-1.1923	0.45068
Segment 10	-1.1997	0.462
Entire Traffic	-1.1949	0.44981
Normalized std	0.0028746	0.016421

As we see from the last row of Tables II, $\sigma_m \ll \sigma_{std}$. We conclude, therefore, that if the logarithm of MAC

layer service time of each segment (short range)are Gaussian with uncertain standard deviation, as shown in Fig.3.

V. Cross-layer Design Using Interval Type-2 Fuzzy Logic System

As we introduce in the preliminaries, the high BER means high packets loss rate. Requests for resends will increase latency. For delay insensitive traffic requires a very low BER. And the MAC later service time is important when we examine the performance of higher protocol layers. So we could know BER and MAC layer service time will manage the packet transmission delay between the mobile nodes. We are now ready to evaluate the packet transmission delay using interval type-2 fuzzy logic systems.

We predict packet transmission delay based on the following two antecedents:

1) Antecedent 1. BER.
2) Antecedent 2. MAC layer service time.

The consequent is depicted as the packet transmission delay. The linguistic variables used to represent the BER and MAC layer service time were divided into three levels: *low*, *moderate*, and *high*. The consequents – the packet transmission delay were divided into 5 levels, *vert low, low, moderate, high and very high.*

We designed questions such as:

IF *BER* is *low* and *MAC layer service time* is *high*, THEN the packet transmission delay is

_____.

So we need to set up $3^2 = 9$ (because every antecedent has 3 fuzzy sub-sets, and there are 2 antecedents) rules for this FLS. We summarized these rules in Table II.

TABLE III
Fuzzy Rules and Consequent

Antecedent1	*Antecedent2*	*Consequent*
Low	*Low*	*VeryLow*
Low	*Moderate*	*Low*
Low	*High*	*Moderate*
Moderate	*Low*	*Low*
Moderate	*Moderate*	*Moderate*
Moderate	*High*	*High*
High	*Low*	*Moderate*
High	*Moderate*	*High*
High	*High*	*VeryHigh*

We used Guassian membership functions (MFs) to represent the antecedents and the consequent.

Fig.4 show the FLS application for the cross-layer design.

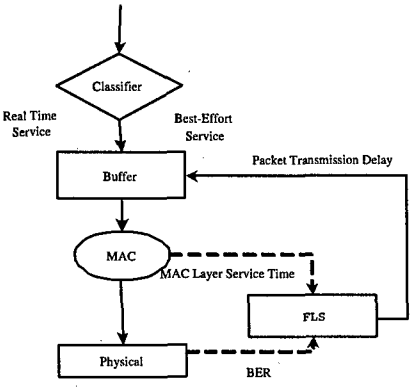

Fig. 4. FLS application for cross-layer design

When a mobile node sends out a packet, it will first predict the packet transmission delay using the FLS algorithm. After that, the node could choose to send the real-time service or not for the real-time service need low delay requirement.

VI. Simulations

We implemented the simulation model using the OPNET modeler. The simulation region is 300×300 meters. There were 12 mobile nodes in the simulation model, and the nodes were roaming independently with variable ground speed between 0 to 10 meters per second. The mobility model was called one-step Markov path model. The movement would change the distance between mobile nodes. We assumed the collecting data distribution of the mobile node was exponential distribution and the arriving interval was 0.2 second and the length of the packet is 512 bits.

Because data communications in the mobile networks had trimming constraints, it was important to design the network algorithm to meet a kind of end-end deadline [14]. We used the packet transmission delay to evaluate the network performance.

Each packet was labeled a timestamp when it was generated by the source mobile node. When its destination mobile node received it, the time interval was the transmission delay.

For type-1 FLS, We chose Gaussian membership function as antecedents; for interval type-2 FLS, we used Gaussian primary MF's with fixed mean and uncertain std for the antecedents. The steepest decent algorithm was used to train all the parameters based on the 300

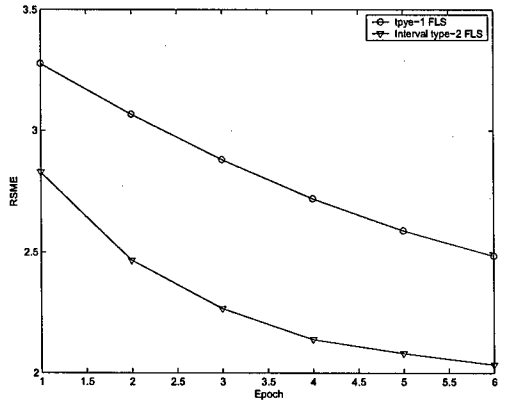

Fig. 5. The RMSE of packet transmission delay prediction for two FLS approaches

data sets. After training, the rules were fixed, and we tested the FLS based on the remaining 300 data sets.

In Fig.5, we summarized the root-mean-square-errors (RMSE) between the estimated packet transmission delay and the actual delay.

$$RMSE = \sqrt{\frac{1}{300}\sum_{i=301}^{600}[d(i) - f(i)]} \qquad (9)$$

where d(i) was the actual packet transmission delay and f(i) was the estimated delay.

The simulation result shows that the interval type-2 FLS for packet transmission delay analysis and prediction outforms the type-1 FLS.

We introduce the fuzzy logic system in the cross-layer design. Compare with other algorithms for cross-layer design, the fuzzy method could be flexible and simpler to implement. We could predict the packet transmission delay according to the information just from physical layer and mac layer. So we have potential application advantage. We could estimate the packet transmission delay before the mobile node sends a packet. Therefore we could assure the service meet the end-to-end delay deadline.

VII. Conclusion

Cross-layer design is a effective method to improve the performance of the mobile ad hoc network. We apply the fuzzy logic system to combine physical layer and data-link layer together. We select BER and MAC layer service time as antecedents to analyze and predict the packet transmission delay. And we apply a type-1 FLS and an interval type-2 FLS for the packet transmission delay analysis and prediction. Simulation result shows that the interval type-2 FLS for packet transmission delay analysis and prediction outform the type-1 FLS.

Acknowledgment

This work was supported by the U.S. Office of Naval Research (ONR) Young Investigator Award under Grant N00014-03-1-0466.

References

[1] A.J. Goldsmith and S.B. Wicker; " Design Challenges for Energy-Constrained Ad Hoc Wireless Networks, " *IEEE Wireless Comm.,* vol. 9, no. 4 , pp. 8-27, 2002.

[2] Q.Liu, S.Zhou and G.Giannakis; " Cross-Layer Combining of Adaptive Modulation and Coding with Truncated ARQ over Wireless Links ," *IEEE Transactions on Wireless Communications*, vol. 3 , no.5 , pp. 1746 - 1755, Sept. 2004.

[3] G. Ahn, A. Campbell, A. Veres and L. Sun; " Support Service Differentiation for Real-Time and Best-Effort Traffic in Stateless Wireless Ad Hoc Networks (SWAN),", *IEEE Transactions on Mobile Computing*, vol. 1, no. 3, pp. 192 - 207, July-Sept. 2002.

[4] O.B.Akan and I.F.Akyildiz; " ATL, An Adaptive Transport Layer Suite for Next Generation on Wireless Internet ,", *IEEE Journal on Selected Areas in Communcations*, June 2004.

[5] D.Qiao, S. Choi, and K.G. Shin " IEEE Trans. On Mobile Computing ,", *IEEE Transactions On Mobile Computing*, Oct. 2002.

[6] L. H. Bao, J. J. Garcia-Luna-Aceves, " Hybrid Channel Access Scheduling in Ad Hoc Networks", *IEEE Computer Society,* Washington, DC, USA.

[7] H. Zhai, Y. Kwon and Y. Fang, "Peformance analysis of IEEE 802.11 MAC protocols in wireless LANs," *Wireless Communication and Mobile Computing*, pp. 917-931, 2004.

[8] Xia, X.;Liang, Q.; "Latency-aware and energy efficiency tradeoffs for sensor networks", *15th IEEE PIMRC(Personal, Indoor and Mobile Radio Communications), 2004.*

[9] Hou T. C., and Tsai T. J.; "Adaptive clustering in a hierarchical ad hoc network", *Proc. Int. Computer Symp.,Tainan, Taiwan,R.O.C.*, Dec. 1998, pp. 171-176.

[10] N. N. Karnik, J. M. Mendel, and Q. Liang, "Type-2 fuzzy logic systems," *IEEE Transactions On Fuzzy Systems*, vol. 7, no. 6, pp. 643-658, Dec. 1999.

[11] J. M. Mendel, "Fuzzy logic systems for engineering: a tutorial," *Proc. of the IEEE*, vol. 83, no. 3, pp. 345-377, March 1995.

[12] L. A. Zadeh, " The concept of a linguistic variable and its application to approximate reasoning - I," *Information Sciences*, vol. 8, pp. 199-249, 1975.

[13] Q. Liang and J. M. Mendel, "Interval type-2 fuzzy logic systems: theory and design," *IEEE Transactions on Fuzzy Systems*, vol. 8, no. 5, pp. 535-550, Oct 2000.

[14] Lu, C. et al; " RAP: a real-time communication architecture for large-scale wireless sensor networks ," *Proceeding of the eighth IEEE real-time and embedded technology and applications Symposium*, San Jose, California, pp. 55 - 66, Sept. 25 - 27, 2002.

Resource Allocation and Latency Estimation in Wireless Sensor Networks Using Maximum Likelihood Decision

Liang Zhao and Qilian Liang
Department of Electrical Engineering
University of Texas at Arlington
Arlington, TX 76010, USA
Email: zhao@wcn.uta.edu, liang@uta.edu

***Abstract*— In this paper, we address a fundamental problem in Wireless Sensor Networks, how many hops does it take for a packet to be relayed for a given distance? For a deterministic topology, this question reduces to a simple geometry problem. However, a statistical study is needed for randomly deployed WSNs. We propose a Maximum Likelihood decision based on the joint pdf of (H, n), which is also derived in this paper. Since the solution is not closed-form, we also propose an attenuated Gaussian approximation for the joint pdf. We show that the approximation visibly simplifies the decision process and the error analysis. The latency and energy consumption estimation are also included as application examples.**

I. Introduction

The recent advances in MEMS, embedded systems and wireless communications enable the realization and deployment of wireless sensor networks (WSN), which consist of a large number of densely deployed and self-organized sensor nodes. The potential applications of WSN, such as environment monitor, often emphasize the importance of location information. Accordingly geographic routing [1] was proposed to handle such requirement. Most likely, a packet is not routed to a specific node, but a given location. An interesting question arises as "how many hops does it take to reach a given location?" The prediction of the number of hops is important not only in itself but also in helping estimating the latency and energy cost, which are both important to the viability of WSN.

The question could become very simple if the sensor nodes are manually placed. For example, suppose sensor nodes are place in a square grid with separation of d. Obviously, the connectivity depends on the comparison of d and the transmission range R. Suppose $d < R < \sqrt{2}d$, this is simply a 4-connectivity network. For any node, the possible distance of its first-hop neighbors is $\{d\}$, the possible distances of its second-hop neighbors are $\{\sqrt{2}d, 2d\}$ and so on. Generally, the possible distances of its nth-hop neighbors are $\{\sqrt{(n-i)^2+i^2}d, i = 0, 1, 2, \cdots, [n/2]\}$, where $[n/2]$ is the smallest integer not less than $n/2$. If we compare the given distance with these distances, the required number of hops can be easily found. For some given distance, there could be two solutions, such as $(8-1)^2+1^2 = (10-5)^2+(10-5)^2 = 50$, then we have to select the number of hops with higher probability. For geographic approach, such conflicts can be easily solved with loss of accuracy. Thus, geographic approach is more efficient and accurate than statistical approach on deterministic topology.

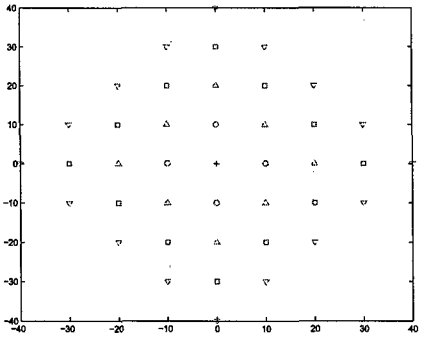

Fig. 1. The nodes in a square grid placement. Only nodes within 4 hops are shown.

However, if sensor nodes are deployed in a random fashion, which is the case for most potential application, the answer is beyond the reach of simple geometry. The stochastic nature of the random deployment calls for a statistical study. A natural and obvious estimation would be dividing the distance by the average inter-

node distance (i.e., the average single-hop distance). However, such estimation may be unable to provide the required accuracy. A probabilistic study is needed here, that is, finding $f(H|d)$, where H is the number of hops. Although the question raised here is not directly addressed before, a mirror problem, finding $f(d|h)$, has been well studied. In [2], Hou and Li studied the 2-D Poisson distribution to find a optimal transmission range. They found that the hop-distance distribution is determined not only by node density and transmission range but also by the routing strategy. They showed results for three routing strategies, Most Forward with Fixed Radius, Nearest with Forward Progress, and Most Forward with Variable Radius. Cheng and Robertazzi in [3] studied the one-dimension Poisson point and found the pdf of r_i as

$$f_{r_i}(r_i) = \frac{\lambda e^{-\lambda(R-r_i)}}{1-e^{-\lambda(R-r_{e_{i-1}})}}, \quad (1)$$

where R is the transmission range, λ is the node density, r_i is the distance from the source to a ith-hop point and r_i is related to r_{e_i} by

$$r_{e_i} + r_i = R. \quad (2)$$

The pdf of r_{e_i} is also obtained,

$$f_{r_{e_i}}(r_{e_i}) = \frac{\lambda e^{-\lambda r_{e_i}}}{1-e^{-\lambda(R-r_{e_{i-1}})}}. \quad (3)$$

Obviously, the distribution of r_i depends on previous r_j, $j < i$. They also pointed out the 2-D Poisson point distribution is analogous to the 1-D case, replacing the length of the segment by the area of the range.

Vural and Ekici reexamined the study under the sensor networks circumstances in [4], and gave the mean and variance of multi-hop distance. They also proposed to approximate the multi-hop distance using Gaussian.

The rest of this paper is organized as follows. We provide some preliminaries on skewness and kurtosis in Sectionsect:Preliminaries. The number of hops predication problem is addressed and solved in Section III. Since this problem has no closed-form solution, we propose an attenuated Gaussian approximation and show how to simplify the error analysis in Section IV. An application example is shown in Section V. Section VI concludes this paper.

II. Preliminaries :Skewness and Kurtosis

In this section, we provide some preliminaries on statistical methods [5]. Skewness is a measure of symmetry, or more precisely, the lack of symmetry. A distribution, or sample set, is symmetric if it looks the same to the left and right of the center point.

Definition 1: [5] For a given sample set X,

$$m_3 = \Sigma(X-\bar{X})^3/n, \quad (4)$$

$$m_2 = \Sigma(X-\bar{X})^2/n, \quad (5)$$

where $\bar{X}$ is the sample mean of X, and n is the size of X. Then a *sample estimate of skewness coefficient* is given by

$$g_1 = \frac{m_3}{m_2^{\frac{3}{2}}}. \quad (6)$$

Skewness is zero for a symmetric distribution. Positive skewness indicates right skewness and negative indicates left.

Kurtosis is a measure of whether the data are peaked or flat relative to a normal distribution.

Definition 2: [5] A sample estimate of kurtosis for a sample set X is given by

$$g_2 = m_4/m_2^2 - 3, \quad (7)$$

where $m_4 = \Sigma(X-\bar{X})^4/n$ is the fourth-order moment of $\bar{X}$ about its mean.

Skewness and kurtosis is useful in determining whether a sample set is normal. Note that the skewness and kurtosis of a normal distribution are both zero; significant skewness and kurtosis clearly indicate that data are not normal.

III. The Number of Hops Prection

A. Problem Formulation

We make the following assumptions.

- The nodes are deployed at random on a plan, that is, the node distribution follows 2D Poisson random process. Thus, the probability of "there is no node in a given area A" is given by [6]

$$Pr(\text{No nodes in } A) = e^{-\lambda A}, \quad (8)$$

  where λ is the density of nodes.
- The distance from the source to the destination d is known, which is common in geographic routing.
- Neither of the source and destination is close to the border. This assumption holds true for most of the nodes if the network size is large enough.

The problem of interest is to find the number of hops, denoted H needed to reach a specific destination r from a given source node. We can make a Maximum Likelihood (ML) decision,

$$H = \arg\max_{H} f(H|r), H = 1, 2, 3, \cdots. \quad (9)$$

Considering

$$f(H|r) = \frac{f(H,r)}{f(r)}, \tag{10}$$

the decision rule can be translated into

$$H = \arg\max_{max} f(H,r), \tag{11}$$

where $f(H,r)$ is also called objective function. In the next subsection, we are concerned with deriving $p(H,r)$.

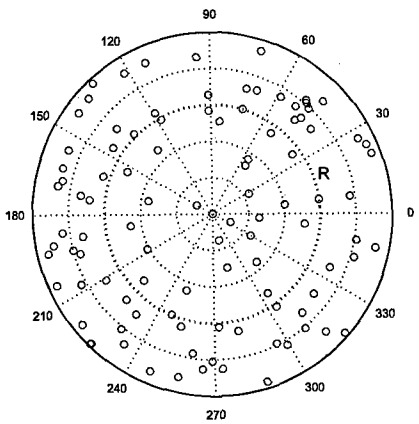

Fig. 2. Poisson node distribution.

B. Derivation of the Joint PDF $p(H,r)$

Let r denote the distance from the source to a node, the cdf of d is

$$F_r(r) = 1 - e^{-\lambda\pi r^2}. \tag{12}$$

And the pdf of d is

$$f_r(r) = \lambda 2\pi r e^{-\lambda\pi r^2}. \tag{13}$$

When $H = 1$, the joint cdf of (H, r_1)

$$p(H=1, r_1) = \begin{cases} 1 - e^{-\lambda\pi r_1^2} & r_1 \le R \\ 0 & r_1 > R \end{cases} \tag{14}$$

and the joint pdf is

$$f(H=1, r_1) = \begin{cases} \lambda 2\pi r_1 e^{-\lambda\pi r_1^2} & r_1 \le R \\ 0 & r_1 > R \end{cases} \tag{15}$$

Note that the conditional pdf of $H = 1$ given $r < R$ is unity for $r < R$, which is intuitively correct but simple, we are more interested in multi-hop distance. In the following, $r > R$ is assumed so that $H > 1$.

The two-hop case is shown in Fig. 3, a second-hop node must satisfy $R < r_2 \le 2R$. Furthermore, the

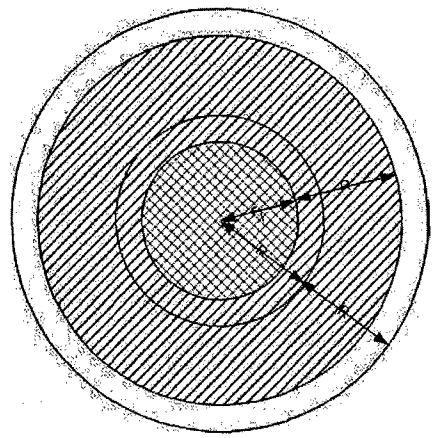

Fig. 3. The second-hop coverage.

farthest first-hop node is not necessarily at the maximum transmission range, which means, there is a gap r_{e_1} between R and r_1, i.e.,

$$r_{e_1} + r_1 = R. \tag{16}$$

Therefore, the joint pdf of (H_1, r_{e_1}) is

$$f(H=1, r_{e_1}) = \begin{cases} \lambda 2\pi (R - r_{e_1}) e^{-\lambda\pi (R - r_{e_1})^2} & r_{e_1} \le R \\ 0 & O.W. \end{cases} \tag{17}$$

And accordingly, the joint cdf of (H_2, r_2) is

$$p(H=1, r_2|r_1) = \begin{cases} e^{-\lambda\pi[(R+r_1)^2 - (r_2+r_1)^2]} - e^{-\lambda\pi[(R+r_1)^2 - r_1^2]} & R < r \le 2R \\ 0 & O.W. \end{cases} \tag{18}$$

Generally, for $H = n$ (shown in Fig.4), we have

$$p(H_n, r_n|r_1, r_2, \cdots, r_n - 1) = \begin{cases} e^{-\lambda\pi[(R+\sum_{i=1}^{n-1} r_i)^2 - (\sum_{i=1}^{n} r_i)^2]} - e^{-\lambda\pi[(R+\sum_{i=1}^{n-1} r_i)^2 - (\sum_{i=1}^{n-1} r_i^2]} & R < r \le nR \\ 0 & O.W. \end{cases} \tag{19}$$

and

$$p(H_n, r_n) = \int_R^{(n-1)R(n-2)R} \int_R^R \cdots \int_0^R p(H_n, r_n|r_1, r_2, \cdots, r_n - 1) f(H_{n-1}, r_{n-1}|r_1, r_2, \cdots, r_n - 2) \cdots f(H_1, r_1) dr_1 \cdots dr_{n-2} dr_{n-1} \tag{20}$$

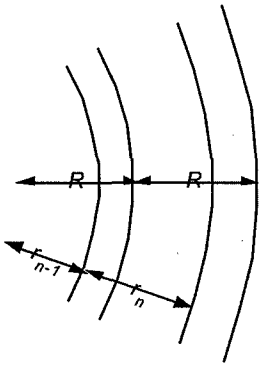

Fig. 4. The ith-hop coverage.

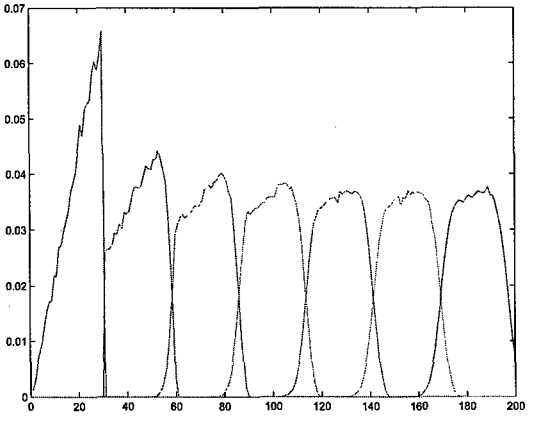

Fig. 5. Histograms of hop-distance joint distribution. ($R = 30$, $\lambda = 6.37(10)^{-3}$)

Theoretically, we can take derivative of (20) with respect to r to obtain the objective function, use (11) to decide the most likely H given r and give the probability of error for such a decision. However, (20) is awkward to evaluate and the computational cost could limit the applicability of such a decision scheme.

IV. Attenuated Gaussian Approximation

TABLE I
STATISTICS OF $f(H = n, r_n), n \geq 3$

Number of Hops	Mean	Std	Skewness	Kurtosis
1	19.991	7.0651	-0.57471	-0.58389
2	45.132	7.8365	-0.16958	-1.0763
3	72.01	8.2129	-0.10761	-1.0332
4	99.45	8.391	-0.07938	-0.97857
5	127.14	8.5323	-0.06445	-0.93104
6	154.96	8.6147	-0.05341	-0.9004
7	182.68	8.573	-0.07738	-0.91687

Since (20) is awkward to evaluate even using numerical methods, we use histograms collected from Monte Carlo simulations as substitute to the joint pdf. All the simulation data are collected from such a scenario that N sensor nodes were uniformly distributed in a circular region of radius of 300 meters. For convenience, polar coordinates were used. The source node was placed at $(0, 0)$. The transmission range was set as R meters. For each setting of (N, R), we ran 300 simulations, in each of which all nodes are re-deployed at random. And the node density is given by

$$\lambda = \frac{N}{\pi R^2} \tag{21}$$

The histograms of $f(H, r)$ are plotted in Fig. 5, which clearly shows that the joint distribution of (H, r) approach the normal when H increases. Table I lists the first-, second-, third- and fourth-order statistics of $f(H, r)$. The skewness and kurtosis clearly satisfy the Gaussianity condition within tolerance of error. Thus, the objective function can be approximated by

$$\begin{aligned} f(H = n, r_n) &= \alpha^n \mathcal{N}(m_n, \sigma_n) \\ &= \frac{\alpha^n}{2\pi\sigma} e^{-\frac{(r-m_n)^2}{2\sigma_n^2}}, \end{aligned} \tag{22}$$

where α is the equivalent attenuation base, m_n and σ_n are the mean and standard deviation(std), respectively. The specific values of these parameters can be evaluated from (20) numerically or estimated from simulations. Observe Table I, for large n, the joint pdf of (H, r) has following properties,

1) $\sigma_n \approx \sigma_{n-1}$, which means the neighboring joint pdf's have similar spread.
2) $m_n - m_{n-1} \approx m_{n+1} - m_n$, which means the joint pdf's are evenly spaced.
3) $3 < \frac{m_n - m_{n-1}}{\sigma_n} < 5$, which means the overlap between the neighboring joint pdf's is small but not negligible. (As a rule of thumbs, $Q(3)$ is considered relatively small and $Q(5)$ is regarded negligible.)
4) $\frac{m_n - m_{n-2}}{\sigma_n} \gg 5$, which means the overlap between the non-neighboring joint pdf's is negligible.
5) $\alpha < 1$. For large density λ, $\alpha \to 1$. Along with Property 1, this tell us that the neighboring joint pdf's have nearly identical shape.

As shown in the following discussion, these properties largely simplify the decision rule and the error analysis. Another interesting observation, besides these properties,

is that the following equations do not stand true.

$$m_n = nm_1 \quad (23)$$
$$m_n = nR \quad (24)$$
$$m_n = (n-1)R + R/2 \quad (25)$$

Although these equations sound plausible, they all give visible errors. The aforementioned estimator $[r/R]+1$ for H, though widely used, is not good in the new light shed by this study. However, Property 2 does tell us the increment for m_n is constant, if denoted by Δ,

$$m_n = m_1 + (n-1)\Delta \quad (26)$$

We showed in [7] that $m_1 = 2/3R$, irrelevant to the node density. Although Δ is a function of λ and R, λ is often regarded constant for a specific application and R varies in a short range, thus, we can safely expect $\Delta = aR$, where a is a constant, for example, $a = 0.9$ for the data in Table I. In summary, the following empirical equation stands for most application for WSN.

$$m_n = R(\frac{2}{3} + (n-1)a) \quad (27)$$

The above results about the constant increment of mean hop-distance is used in Section V-B for energy consumption estimation.

A. Decision Boundaries

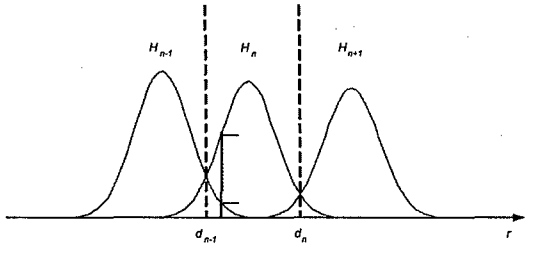

Fig. 6. Gaussian Approximation.

Following (11), we decide H given r using the following rule.

$$H = arg_{max} f(H, r) \quad (28)$$

Observe the $f(H_n, r_n)$ in Fig. 6, the decision is needed only between neighboring H, that is,

$$f(H = n, r) \underset{n+1}{\overset{n}{\gtrless}} f(H = n+1, r). \quad (29)$$

This is because, for a specific value of r, there are only two H_n with dominating $f(H = n+1, r)$, compared to which $f(H = n+1, r)$ for other values of H_n is negligible. Substitute (22) into (29), we obtain the decision boundary d_n between the regions $H = n$ and $H = n+1$.

$$\begin{aligned} d_n &= \frac{B + \sqrt{B^2 + AC)}}{A} \\ A &= \sigma_{n+1}^2 - \sigma_n^2 \\ B &= m_n\sigma_{n+1}^2 - m_{n+1}\sigma_n^2 \\ C &= m_n^2\sigma_{n+1}^2 - m_{n+1}^2\sigma_n^2 + 2\sigma_n^2\sigma_{n+1}^2 \ln\alpha \end{aligned} \quad (30)$$

Using Property 1,

$$d_n = \frac{m_{n+1}^2 - m_n^2 - 2\sigma_n^2 \ln\alpha}{2(m_{n+1} - m_n)} \quad (31)$$

For large density λ, Property 5 is applicable, (30) simplifies to

$$d_n = \frac{\sigma_n^2 m_{n+1} + \sigma_{n+1}^2 m_n}{\sigma_n^2 + \sigma_{n+1}^2} \quad (32)$$

Applying Property 1 to (32),

$$d_n = \frac{m_n + m_{n+1}}{2} \quad (33)$$

If we use the empirical equation (27),

$$d_n = \frac{2}{3}R + (n - \frac{1}{2})aR \quad (34)$$

No matter which approximate solution we choose for d_n, the decision rule is given by

$$r \underset{n}{\overset{n+1}{\gtrless}} d_n. \quad (35)$$

In other words,

$$\text{we decide } H = \hat{n} \text{ if } d_{\hat{n}-1} < r \leq d_{\hat{n}}, \quad (36)$$

which is equivalent to

$$n = [\frac{r - \frac{2}{3}R}{aR} + \frac{1}{2}] + 1. \quad (37)$$

B. Error Performance Analysis

For out decision rule, a decision error occurs when $H = n \neq \hat{n}$. Thus, the probability of error with a specific r is

$$p(\epsilon, r) = \sum_{n \neq \hat{n}} f(n, r). \quad (38)$$

The total probability of error is obtained by integrating (38) over all possible r.

$$p(\epsilon) = \int p(\epsilon, r) dr \quad (39)$$

According to Property 4, only $f(n-1,r)$ and $f(n+1,r)$ could have outstanding value over the decision region $[d_{n-1}, d_n]$.

$$\begin{aligned} p(\epsilon) &\approx \sum_{n=2}^{\infty} \int_{d_{n-1}}^{d_n} f(n-1,r) + f(n+1,r) dr \\ &= \sum_{n=2}^{\infty} \alpha^{n-1} [Q(\frac{d_{n-1} - m_{n-1}}{\sigma_{n-1}}) - Q(\frac{d_n - m_{n-1}}{\sigma_{n-1}})] \\ &\quad + \alpha^{n+1} [Q(\frac{m_{n+1} - d_n}{\sigma_{n+1}}) - Q(\frac{m_{n+1} - d_{n-1}}{\sigma_{n+1}})] \end{aligned} \tag{40}$$

Note that

$$\begin{aligned} &\frac{d_n - m_{n-1}}{\sigma_{n-1}} - \frac{d_{n-1} - m_{n-1}}{\sigma_{n-1}} \\ &= \frac{d_n - d_{n-1}}{\sigma_{n-1}} \gg 1, \end{aligned} \tag{41}$$

therefore, $Q(\frac{d_n - m_{n-1}}{\sigma_{n-1}})$ is negligible compared to $Q(\frac{d_{n-1} - m_{n-1}}{\sigma_{n-1}})$. Similarly, $Q(\frac{m_{n+1} - d_n}{\sigma_{n+1}})$ is negligible. (40) is approximated by

$$\begin{aligned} p(\epsilon) &\approx \alpha^3 Q(\frac{m_3 - d_2}{\sigma_3}) + \sum_{n=3}^{\infty} [\alpha^{n-1} Q(\frac{d_{n-1} - m_{n-1}}{\sigma_{n-1}}) \\ &\quad + \alpha^{n+1} Q(\frac{m_{n+1} - d_n}{\sigma_{n+1}})] \\ &= \alpha^2 Q(\frac{d_2 - m_2}{\sigma_2}) + \sum_{n=3}^{\infty} \alpha^n [Q(\frac{m_n - d_{n-1}}{\sigma_n}) \\ &\quad + Q(\frac{d_n - m_n}{\sigma_n})] \end{aligned} \tag{42}$$

Substituting an appropriate solution of d_n into (42) would give us the probability of error within required accuracy. For example, if we choose (33),

$$\begin{aligned} p(\epsilon) &\approx \alpha^2 Q(\frac{m_3 - m_2}{2\sigma_2}) + \sum_{n=3}^{\infty} \alpha^n [Q(\frac{m_n - m_{n-1}}{2\sigma_n}) \\ &\quad + Q(\frac{m_{n+1} - m_n}{2\sigma_n})] \end{aligned} \tag{43}$$

V. Application Examples

A. Latency Estimation

Suppose it takes T_{rx} for a sensor node to receive 1 bit of message and T_{tx} to transmit. Considering the transmission range in sensor networks is usually short compared to the light speed, the propagation time T_{pr} is negligible. Shown in Fig. 7, given the end-to-end distance r, we can find the required number of hops $H = \hat{n}$ according to (35), thus, a good estimator of the total latency of a l-bit message is

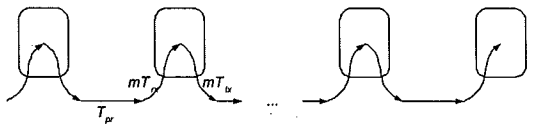

Fig. 7. Time Model.

$$\begin{aligned} &l[T_{tx} + (\hat{n}-1)(T_{tx} + T_{rx}) + T_{rx}] &(44)\\ &= l\hat{n}(T_{tx} + T_{rx}) &(45) \end{aligned}$$

B. Energy Consumption Estimation

The following model is adopted from [8] where perfect power control is assumed. To transmit l bits over distance d, the sender's radio expends

$$E_{tx}(l,d) = \begin{cases} lE_{elec} + l\epsilon_{fs} d^2 & d < d_0 \\ lE_{elec} + l\epsilon_{mp} d^4 & d \geq d_0 \end{cases} \tag{46}$$

and the receiver's radio expends

$$E_{rx}(l,d) = lE_{elec}. \tag{47}$$

E_{elec} is the unit energy consumed by the electronics to process one bit of message, ϵ_{fs} and ϵ_{mp} are the amplifier factor for free-space and multi-path models, respectively, and d_0 is the reference distance to determine which model to use. The values of these communication energy parameters are set as in Table II.

TABLE II
Energy Consumpton Parameters

Name	Value
d_0	86.2m
E_{elec}	$50nJ/bit$
E_{DA}	$5nJ/bit$
ϵ_{fs}	$10pJ/bit/m^2$
ϵ_{mp}	$0.0013pJ/bit/m^4$

Let s_n denote the single-hop distance from the $(n-1)$th-hop to the nth-hop. Obviously, $s_n \leq R$. In our experimental setting, $R = 30m < d_0$ so that the free space model is always used. This agrees well with most applications, in which multi-hop short-range transmission is preferred to avoid the exponential increase in energy consumption for long-range transmission. Naturally, the

end-to-end energy consumption for sending 1 bits over distance r is given by

$$\begin{aligned} E_{total}(l,r) &= \sum_{1}^{\hat{n}}\{E_{tx}(l,r)+E_{rx}(l)\} \\ &= l\sum_{1}^{\hat{n}}\{E_{elec}+\epsilon_{fs}s_n^2+E_{elec}\}, \quad (48) \end{aligned}$$

where $\hat{n}$ is the decision result for given r. On the average,

$$\bar{E}_{total}(l,r) = 2\hat{n}lE_{elec}+\epsilon_{fs}\sum_{1}^{\hat{n}}E[s_n^2] \quad (49)$$

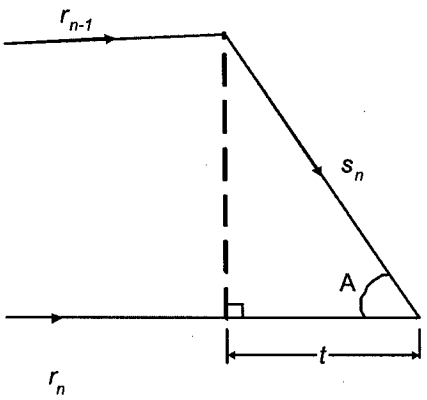

Fig. 8. The relationship between r_n, r_{n-1} and s_n.

The relationship between r_n, r_{n-1} and s_n is depicted in Fig.8.

$$\begin{aligned} t &= s_n\cos A \\ \cos A &= \frac{s_n^2+r_n^2-r_{n-1}^2}{2s_nr_n} \\ \therefore s_n^2 &= r_{n-1}^2-r_n^2+2tr_n \quad (50) \end{aligned}$$

For large n, $r_n \gg s_n$ and $r_{n-1} \gg s_n$, therefore, $t \to \Delta$. According to Property 2, Δ can be treated as a constant.

$$\begin{aligned} E[s_n^2] &\approx E[r_{n-1}^2]-E[r_n^2]+2\Delta E[r_n] \\ &= \sigma_{n-1}^2-\sigma_n^2+2\Delta m_n \quad (51) \\ (\because \text{Property 1}) &\approx 2\Delta m_n \quad (52) \end{aligned}$$

Substitute (52) into (49),

$$\bar{E}_{total}(l,r) = 2\hat{n}lE_{elec}+2\epsilon_{fs}\Delta\sum_{1}^{\hat{n}}m_n \quad (53)$$

VI. Conclusion

To predict the number of hops H needed to reach a given distance r in randomly deployed sensor networks, we proposed a ML decision based on the joint pdf of (H,n), which was also derived in this paper. Since the solution is not closed-form, we also proposed an attenuated Gaussian approximation for the joint pdf. We show that the approximation visibly simplifies the decision process and the error analysis. The latency and energy consumption estimation are also included as application examples.

Acknowledgment

This work was supported by the U.S. Office of Naval Research (ONR) Young Investigator Award under Grant N00014-03-1-0466.

References

[1] R. Jain, A. Puri, and R. Sengupta, "Geographical routing using partial information for wireless ad hoc networks," *IEEE Personal Communications*, vol. 8, pp. 48 – 57, Feb 2001.

[2] T.-C. Hou and V. Li, "Transmission range control in multihop packet radio networks," *Communications, IEEE Transactions on [legacy, pre - 1988]*, vol. 34, no. 1, pp. 38–44, 1986.

[3] Y.-C. Cheng and T. Robertazzi, "Critical connectivity phenomena in multihop radio models," *Communications, IEEE Transactions on*, vol. 37, no. 7, pp. 770–777, 1989.

[4] S. Vural and E. Ekici, "Analysis of hop-distance relationship in spatially random sensor networks," in *MobiHoc '05: Proceedings of the 6th ACM international symposium on Mobile ad hoc networking and computing*. New York, NY, USA: ACM Press, 2005, pp. 320–331.

[5] G. Snedecor and W. Cochran, *Statistical Methods*. Iowa State University Press / AMES, 1989.

[6] M. G. Kendall and P. A. P. Moran, *Geometrical Probability*. Charles Griffin & Co. Ltd., 1963.

[7] L. Zhao and Q. Liang, "Modeling end-to-end distance for given number of hops in wireless sensor networks," in *WCNC'06*, under review, 2006.

[8] W. B. Heinzelman, A. P. Chandrakasan, and H. Balakrishnan, "An application-specific protocol architecture for wireless microsensor networks," *IEEE Trans. Wireless Commun.*, vol. 1, no. 4, pp. 660 – 670, Oct. 2002.

Modeling End-to-end Distance for Given Number of Hops in Wireless Sensor Networks

Liang Zhao and Qilian Liang
Department of Electrical Engineering
University of Texas at Arlington
Arlington, TX 76010, USA
Email: zhao@wcn.uta.edu, liang@uta.edu

Abstract—**We model the end-to-end distance for given hops in Wireless Sensor Networks in this paper. We derive that the single-hop distance follows the distribution $2r/R^2$, where R is the transmission range. The end-to-end distance shows beta distribution for two hops, and approaches Gaussian distribution when the number of hops is beyond three. As an application example, we propose Statistical Distance Estimation, which shows less distance error than Hop-TERRAIN and APS (Ad hoc Positioning System). Our results are also applicable to other applications for Wireless Sensor Networks.**

I. Introduction and Motivation

In Wireless Sensor Networks (WSN), knowledge of node location is often required in many applications. The examples include events report, target tracking, geographical routing, and coverage evaluation. Generally, the distances from a node with unknown location to several anchor nodes are estimated, and then a multilateration is applied to estimate the node location. Distance is often estimated based on received signal strength, time of arrival (TOA), time difference of arrival (TDOA) or angle of arrival [1]. The angle-of-arrival based ranging requires directive antennas or arrays, which is not suitable for most microsensors. Similarly, measuring time of flight requires timing device with satisfactory resolution like in GPS. Although TDOA needs much less resolution, it often requires extra acoustic or ultrasound emission, which comes with higher price, larger size and more energy consumption, all seeming impractical for microsensors. Thus, most technically available ranging is based on received signal strength; in fact, RSSI (Received Signal Strength Indication) is widely used in wireless communications to provide distance estimation.

The underlying observation is that the average large-scale path loss can be expressed as a function of distance by using a path loss exponent, n [2].

$$\bar{PL}(d) = \bar{PL}(d_0)(\frac{d}{d_0})^n \tag{1}$$

where n is the path loss exponent, which indicates the rate at which the path loss increases with distance, d_0 is the close-in reference distance, which is determined from measurement close to the transmitter, and d is the distance from the source to the receiving point. Measurements have also shown that at any value of d, the path loss $PL(d)$ at a particular location is random and distributed log-normally (normal in dB) about the mean distance-dependent value.

$$PL(d)[dB] = \bar{PL}(d)[dB] + X_\sigma, \tag{2}$$

where X_σ is a zero-mean Gaussian distributed random variable (in dB) with standard deviation σ (also in dB). The log-normal shadowing is the main source of distance error for received-signal-strength-based ranging methods. The values of n and σ are often estimated empirically, for example, n could vary from 2 to 10 for different environments, and typical value of σ in urban area is around 10 dBs.

Due to the log-normal shadowing, the RSS-based ranging could be very rough, especially indoors. For example, the median localization error of commodity 802.11 technology is $10ft$ [3], such accuracy may be achieved by alternative techniques, for example, exploiting the density of sensor deployment to estimate distance between nodes. Since the sensor nodes are over-densely deployed, the distance between the nodes are short and the variance of such distance is also small. Therefore, it is quite promising to use the end-to-end distance to obtain distance estimation [4], [5].

For example, both APS [4] and Hop-TERRAIN [6] find the number of hops from a node to each of the anchors and then multiplie this hop count by a shared metric (average single-hop distance) to estimate the range between the node and each anchor. The known positions of anchor nodes and these computed ranges are then used to perform a triangulation to obtain estimated node positions. A further refinement phase is proposed in [6], which uses least squares on local computation. However, as we show later, the distance does not increase linearly with the number of hops. Therefore, a better knowledge about the distribution of end-to-end distance for given number of hops could cast new light on distance estimation.

Geometrical probabilistic study on randomly distributed nodes may date back to centuries ago. More recent studies include [7], which inspected a stochastic modeling of broadcast percolation in one-dimension and obtain the pdf of the hop-distance based on Poisson node distribution [8]. Vural and Ekici [9] reexamined this problem for WSN, and proposed Gaussian approximations for multi-hop end-to-end distance. In these studies, the following equation is widely cited as the

pdf for single-hop distance on a line [9].

$$f(r_e^i) = \frac{\lambda e^{-\lambda r_e^i}}{1 - e^{-\lambda(R - r_e^{i-1})}}, \quad (3)$$

where λ is the node density and R is the transmission range. However, these studies are based on farthest delivery, that is, only the farthest node in the desired direction within the transmission range would relay the beacon packets. In [7], the locations of nodes are known so that the farthest node could be chosen as the next hop. When we plan to exploit node distribution to estimate distance between nodes, we cannot guarantee the beacon packets are relayed in such a fashion, because it is impossible for any nodes to have such location information *a priori*. In fact, routing does not necessarily choose the farthest node for reasons such as energy efficiency, minimizing interference, robustness and so forth. A new study must be carried out in the background of distance estimation.

The rest of this paper is organized as follow. Section II provides some preliminaries for statistical analysis. We model the single-hop distance and show that the derivation for higher-hop end-to-end distance is beyond practical complexity in Section III. Computer simulations and analysis are presented in Section IV. In Section V, based on the knowledge of hop-distance distribution, we propose Statistical Distance Estimation (SDE), independent of ranging techniques. Section VI concludes this paper.

II. Preliminaries

In this section, we provide some preliminaries on statistical methods [10].

A. Skewness and Kurtosis

Skewness is a measure of symmetry, or more precisely, the lack of symmetry. A distribution, or sample set, is symmetric if it looks the same to the left and right of the center point.

Definition 1: [10] For a given sample set X,

$$m_3 = \Sigma(X - \bar{X})^3/n, \quad (4)$$

$$m_2 = \Sigma(X - \bar{X})^2/n, \quad (5)$$

where $\bar{X}$ is the sample mean of X, and n is the size of X. Then a *sample estimate of skewness coefficient* is given by

$$g_1 = \frac{m_3}{m_2^{\frac{3}{2}}}. \quad (6)$$

Skewness is zero for a symmetric distribution. Positive skewness indicates right skewness and negative indicates left.

Kurtosis is a measure of whether the data are peaked or flat relative to a normal distribution.

Definition 2: [10] A sample estimate of kurtosis for a sample set X is given by

$$g_2 = m_4/m_2^2 - 3, \quad (7)$$

where $m_4 = \Sigma(X - \bar{X})^4/n$ is the fourth-order moment of $\bar{X}$ about its mean.

Skewness and kurtosis is useful in determining whether a sample set is normal. Note that the skewness and kurtosis of a normal distribution are both zero; significant skewness and kurtosis clearly indicate that data are not normal.

B. Chi-Square Test

Chi-square test is widely used to determine the goodness of fit of a distribution to a set of experimental data. It works as follows:

- 1. Partition the sample space into the union of K disjoint intervals.
- 2. Compute the probability b_k that an outcome falls in the kth interval under the postulated distribution. The $m_k = nb_k$ is the expected number of outcomes that fall in the kth interval in n repetitions of the experiment.
- 3. The chi-square statistic is defined as the weighted difference between the observed number of outcomes, N_k, that fall in the kth interval, and the expected number m_k.

$$D^2 = \Sigma_{k=1}^{K} \frac{(N_k - m_k)^2}{m_k} \quad (8)$$

- 4. The hypothesis is rejected if $D^2 \geq t_\alpha$, where t_α is a threshold determined by a given significance level. Otherwise, the fit is considered good.

III. Modeling End-to-end Distance for Given Number of Hops

A. Problem Formulation

We assume a general beacon scenario, in which anchors sends out beacon packets informing other nodes about their locations. These beacon packets are also relayed so that nodes outside the anchors' transmission range could also have knowledge about their locations. Nonetheless, clarifications about several terms are necessary, because they have been used in a wide variety of senses.

Firstly, our study on end-to-end distance for given number of hops is based on local coordinate system, which could be translated into a global coordinate system if enough nodes in the local coordinate system have known global coordinates. In previous research, anchors refer to beacons, whose locations are known and broadcast to other nodes. However, in our study, an anchor is simply a specific node used in establishing the local coordinate system. An anchor could have global coordinates or not, which is of no interest to our study. Therefore, our study is applicable to both anchor-based and anchor-free approaches.

Secondly, we assume the beacon packets are distributed in an ad hoc fashion. Although better routing, such as geographic routing, are proposed for WSN, they are not suitable for relaying beacon packets, because during this phase, most nodes have no knowledge about locations of their own and neighbors'. Under such circumstances, we have to assume the beacon packets are simply flooded throughout the sensor network, except that nodes can only relay the beacon packets incoming with least number of hops and discard those via more hops.

Suppose the sensor nodes are placed on a plane at random at an average density of λ nodes per square meters. Let $N(A)$ be the number of nodes in area A, it can be shown

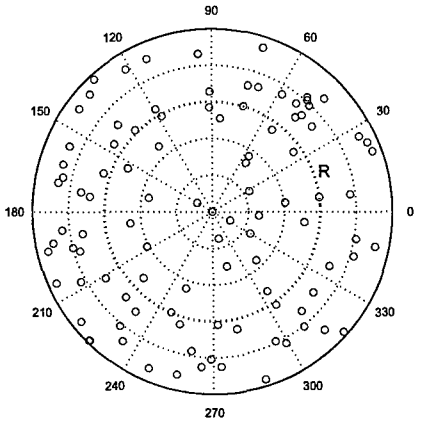

Fig. 1. Uniform node distribution.

that $N(A)$ is a two-dimensional Poisson point process with density λ. One property of the Poisson process is that *if the number of nodes occurring in the area A is N, then the individual outcomes are distributed independently and uniformly in the area A.* That is, if N nodes are placed at random in the area A, then the probability of a specific node in the subarea B is B/A, given B is included by A.

Assume the area A is large enough and none of the anchor nodes is near the border. Without loss of generality, we center the polar coordinates at an arbitrary anchor node (Fig.1). This node could communicate directly with any other nodes within the transmission range, say R. The problem of interest is to find the distance from a specific node to the anchor given this node is within i hops from the anchor. The definitions of variables we are working with are listed in Table I. Note that the event Hop_i can

TABLE I
DEFINITION OF VARIABLES

Variable	Definition
$\vec{r}_i = (r_i, \theta_i)$	the polar coordinates of the i-hop node
s_i	the distance from the anchor to the i-hop node
t_i	the distance from the $(i-1)$-hop node to the i-hop node
$Hop\ i$	the event "the specific node is within i hop, but beyond $i-1$ hops from the anchor."

also be described as "the minimum number of hops from the anchor to the specific node is i".

B. Single-Hop Case

Consider the first hop case, the conditional cdf can be expressed by

$$\begin{aligned} P[s_1 < s|Hop_1] &= P[s_1 < s|r_1 < R] \\ &= \frac{P[s_1 < s]}{P[r_1 < R]} \\ &= \frac{\pi s^2}{\pi R^2} \\ &= \frac{s^2}{R^2} \end{aligned} \tag{9}$$

Note that since the anchor node is placed at the origin, the single-hop distance $d^{[1]}$ equals r_1. The conditional pdf is the derivative of (9).

$$f_{(s_1|Hop_1)}(s) = \frac{2s}{R^2} \tag{10}$$

The conditional expected value and variance can be easily computed by

$$\begin{aligned} E[s_1|Hop_1] &= \int_0^R s\frac{2s}{R^2}ds \\ &= \frac{2R}{3} \end{aligned} \tag{11}$$

$$\begin{aligned} VAR[s_1|Hop_1] &= E[(s_1)^2] - E^2[s_1] \\ &= \int_0^R s^2\frac{2s}{R^2}ds - \frac{4R^2}{9} \\ &= \frac{R^2}{18} \end{aligned} \tag{12}$$

(11) and (12) show that the expected value and variance of single-hop distance is solely determined by the transmission range R and irrelevant to the node distribution density λ. This is due to the uniform node distribution; no matter how large the density could be, it would not give any bias to $E[s_1|Hop_1]$ and $VAR[s_1|Hop_1]$.

C. Two-Hop Case

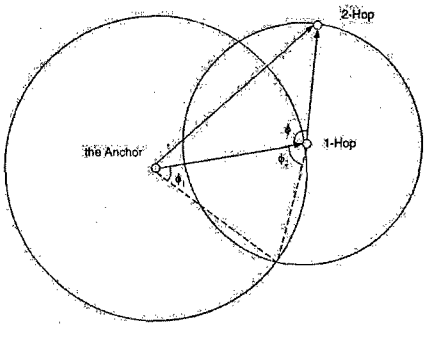

Fig. 2. Two hops.

Consider the two-hop case shown in Fig. 2. The distribution of s_1,which is equal to t_1, is given in (9). Conditional on the value of s_1, the cdf for t_2 is

$$P(t_2 < t|s_1|Hop2) = \frac{B}{\pi R^2}, \tag{13}$$

where B is the area of the region inside the circle of center $\vec{r}_1$ but outside the circle of center $\vec{r}_0$. B is equal to

$$\pi(t_2)^2 - (t_1)^2(\phi_1 - \frac{1}{2}\sin 2\phi_1) - (t_2)^2(\phi_2 - \frac{1}{2}\sin 2\phi_2), \tag{14}$$

where

$$\phi_1 = \cos^{-1}(1 - \frac{(t_2)^2}{2(t_1)^2}), \quad (15)$$

$$\phi_2 = \cos^{-1}(\frac{t_2}{2t_1}). \quad (16)$$

The conditional pdf of t_2 is obtained by taking the derivative of (13).

$$f_{t_2|s_1|Hop2}(r) = \frac{d}{dt}\frac{B}{\pi R^2}, \quad (17)$$

By taking expected value of (17),

$$f_{t_2|Hop2}(t) = \int_0^R f_{s_1}(s)\frac{d}{dt}\frac{B}{\pi R^2}ds, \quad (18)$$

s_2 is determined by

$$s_2 = \sqrt{(t_1)^2 + (t_2)^2 - 2t_1t_2\cos\phi}, \quad (19)$$

where ϕ is the angle between t_1 and t_2 and uniformly distributed in $[-\phi_2, \phi_2]$. Although it is possible to derive the pdf of s_2 from (19), it is awkward to evaluate explicitly. Thus, for the end-to-end distance for two and more hops, we will postulate their distribution from the collected simulation data in the next section.

IV. Simulations and Analysis

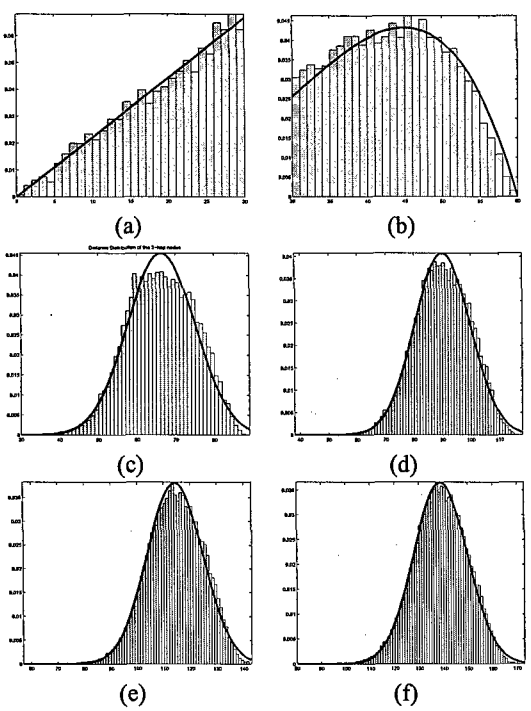

Fig. 3. The histogram vs. postulated distribution for end-to-end distances for given number of hops. (a) One-hop. (b) Two-hop. (c) Three-hop. (d) Four-hop. (e) Five-hop. (f) Six-hop.

All the simulation data are collected from such a scenario that N sensor nodes were uniformly distributed in a circular region of radius of 300 meters. For convenience, polar coordinates were used. The anchor node was placed at $(0, 0)$. The transmission range was set as R meters. For each setting of (N, R), we ran 300 simulations, in each of which all nodes are re-deployed from the beginning.

A. Single-Hop Distance

We plot (10) and the histogram of single-hop distance collected from simulations together in Fig. 3 (a), which clearly shows that (10) fits the experimental data very well. Furthermore, a chi-square test was carried out to determine the goodness of fit of (10) to the experimental data.

TABLE II
Chi-Square Test for Single-Hop Distance Distribution.

Interval	Observed	Expected	$(O-E)^2/E$
1	539	555.37	0.48233
2	543	555.37	0.27538
3	546	555.37	0.15798
4	560	555.37	0.038655
5	583	555.37	1.3749
6	507	555.37	4.2122
7	541	555.37	0.37165
8	571	555.37	0.44007
9	562	555.37	0.079229
10	538	555.37	0.54307
11	583	555.37	1.3749
12	564	555.37	0.13421
13	593	555.37	2.5501
14	555	555.37	0.00024208
15	577	555.37	0.84269
16	563	555.37	0.10492
17	566	555.37	0.20359
18	537	555.37	0.60741
19	549	555.37	0.072987
20	499	555.37	5.7209
21	577	555.37	0.84269
22	535	555.37	0.7469
23	552	555.37	0.020409
24	550	555.37	0.05186
25	611	555.37	5.573
26	552	555.37	0.020409
27	566	555.37	0.20359
28	541	555.37	0.37165
29	570	555.37	0.38557
30	531	555.37	1.0691
		Chi-Square Value =	28.8728

The threshold for $30 - 1 = 29$ degrees of freedom at a 0.005 significance level is 52.34. Compared to this, $D^2 = 28.8728$ is well within the threshold. Thus, we establish that the data is in good agreement with (10).

B. Two-Hop End-to-end Distance

Since there is no close-form formula for the conditional pdf of end-to-end distance for two and more hops, we have to find a fit for it. We postulate the following pdf for the conditional pdf of two-hop end-to-end distance according to the experimental data plotted in Fig. 3 (b). The characteristic curve in Fig. 3 (b) clearly shows a Beta distribution shape. The general pdf of Beta distribution is

$$f_X(x) = \frac{(x-a)^{p-1}(b-x)^{q-1}}{\mathcal{B}(p,q)(b-a)^{p+q-1}}, \quad (20)$$

where p and q are the shape parameters, a and b are the lower and upper bounds, respectively, of the distribution, and $\mathcal{B}(p,q)$ is the beta function. The beta function has the formula

$$\mathcal{B}(p,q) = \int_0^1 t^{p-1}(1-t)^{q-1}dt. \quad (21)$$

The bounds a and b can be easily determined as $a = 0$ and $b = 2R$. Since the maximum of (20) occurs at $\frac{p}{p+q}b$, which is at $\frac{3R}{2}$ in Fig. 3 (b), $p = 3$ and $q = 1$ would be a good guess.

Another noteworthy fact is (20) is valid in $[0, 2R]$ while we only consider $x \in [R, 2R]$ for the conditional two-hop end-to-end distance distribution. Therefore, (20) should be modified for the given condition $x \in [R, 2R]$, that is,

$$f_{X|x\in[R,2R]} = \frac{f_X(x)}{F_X(2R) - F_X(R)}, \quad (22)$$

where $F_X(x)$ is the cdf of $f_X(x)$. Thus,

$$f_{s_2|Hop2}(s) = \frac{(2R-s)s^3}{C\mathcal{B}(2,4)(2R)^5} \qquad R \le s < 2R, (23)$$

where $\mathcal{B}(p,q)$ is the beta function and $C = F_X(2R) - F_X(R)$. Note that C is simply a constant making

$$\int_R^{2R} \frac{(2R-s)s^3}{\mathcal{B}(2,4)(2R)^5} = 1. \quad (24)$$

When $R = 30$, (24) gives us

$$\begin{aligned} C &= \int_{30}^{60} \frac{(60-s)s^3}{\mathcal{B}(2,4)(60)^5} ds \\ &= 0.8125 \end{aligned} \quad (25)$$

C. Three-And-More-Hop End-to-end Distance

When the number of hops increases beyond three, the end-to-end distance distribution approaches Gaussian (See Fig. 3 (d)(e)(f)). For a more formal analysis about its Gaussianity, we list their skewness and kurtosis in Table III. Note that both skewness and kurtosis are virtually zero within tolerance, we postulate Gaussian distribution for three-and-more-hop end-to-end distance. The mean and std can be estimated from the experimental data (see Table III). The postulated distribution and histogram are drawn together in Fig. 3 (d)(e)(f), which clearly shows a close match for each case.

TABLE III
MEANS AND STDS FOR THREE-AND-MORE-HOP END-TO-END DISTANCES

Number of Hops	Mean	Std	Skewness	Kurtosis
3	72.01	8.2129	-0.10761	-1.0332
4	99.45	8.391	-0.079383	-0.97857
5	127.14	8.5323	-0.064453	-0.93104
6	154.96	8.6147	-0.053416	-0.9004

V. AN APPLICATION EXAMPLE: STATISTICAL DISTANCE ESTIMATION

The knowledge about the end-to-end distance for given number of hops can used widely in applications for WSN. For example, we here propose Statistical Distance Estimation (SDE).

A. Protocol Description

SDE is designed for randomly over-densely deployed WSN so that a smaller transmission range can be used without loss of connectivity. SDE is used to obtain relative rough distance between nodes in order to establish a local coordinate system. SDE starts with a core of anchors with assigned coordinates. These anchors broadcast their coordinates throughout the sensor network. Other nodes keep and relay a minimum-hop beacon from each anchor. A node can estimate its distance from an anchor based on the minimum number of hops it takes the beacons to travel from the anchor. Instead of using the product of an average single-hop distance and the number of hops in Hop-TERRAIN, SDE uses the mean of end-to-end distance for minimum number of hops as the estimator. Once a node's distances from three and more non-collinear anchors are estimated, multilateration can be used to determine its location.

In SDE, sensor nodes do not need to have the full knowledge on the end-to-end distance distribution. In fact, a table of the mean distance for each possible number of hops is sufficient. This table can be compiled empirically from simulations for different node densities and transmission ranges. According the minimum number of hops from the anchor, a node can look up the corresponding mean in the table.

B. Error Analysis

For the single-hop distance, we have derived the theoretical distribution given by (10). From (12), we obtain

$$MSE(Hop_1) = \sqrt{VAR[s_1|Hop1]} = \frac{R}{3\sqrt{2}} \quad (26)$$

Note that MSE increases linearly with the transmission range R. When $R = 30m$, (26) gives us 7.0711, which agrees well with the collected MSE 7.1246 from simulations. Other MSEs collected from simulations are also listed in Table IV, which clearly shows the distance accuracy, indicated by MSE, decreases monotonously with the number of hops. Consider a specific node, if we decrease R in the hope of decreasing MSE, it would take more hops for the beacon to reach this node, which could counteract the MSE reduction due to reduced R. As rule of thumb, we found the best number of hops is two, that is, it would be advisable to choose a transmission range to keep all nodes within two hops from the anchors. Considering only the nodes within two hops from the

anchors, the average MSE is

$$= \frac{7.12 \times 5428 + 7.33 \times 11376}{5428 + 11376} = 7.27, \quad (27)$$

which is approximately $0.24R$. Compared to $R/3$ distance error provided by [4], [6], our statistical approach achieved a lesser error, which is within a quarter of the transmission range.

TABLE IV
MSE FROM SIMULATIONS (R=30M)

Number of Hops	MSE	Sample Size
1	7.12	5428
2	7.33	11376
3	8.75	18607
4	9.77	26042
5	10.46	33804
6	10.89	40770

VI. CONCLUSION

In this paper, we study the modeling of the end-to-end distance for given number of hops in WSN. The experiments showed that the distance does not increase linearly with the number of hops. Therefore, the distance should be analyzed for each number of hops. We derived the distribution for single-hop distance and also showed that the complexity of derivation for multiple-hop distance is beyond practical interest. Thus, we postulate gamma distribution for two-hop end-to-end distance and Gaussian distribution for three-and-more-hop end-to-end distance. Computer simulations showed our postulated distributions agree well with the histograms.

We also propose Statistical Distance Estimation, in which statistically exploiting the knowledge of hop-distance distribution reduces the distance error from $R/3$ to $R/4$. Such fundamental knowledge about end-to-end distance distribution is applicable to other applications for WSN, such planning and/or optimization in deployment and resource management.

VII. ACKNOWLEDGMENT

This work was supported by the U.S. Office of Naval Research (ONR) Young Investigator Award under Grant N00014-03-1-0466.

REFERENCES

[1] J. Hightower and G. Borriello, "Location systems for ubiquitous computing," *IEEE Computer*, vol. 34, no. 8, pp. 57–66, August 2001, this article is also excerpted in "IT Roadmap to a Geospatial Future," a 2003 report from the Computer Science and Telecommunications Board of the National Research Council. [Online]. Available: http://seattle.intel-research.net/people/jhightower/pubs/hightower2001location/hightower2001location.pdf

[2] T. S. Rappaport, *Wireless Communications:Principles and Practice*. Upper Saddle River, NJ: Prentice-Hall, 2002.

[3] E. Elnahrawy, X. Li, and R. Martin, "The limits of localization using signal strength: a comparative study," in *Sensor and Ad Hoc Communications and Networks, 2004. IEEE SECON 2004. 2004 First Annual IEEE Communications Society Conference on*, 2004, pp. 406–414.

[4] D. Niculescu and B. Nath, "Ad hoc positioning system (aps)," in *Global Telecommunications Conference, 2001. GLOBECOM '01. IEEE*, vol. 5, 2001, pp. 2926–2931 vol.5.

[5] ——, "Dv based positioning in ad hoc networks," *Telecommunication Systems*, pp. 22(1–4):267–280, 2003.

[6] C. Savarese, J. Rabay, and K. Langendoen, "Robust positioning algorithms for distributed ad-hoc wireless sensor networks," in *USENIX Technical Annual Conference*, Monterey, CA, June 2002. [Online]. Available: citeseer.ist.psu.edu/savarese02robust.html

[7] Y.-C. Cheng and T. Robertazzi, "Critical connectivity phenomena in multihop radio models," *Communications, IEEE Transactions on*, vol. 37, no. 7, pp. 770–777, 1989.

[8] M. G. Kendall and P. A. P. Moran, *Geometrical Probability*. Charles Griffin & Co. Ltd., 1963.

[9] S. Vural and E. Ekici, "Analysis of hop-distance relationship in spatially random sensor networks," in *MobiHoc '05: Proceedings of the 6th ACM international symposium on Mobile ad hoc networking and computing*. New York, NY, USA: ACM Press, 2005, pp. 320–331.

[10] G. Snedecor and W. Cochran, *Statistical Methods*. Iowa State University Press / AMES, 1989.